bioRxiv preprint doi: https://doi.org/10.1101/708701; this version posted July 19, 2019. The copyright holder for this preprint (which was not certified by peer review) is the author/funder, who has granted bioRxiv a license to display the preprint in perpetuity. It is made available under aCC-BY-ND 4.0 International license.

The *in vivo* endothelial cell translatome is highly heterogeneous across vascular beds

Audrey C.A. Cleuren[1], Martijn A. van der Ent[2], Hui Jiang[3], Kristina L. Hunker[2], Andrew Yee[1*], David R. Siemieniak[1,4], Grietje Molema[5], William C. Aird[6], Santhi K. Ganesh[2,7] and David Ginsburg[1,2,4,7,8,§]

[1]Life Sciences Institute, [2]Department of Internal Medicine, [3]Department of Biostatistics, [4]Howard Hughes Medical Institute, University of Michigan, Ann Arbor, Michigan, USA, [5]Department of Pathology and Medical Biology, University of Groningen, Groningen, the Netherlands, [6]Center for Vascular Biology Research, Beth Israel Deaconess Medical Center, Boston, Massachusetts, USA, [7]Department of Human Genetics and [8]Department of Pediatrics, University of Michigan, Ann Arbor, Michigan, USA

* Current address: Department of Pediatrics, Baylor College of Medicine, Houston, TX

§ Corresponding author; email ginsburg@umich.edu

Running title: *in vivo* endothelial cell heterogeneity

Key words: endothelial cells, RiboTag, gene expression profiling, RNA sequencing

bioRxiv preprint doi: https://doi.org/10.1101/708701; this version posted July 19, 2019. The copyright holder for this preprint (which was not certified by peer review) is the author/funder, who has granted bioRxiv a license to display the preprint in perpetuity. It is made available under aCC-BY-ND 4.0 International license.

Abstract

Endothelial cells (ECs) are highly specialized across vascular beds. However, given their interspersed anatomic distribution, comprehensive characterization of the molecular basis for this heterogeneity *in vivo* has been limited. By applying endothelial-specific translating ribosome affinity purification (EC-TRAP) combined with high-throughput RNA sequencing analysis, we identified pan EC-enriched genes and tissue-specific EC transcripts, which include both established markers and genes previously unappreciated for their presence in ECs. In addition, EC-TRAP limits changes in gene expression following EC isolation and *in vitro* expansion, as well as rapid vascular bed-specific shifts in EC gene expression profiles as a result of the enzymatic tissue dissociation required to generate single cell suspensions for fluorescence-activated cell sorting (FACS) or single cell RNA sequencing analysis. Comparison of our EC-TRAP to published single cell RNA sequencing data further demonstrates considerably greater sensitivity of EC-TRAP for the detection of low abundant transcripts. Application of EC-TRAP to examine the *in vivo* host response to lipopolysaccharide (LPS) revealed the induction of gene expression programs associated with a native defense response, with marked differences across vascular beds. Furthermore, comparative analysis of whole tissue and TRAP-selected mRNAs identified LPS-induced differences that would not have been detected by whole tissue analysis alone. Together, these data provide a resource for the analysis of EC-specific gene expression programs across heterogeneous vascular beds under both physiologic and pathologic conditions.

bioRxiv preprint doi: https://doi.org/10.1101/708701; this version posted July 19, 2019. The copyright holder for this preprint (which was not certified by peer review) is the author/funder, who has granted bioRxiv a license to display the preprint in perpetuity. It is made available under aCC-BY-ND 4.0 International license.

Significance

Endothelial cells (ECs), which line all vertebrate blood vessels, are highly heterogeneous across different tissues. The present study uses a genetic approach to specifically tag mRNAs within ECs of the mouse, thereby allowing recovery and sequence analysis to evaluate the EC-specific gene expression program directly from intact organs. Our findings demonstrate marked heterogeneity in EC gene expression across different vascular beds under both normal and disease conditions, with a more accurate picture than can be achieved using other methods. The data generated in these studies advance our understanding of EC function in different blood vessels and provide a valuable resource for future studies.

bioRxiv preprint doi: https://doi.org/10.1101/708701; this version posted July 19, 2019. The copyright holder for this preprint (which was not certified by peer review) is the author/funder, who has granted bioRxiv a license to display the preprint in perpetuity. It is made available under aCC-BY-ND 4.0 International license.

Introduction

Endothelial cells (ECs) form the inner lining of all vertebrate blood vessels, providing a critical barrier between circulating blood and parenchymal cells. In addition to maintaining blood fluidity and regulating vascular tone, ECs control the transport of nutrients and metabolites to and from underlying tissues while also contributing to host defense and the control of inflammatory processes. Consistent with their diverse microenvironments and specialized functions, ECs display remarkable morphologic and structural heterogeneity across organs (1-5). Initial studies of well-established EC markers including von Willebrand factor (*Vwf*), platelet endothelial cell adhesion molecule (*Pecam*) and *Cd34* demonstrated heterogeneous expression of these genes across the vascular tree and in distinct vascular beds (6, 7). However, more comprehensive characterization of the EC transcriptome has been largely limited by the challenge of purifying ECs, given their highly interspersed anatomic distribution among parenchymal cells in various tissues.

Previous studies have focused on human umbilical vein endothelial cells (HUVECs) expanded in cell culture, or isolation and *in vitro* expansion of ECs from distinct vascular beds such as the brain or liver (8-10). Although ECs expanded *in vitro* may retain some tissue-specific characteristics, the loss of microenvironmental cues could result in shifts in the expression program that no longer faithfully reflect the *in vivo* EC transcriptome (11-14). Several *in vivo* phage display approaches have been used to identify vascular bed-specific markers or 'vascular zip codes', though generally resulting in the identification of only a limited number of EC binding peptides (15-18). In addition, fluorescence-activated cell sorting (FACS) of cells endogenously marked with a fluorescent protein (19-23) or via intravital staining (24), and more recently single cell RNA sequencing (RNASeq) analyses (25-30), have been performed to determine cell type-specific transcriptomes. However, these latter methods rely on the preparation of single cell suspensions following enzymatic tissue dissociation often followed by flow sorting under high shear stress, which may affect gene expression programs.

Mouse transgenic approaches have enabled transcriptional profiling directly *in vivo* via translating ribosome affinity purification (TRAP) (31-36). This method relies on the inducible expression of an epitope-tagged ribosomal protein in a cell type-specific pattern, thus facilitating isolation of ribosome-associated transcripts, also known as the translatome (37), for particular cellular subsets directly from a complex mixture of cells. Here we report the application of EC-specific TRAP (EC-TRAP) combined with high-throughput RNASeq analysis to characterize EC

bioRxiv preprint doi: https://doi.org/10.1101/708701; this version posted July 19, 2019. The copyright holder for this preprint (which was not certified by peer review) is the author/funder, who has granted bioRxiv a license to display the preprint in perpetuity. It is made available under aCC-BY-ND 4.0 International license.

translatomes across multiple vascular beds. Our findings demonstrate a high degree of tissue-specific endothelial heterogeneity, as well as notable shifts in EC mRNA content during the process of enzymatic tissue dissociation. Using EC-TRAP we also demonstrate vascular bed-specific variation in endothelial reactivity in response to lipopolysaccharide (LPS) exposure, which would not have been identified by whole tissue RNASeq data analysis.

Results and Discussion

In vitro expansion of ECs leads to phenotypic drift

Microarray analysis was performed on ECs isolated from heart or kidney, either directly after isolation (day 0) or after additional expansion in culture for 3 days. As shown by principal component analysis (Figure 1), *in vitro* expansion of primary ECs results in major shifts in gene expression profiles, with the expression profiles of heart and kidney more closely resembling each other after 3 days in culture, than compared to freshly isolated ECs at day 0. These data suggest that removal of the native environment results in phenotypic drift with regression toward a common EC transcription profile. This finding supports previous reports (11-14) demonstrating an important role for microenvironmental cues in maintaining the molecular heterogeneity of ECs.

Rpl22 isoform analysis to assess tissue-specific EC content

To probe EC heterogeneity directly *in vivo,* we applied TRAP by taking advantage of the RiboTag mouse, which carries a conditional *Rpl22* allele (35). We, and others, have previously shown effective EC targeting using *Cre*-recombinase driven by the *Tek* promoter in evaluating the cellular origin of coagulation factor VIII (38, 39). As shown in Figure 2A-D, analysis of mice carrying a *Tek-Cre* transgene (*Tek-Cre*$^{+/0}$) (40, 41) together with the *Rosa*^{mTmG} reporter (42) confirms efficient targeting of ECs *in vivo*. The high degree of EC sensitivity and specificity observed for the *Tek-Cre* transgene suggests that the extent of genomic *Rpl22* excision in organs from *Rpl22*$^{fl/fl}$, *Tek-Cre*$^{+/0}$ mice should accurately reflect the relative fraction of ECs within those tissues. Quantitative analysis of *Rpl22* targeting by direct high-throughput genomic sequence analysis demonstrated the lowest fraction of ECs in brain (5.5±0.9%), followed by liver (13.5±1.7%), kidney (16.3±2.6%), and heart (38.6±3.8), with the highest fraction observed in the lung

bioRxiv preprint doi: https://doi.org/10.1101/708701; this version posted July 19, 2019. The copyright holder for this preprint (which was not certified by peer review) is the author/funder, who has granted bioRxiv a license to display the preprint in perpetuity. It is made available under aCC-BY-ND 4.0 International license.

(48.4±6.7%) (Figure 2E). Although we cannot exclude a minor contribution from non-ECs (transiently) expressing *Tek* by this approach (see below), the quantitative *Rpl22* data are consistent with our microscopic images from *Rosa*$^{mT/mG}$, *Tek-Cre*$^{+/0}$ mice (Figure 2A-D) and comparable to previous estimates of EC content based on histologic examination and FACS analysis (20, 43).

Evaluation of EC-specific translatomes by TRAP

TRAP specifically captures actively translated mRNAs (translatome), which may differ quantitatively from the total cellular mRNA pool (transcriptome). To determine if tissue transcriptomes obtained prior to EC-TRAP are comparable to tissue translatomes, or if corrections are needed for potential disproportional mRNA capture due to differences in ribosome density across mRNAs, we performed TRAP and RNAseq analysis on tissues of mice expressing HA-tagged ribosomes in all cell types (*Rpl22*$^{fl/fl}$, *EIIa-Cre*$^{+/0}$). Before tissue isolation, animals were perfused with cycloheximide to block translation and stabilize tagged ribosomes on their cognate mRNAs to minimize potential shifts in ribosome distribution during tissue collection and immunoprecipitation (44). Expression profiles obtained before and after TRAP were highly reproducible between biologic replicates, with distinct patterns evident across organs. Only minor changes were observed between the total mRNA and actively translated mRNA within a given tissue (Figure 3A), resulting in a limited number of transcripts that were significantly different between the 2 mRNA pools (Supplemental Figure S1; Supplemental Table S1). These data demonstrate that signatures obtained after EC-TRAP should primarily reflect cell-specific gene expression programs, with little or no contribution from shifts in ribosome distribution, and that the transcriptome of a tissue lysate can serve as a proxy for the corresponding tissue translatome.

We next analyzed TRAP-selected mRNA fractions collected from multiple tissues of *Rpl22*$^{fl/fl}$, *Tek-Cre*$^{+/0}$ mice after cycloheximide perfusion. To avoid contamination of TRAP-selected mRNAs with transcripts originating from parenchymal cells (35), we also evaluated the accompanying unselected tissue transcriptomes by RNAseq analysis, and calculated relative enrichment scores. These scores identify those transcripts that are more abundant in *Tek*$^{+}$ cells (enriched genes, $\log_2$ fold change >0), or more abundant in *Tek*$^{-}$ cells (depleted genes, $\log_2$ fold change <0), where the former should represent EC-specific genes and the latter parenchymal cell-specific genes

bioRxiv preprint doi: https://doi.org/10.1101/708701; this version posted July 19, 2019. The copyright holder for this preprint (which was not certified by peer review) is the author/funder, who has granted bioRxiv a license to display the preprint in perpetuity. It is made available under aCC-BY-ND 4.0 International license.

(Supplemental Figure S1). As expected, GO analysis of TRAP-enriched transcripts showed highly significant associations with endothelial and hematopoietic biologic processes including "vasculature development", "immune response" and "hemopoiesis", while depleted gene sets showing signals consistent with parenchymal, tissue-specific processes (Supplemental Figure S2).

Correction of TRAP-enriched genes for hematopoietic cell content

Although the *Tek-Cre* transgene provides an efficient and specific marker of the EC compartment, the *Tek* gene is also transiently expressed in hematopoietic cells (45), which could result in the false identification of mRNAs as EC-specific as a result of blood contamination of tissues. For example, despite exsanguination and cardiac perfusion prior to organ harvest to remove circulating blood cells, the genes encoding hemoglobin α and β (*Hba-a1*, *Hba-a2*, *Hbb-bs* and *Hbb-bt*) were among the most enriched transcripts across all tissues and although α-hemoglobin gene expression has been reported in arterial ECs, β-hemoglobin has not directly been associated with the endothelium (46, 47). Thus, the similar degree of enrichment observed for both α- and β-hemoglobin in our EC-TRAP suggests a contribution of HA-tagged polysomes derived from circulating blood cells that were not completely removed by perfusion prior to tissue isolation. To eliminate transcripts originating from hematopoietic cells, we applied additional computational filters based on data obtained from TRAP performed directly on peripheral blood samples from *Rpl22*$^{fl/fl}$, *Tek-Cre*$^{+/0}$, as well as EC-TRAP on tissues collected from an *Rpl22*$^{fl/fl}$, *Tek-Cre*$^{+/0}$ recipient following bone marrow transplant using an *Rpl22*$^{fl/fl}$, *Tek-Cre*$^{-}$ donor (see Supporting Information). In addition to removing the hemoglobin genes and other known lymphoid and myeloid cell markers, including a number of established EC markers known to be expressed by megakaryocytes/platelets (48), applying these filters provides the most specific set of EC-enriched genes. GO analysis of this more restricted EC gene set now showed enrichment limited to vascular-related biologic processes (Figure 4A) with loss of the GO terms for marrow-derived cell populations identified in the broader analysis (Supplemental Figure S2).

TRAP identifies EC heterogeneity across vascular beds

Principal component analysis of EC translatomes demonstrates distinct, reproducible patterns for each organ (Figure 3B). This observation is confirmed by hierarchical clustering of enrichment

bioRxiv preprint doi: https://doi.org/10.1101/708701; this version posted July 19, 2019. The copyright holder for this preprint (which was not certified by peer review) is the author/funder, who has granted bioRxiv a license to display the preprint in perpetuity. It is made available under aCC-BY-ND 4.0 International license.

scores where, consistent with the high percentage of ECs in the lung and heart, the degree of enrichment for EC transcripts in these organs is generally lower than that observed in brain, kidney and liver (Figure 4B).

Overlap in expression across the different vascular beds for the 500 top-ranked genes based on enrichment scores for each tissue is shown in Figure 4C, identifying 82 genes shared among all 5 vascular beds, including *Tek*, as expected, as well as other established pan-EC markers such as *Cdh5*, *Nos3*, *Eng* and *Robo4*. This list also includes *Ephb4*, *Dll4* and *Flt4*, specifically marking arterial, venous and lymphatic ECs, respectively, demonstrating efficient targeting of all 3 EC subtypes (49, 50) (Table 1). In addition to the pan-EC markers that have previously been associated with EC function and/or localization (23, 32, 51-53), our EC-TRAP analysis also identified potential novel pan-EC genes, including *Gm20748* (also known as *Bvht*) and *Eva1b*, with *in situ* hybridization confirming colocalization of these transcripts with *Tek* transcripts in ECs of brain, kidney and liver (Figure 5A-B).

The EC-TRAP data identify marked heterogeneity of gene expression levels for EC-enriched genes across tissues, including genes restricted to a single or several vascular beds. An interesting subset of genes appears to be EC-enriched in one or more tissue(s), with expression levels more abundant in non-ECs in another tissue (Supplemental Figure S3; Supplemental Table S2). For example, whereas several solute carriers play important roles in proximal tubules in the kidney, and are thus depleted after kidney EC-TRAP, a number of these genes are significantly enriched in brain ECs (Supplemental Table S2). Focusing on EC-specific genes with expression restricted to a single vascular bed identified the largest number of unique markers for brain ECs, including several genes previously associated with the blood brain barrier (e.g. *Rad54b*, *Zic3* and *Slco1c*) (20, 25, 27, 54). Smaller subsets of tissue-specific EC markers were also identified for heart, kidney, liver and lung (Table 2), with specific kidney EC expression of lincRNA *3110099E03Rik* and liver EC expression of *Wnt9b* confirmed by *in situ* hybridization (Figure 5C-D).

Comparison between EC-TRAP and single cell RNASeq

Recently developed single cell RNASeq methods make it possible to distinguish cellular subtypes within complex mixtures of cells, including multiple subsets of ECs, as previously reported for the brain (23, 27). However, several studies raise the concern that the isolation procedures required

bioRxiv preprint doi: https://doi.org/10.1101/708701; this version posted July 19, 2019. The copyright holder for this preprint (which was not certified by peer review) is the author/funder, who has granted bioRxiv a license to display the preprint in perpetuity. It is made available under aCC-BY-ND 4.0 International license.

to obtain individual cells for RNASeq analysis may perturb relative mRNA abundance (55-57). To evaluate the potential impact of such changes in EC expression programs across tissues, perfusion and enzymatic tissue dissociation were performed in the absence of cycloheximide, to mimic the effects of single cell isolation procedures (including continuing changes in mRNA transcription and translation), until the addition of cycloheximide-containing buffer prior to TRAP, approximately 90 minutes after organ harvest.

Although some degree of vascular bed-specific gene expression patterns persist, substantial changes are observed when compared to the profiles obtained from cycloheximide-perfused animals (Figure 6A). Whereas the kidney endothelium showed relatively small shifts in expression profiles between isolation methods, liver and brain ECs exhibit larger deviations as well as lower correlations between biologic replicates. Indeed, 48.2% of genes expressed in brain ECs (3794/7866) and 21.6% expressed in liver ECs (2306/10696) are differentially expressed when comparing the 2 preparation methods, with only 7.4% for kidney EC genes (779/10475). As a result, hierarchical clustering of EC translatomes identify liver and brain ECs as more similar based on sample preparation method than by tissue of origin (Figure 6B).

In addition to the potential for shifts in the EC expression program during the preparation of single cells, current single cell RNASeq methods exhibit a relatively limited sensitivity to detect low abundance transcripts (58, 59). Consistent with these previous reports, of the 100 most abundant EC-enriched transcripts per tissue identified in our EC-TRAP data set, many have also been identified in ECs based on single cell RNASeq data (median 50, range 28-77; Supplemental Table S3). In contrast, only a few of the 100 lowest abundant genes were detected by single cell RNAseq (median 2, range 0-24) (25-27, 29).

Taken together, the EC-TRAP approach combined with *in vivo* cycloheximide perfusion prior to mRNA preparation reported here, should result in a more accurate snapshot of native EC profiles across different vascular beds, including low abundant transcripts, than is possible with current single cell isolation and RNASeq methods.

Endotoxemia induces tissue-specific changes in the EC gene expression program

bioRxiv preprint doi: https://doi.org/10.1101/708701; this version posted July 19, 2019. The copyright holder for this preprint (which was not certified by peer review) is the author/funder, who has granted bioRxiv a license to display the preprint in perpetuity. It is made available under aCC-BY-ND 4.0 International license.

The endothelium provides a key line of host defense in response to microbial pathogens. To examine the tissue-specific response in an animal model for bacterial endotoxemia, *Rpl22*$^{fl/fl}$, *Tek-Cre*$^{+/0}$ mice were injected with lipopolysaccharide (LPS). Analysis of whole organ transcriptomes (including both ECs and parenchymal cells) demonstrated marked changes in gene expression in response to LPS, with gene ontology analysis yielding highly significant values for terms associated with host defense and immune response (Supplemental Figure S4A). The extent of gene changes was highly variable across tissues, with a markedly reduced number of LPS responsive mRNAs evident for intact brain tissue (Figure 7A). Analysis of the EC-specific response, however, showed similar numbers of genes affected by LPS treatment across all tissues, including brain (Figure 7B). These data suggest a dramatic reduction in the effect of LPS on brain parenchymal cells compared to other tissues, consistent with a high degree of protection provided by the blood-brain barrier (60). In addition, this also illustrates a limitation of RNASeq of whole tissues, where cell type-specific responses can be masked by changes in more abundant cellular subsets. Interestingly, whereas most vascular bed-specific EC translatomes exhibited considerably more downregulated than upregulated transcripts in response to LPS, the opposite pattern was observed for brain ECs (Figure 7B, Supplemental Figure S4B-C).

Consistent with previous reports (61-63), EC-enriched genes upregulated by LPS include several adhesion molecules required for leukocyte recruitment and migration, while genes involved in maintenance of the EC barrier were downregulated. Furthermore, a shift toward a procoagulant state was observed, with reduced expression of anticoagulant and profibrinolytic genes (Supplemental Table S4). Within this limited set of genes, expression of the protein C receptor (*Procr*) provides an example of vascular bed-specific variation in EC reactivity in response to LPS, with significant downregulation of *Procr* in brain, kidney and heart, while expression in liver and lung was increased. These data could explain the organ-specific susceptibility to increased vascular leakage after LPS challenge previously reported for mice with reduced *Procr* expression (64).

Conclusion

The interspersed anatomic distribution of ECs and marked dependence of their gene expression programs on microenvironmental cues have constituted major challenges to the study of EC

bioRxiv preprint doi: https://doi.org/10.1101/708701; this version posted July 19, 2019. The copyright holder for this preprint (which was not certified by peer review) is the author/funder, who has granted bioRxiv a license to display the preprint in perpetuity. It is made available under aCC-BY-ND 4.0 International license.

function and responses to (patho)physiological stimuli *in vivo*. The EC-TRAP strategy described here provides a powerful tool for the analysis of the EC translatome across multiple vascular beds and in response to pathologic challenges in the whole animal. Our findings demonstrate that this method offers an accurate *in vivo* snapshot of tissue-specific EC expression profiles, resulting in better cellular resolution than whole tissue RNASeq, while maintaining a high degree of sensitivity to detect low abundant transcripts. In addition, these data provide a database of tissue-specific EC gene expression that should be a useful reference for other studies, including the identification of tissue-specific targets for drug delivery. Future refinement of EC-TRAP taking advantage of intersectional genetic approaches based on combined expression of 2 or more EC markers (65) may lead to greater resolution of EC subsets within a tissue, particularly in combination with single cell RNAseq methods. Finally, future applications of this approach should significantly advance our understanding of EC function *in vivo* under both physiologic and pathophysiologic conditions, potentially leading to the identification of new disease-specific biomarkers as well as potential novel therapeutic targets.

Material and Methods

All animal experiments were approved by the Institutional Animal Care and Use Committee of the University of Michigan. Detailed descriptions of the mice and procedures used in these studies, including sample preparations for TRAP and high-throughput RNA sequencing, data analysis and follow-up validation by single-molecule fluorescent *in situ* hybridization assays, are provided in the Supporting Information Materials and Methods.

Data availability

All RNASeq data supporting these studies will be made available through the Gene Expression Omnibus.

Acknowledgements

bioRxiv preprint doi: https://doi.org/10.1101/708701; this version posted July 19, 2019. The copyright holder for this preprint (which was not certified by peer review) is the author/funder, who has granted bioRxiv a license to display the preprint in perpetuity. It is made available under aCC-BY-ND 4.0 International license.

We would like to thank Lauren Janes, Kate Spokes and Peter Zwiers for their expert technical assistance with the *in vitro* experiments, and Eliane Popa for the helpful discussions. This research was supported by grants from the National Institutes of Health (R35HL135793 to D.G. and R01HL122684 to S.G.), and the American Heart Association (16POST27770093 to A.C.). D.G. is an investigator of the Howard Hughes Medical Institute.

bioRxiv preprint doi: https://doi.org/10.1101/708701; this version posted July 19, 2019. The copyright holder for this preprint (which was not certified by peer review) is the author/funder, who has granted bioRxiv a license to display the preprint in perpetuity. It is made available under aCC-BY-ND 4.0 International license.

References

1. Aird WC (2007) Phenotypic heterogeneity of the endothelium: II. Representative vascular beds. *Circulation research* 100(2):174-190.
2. Potente M & Makinen T (2017) Vascular heterogeneity and specialization in development and disease. *Nature reviews. Molecular cell biology* 18(8):477-494.
3. Ribatti D, Nico B, Vacca A, Roncali L, & Dammacco F (2002) Endothelial cell heterogeneity and organ specificity. *Journal of hematotherapy & stem cell research* 11(1):81-90.
4. Atkins GB, Jain MK, & Hamik A (2011) Endothelial differentiation: molecular mechanisms of specification and heterogeneity. *Arteriosclerosis, thrombosis, and vascular biology* 31(7):1476-1484.
5. McCarron JG*, et al.* (2019) Heterogeneity and emergent behaviour in the vascular endothelium. *Current opinion in pharmacology* 45:23-32.
6. Aird WC*, et al.* (1997) Vascular bed-specific expression of an endothelial cell gene is programmed by the tissue microenvironment. *The Journal of cell biology* 138(5):1117-1124.
7. Pusztaszeri MP, Seelentag W, & Bosman FT (2006) Immunohistochemical expression of endothelial markers CD31, CD34, von Willebrand factor, and Fli-1 in normal human tissues. *The journal of histochemistry and cytochemistry : official journal of the Histochemistry Society* 54(4):385-395.
8. Aman J, Weijers EM, van Nieuw Amerongen GP, Malik AB, & van Hinsbergh VW (2016) Using cultured endothelial cells to study endothelial barrier dysfunction: Challenges and opportunities. *American journal of physiology. Lung cellular and molecular physiology* 311(2):L453-466.
9. Helms HC*, et al.* (2016) In vitro models of the blood-brain barrier: An overview of commonly used brain endothelial cell culture models and guidelines for their use. *Journal of cerebral blood flow and metabolism : official journal of the International Society of Cerebral Blood Flow and Metabolism* 36(5):862-890.
10. Meyer J, Gonelle-Gispert C, Morel P, & Buhler L (2016) Methods for Isolation and Purification of Murine Liver Sinusoidal Endothelial Cells: A Systematic Review. *PloS one* 11(3):e0151945.
11. Amatschek S*, et al.* (2007) Blood and lymphatic endothelial cell-specific differentiation programs are stringently controlled by the tissue environment. *Blood* 109(11):4777-4785.

bioRxiv preprint doi: https://doi.org/10.1101/708701; this version posted July 19, 2019. The copyright holder for this preprint (which was not certified by peer review) is the author/funder, who has granted bioRxiv a license to display the preprint in perpetuity. It is made available under aCC-BY-ND 4.0 International license.

12. Durr E*, et al.* (2004) Direct proteomic mapping of the lung microvascular endothelial cell surface in vivo and in cell culture. *Nature biotechnology* 22(8):985-992.
13. Lacorre DA*, et al.* (2004) Plasticity of endothelial cells: rapid dedifferentiation of freshly isolated high endothelial venule endothelial cells outside the lymphoid tissue microenvironment. *Blood* 103(11):4164-4172.
14. Calabria AR & Shusta EV (2008) A genomic comparison of in vivo and in vitro brain microvascular endothelial cells. *Journal of cerebral blood flow and metabolism : official journal of the International Society of Cerebral Blood Flow and Metabolism* 28(1):135-148.
15. Pasqualini R & Ruoslahti E (1996) Organ targeting in vivo using phage display peptide libraries. *Nature* 380(6572):364-366.
16. Rajotte D*, et al.* (1998) Molecular heterogeneity of the vascular endothelium revealed by in vivo phage display. *The Journal of clinical investigation* 102(2):430-437.
17. Simonson AB & Schnitzer JE (2007) Vascular proteomic mapping in vivo. *Journal of thrombosis and haemostasis : JTH* 5 Suppl 1:183-187.
18. Tang FHF*, et al.* (2019) A ligand motif enables differential vascular targeting of endothelial junctions between brain and retina. *Proceedings of the National Academy of Sciences of the United States of America* 116(6):2300-2305.
19. Brunskill EW & Potter SS (2010) Gene expression programs of mouse endothelial cells in kidney development and disease. *PloS one* 5(8):e12034.
20. Daneman R*, et al.* (2010) The mouse blood-brain barrier transcriptome: a new resource for understanding the development and function of brain endothelial cells. *The Journal of neuroscience : the official journal of the Society for Neuroscience* 5(10):e13741.
21. Zhang Y*, et al.* (2014) An RNA-sequencing transcriptome and splicing database of glia, neurons, and vascular cells of the cerebral cortex. 34(36):11929-11947.
22. Schlereth K, Weichenhan D, & Bauer T (2018) The transcriptomic and epigenetic map of vascular quiescence in the continuous lung endothelium. *Science (New York, N.Y.)* 7.
23. Sabbagh MF*, et al.* (2018) Transcriptional and epigenomic landscapes of CNS and non-CNS vascular endothelial cells. *eLife* 7.
24. Nolan DJ*, et al.* (2013) Molecular signatures of tissue-specific microvascular endothelial cell heterogeneity in organ maintenance and regeneration. *Developmental cell* 26(2):204-219.

bioRxiv preprint doi: https://doi.org/10.1101/708701; this version posted July 19, 2019. The copyright holder for this preprint (which was not certified by peer review) is the author/funder, who has granted bioRxiv a license to display the preprint in perpetuity. It is made available under aCC-BY-ND 4.0 International license.

25. Han X*, et al.* (2018) Mapping the Mouse Cell Atlas by Microwell-Seq. *Cell* 172(5):1091-1107.e1017.
26. Lother A*, et al.* (2018) Cardiac Endothelial Cell Transcriptome. *Arteriosclerosis, thrombosis, and vascular biology* 38(3):566-574.
27. Vanlandewijck M*, et al.* (2018) A molecular atlas of cell types and zonation in the brain vasculature. *Nature* 554(7693):475-480.
28. He L & Vanlandewijck M (2018) Single-cell RNA sequencing of mouse brain and lung vascular and vessel-associated cell types. 5:180160.
29. Anonymous (2018) Single-cell transcriptomics of 20 mouse organs creates a Tabula Muris. *Nature* 562(7727):367-372.
30. Karaiskos N*, et al.* (2018) A Single-Cell Transcriptome Atlas of the Mouse Glomerulus. *Journal of the American Society of Nephrology : JASN* 29(8):2060-2068.
31. Heiman M*, et al.* (2008) A translational profiling approach for the molecular characterization of CNS cell types. *Cell* 135(4):738-748.
32. Hupe M, Li MX, Gertow Gillner K, Adams RH, & Stenman JM (2014) Evaluation of TRAP-sequencing technology with a versatile conditional mouse model. *Science signaling* 42(2):e14.
33. Liu J*, et al.* (2014) Cell-specific translational profiling in acute kidney injury. *The Journal of clinical investigation* 124(3):1242-1254.
34. Santhosh D & Huang Z (2016) A Tie2-driven BAC-TRAP transgenic line for in vivo endothelial gene profiling. *Genesis (New York, N.Y. : 2000)* 54(3):136-145.
35. Sanz E*, et al.* (2009) Cell-type-specific isolation of ribosome-associated mRNA from complex tissues. *Proceedings of the National Academy of Sciences of the United States of America* 106(33):13939-13944.
36. Zhou P*, et al.* (2013) Interrogating translational efficiency and lineage-specific transcriptomes using ribosome affinity purification. *Proceedings of the National Academy of Sciences of the United States of America* 110(38):15395-15400.
37. King HA & Gerber AP (2016) Translatome profiling: methods for genome-scale analysis of mRNA translation. *Briefings in functional genomics* 15(1):22-31.
38. Everett LA, Cleuren AC, Khoriaty RN, & Ginsburg D (2014) Murine coagulation factor VIII is synthesized in endothelial cells. *Blood* 123(24):3697-3705.

bioRxiv preprint doi: https://doi.org/10.1101/708701; this version posted July 19, 2019. The copyright holder for this preprint (which was not certified by peer review) is the author/funder, who has granted bioRxiv a license to display the preprint in perpetuity. It is made available under aCC-BY-ND 4.0 International license.

39. Fahs SA, Hille MT, Shi Q, Weiler H, & Montgomery RR (2014) A conditional knockout mouse model reveals endothelial cells as the principal and possibly exclusive source of plasma factor VIII. *Blood* 123(24):3706-3713.

40. de Lange WJ, Halabi CM, Beyer AM, & Sigmund CD (2008) Germ line activation of the Tie2 and SMMHC promoters causes noncell-specific deletion of floxed alleles. *Physiological genomics* 35(1):1-4.

41. Koni PA*, et al.* (2001) Conditional vascular cell adhesion molecule 1 deletion in mice: impaired lymphocyte migration to bone marrow. *The Journal of experimental medicine* 193(6):741-754.

42. Muzumdar MD, Tasic B, Miyamichi K, Li L, & Luo L (2007) A global double-fluorescent Cre reporter mouse. *Genesis (New York, N.Y. : 2000)* 45(9):593-605.

43. Hsieh PC, Davis ME, Lisowski LK, & Lee RT (2006) Endothelial-cardiomyocyte interactions in cardiac development and repair. *Annual review of physiology* 68:51-66.

44. Ingolia NT, Lareau LF, & Weissman JS (2011) Ribosome profiling of mouse embryonic stem cells reveals the complexity and dynamics of mammalian proteomes. *Cell* 147(4):789-802.

45. Tang Y, Harrington A, Yang X, Friesel RE, & Liaw L (2010) The contribution of the Tie2+ lineage to primitive and definitive hematopoietic cells. *Genesis (New York, N.Y. : 2000)* 48(9):563-567.

46. Lechauve C*, et al.* (2018) Endothelial cell alpha-globin and its molecular chaperone alpha-hemoglobin-stabilizing protein regulate arteriolar contractility. *The Journal of clinical investigation* 128(11):5073-5082.

47. Straub AC*, et al.* (2012) Endothelial cell expression of haemoglobin alpha regulates nitric oxide signalling. *Nature* 491(7424):473-477.

48. Rowley JW*, et al.* (2011) Genome-wide RNA-seq analysis of human and mouse platelet transcriptomes. *Blood* 118(14):e101-111.

49. Aitsebaomo J, Portbury AL, Schisler JC, & Patterson C (2008) Brothers and sisters: molecular insights into arterial-venous heterogeneity. *Circulation research* 103(9):929-939.

50. Podgrabinska S*, et al.* (2002) Molecular characterization of lymphatic endothelial cells. *Proceedings of the National Academy of Sciences of the United States of America* 99(25):16069-16074.

bioRxiv preprint doi: https://doi.org/10.1101/708701; this version posted July 19, 2019. The copyright holder for this preprint (which was not certified by peer review) is the author/funder, who has granted bioRxiv a license to display the preprint in perpetuity. It is made available under aCC-BY-ND 4.0 International license.

51. Bhasin M*, et al.* (2010) Bioinformatic identification and characterization of human endothelial cell-restricted genes. *BMC genomics* 11:342.
52. Wallgard E*, et al.* (2008) Identification of a core set of 58 gene transcripts with broad and specific expression in the microvasculature. *Arteriosclerosis, thrombosis, and vascular biology* 28(8):1469-1476.
53. Butler LM*, et al.* (2016) Analysis of Body-wide Unfractionated Tissue Data to Identify a Core Human Endothelial Transcriptome. *Cell systems* 3(3):287-301.e283.
54. Rosenberg AB & Roco CM (2018) Single-cell profiling of the developing mouse brain and spinal cord with split-pool barcoding. 360(6385):176-182.
55. Adam M, Potter AS, & Potter SS (2017) Psychrophilic proteases dramatically reduce single-cell RNA-seq artifacts: a molecular atlas of kidney development. 144(19):3625-3632.
56. Kang SS, Baker KE, Wang X, Kocher J-P, & Fryer JD (2017) Translational profiling of microglia reveals artifacts of cell sorting. *bioRxiv*.
57. van den Brink SC, Sage F, & Vertesy A (2017) Single-cell sequencing reveals dissociation-induced gene expression in tissue subpopulations. 14(10):935-936.
58. Hicks SC, Townes FW, Teng M, & Irizarry RA (2018) Missing data and technical variability in single-cell RNA-sequencing experiments. *Biostatistics (Oxford, England)* 19(4):562-578.
59. Cuevas-Diaz Duran R, Wei H, & Wu JQ (2017) Single-cell RNA-sequencing of the brain. *Clinical and translational medicine* 6(1):20.
60. Banks WA & Robinson SM (2010) Minimal penetration of lipopolysaccharide across the murine blood-brain barrier. *Brain, behavior, and immunity* 24(1):102-109.
61. Aird WC (2003) The role of the endothelium in severe sepsis and multiple organ dysfunction syndrome. *Blood* 101(10):3765-3777.
62. Ince C*, et al.* (2016) THE ENDOTHELIUM IN SEPSIS. *Shock (Augusta, Ga.)* 45(3):259-270.
63. Komarova YA, Kruse K, Mehta D, & Malik AB (2017) Protein Interactions at Endothelial Junctions and Signaling Mechanisms Regulating Endothelial Permeability. *Circulation research* 120(1):179-206.
64. von Drygalski A, Furlan-Freguia C, Ruf W, Griffin JH, & Mosnier LO (2013) Organ-specific protection against lipopolysaccharide-induced vascular leak is dependent on the endothelial protein C receptor. *Arteriosclerosis, thrombosis, and vascular biology* 33(4):769-776.

bioRxiv preprint doi: https://doi.org/10.1101/708701; this version posted July 19, 2019. The copyright holder for this preprint (which was not certified by peer review) is the author/funder, who has granted bioRxiv a license to display the preprint in perpetuity. It is made available under aCC-BY-ND 4.0 International license.

65. Pu W*, et al.* (2018) Genetic Targeting of Organ-Specific Blood Vessels. *Circulation research* 123(1):86-99.

bioRxiv preprint doi: https://doi.org/10.1101/708701; this version posted July 19, 2019. The copyright holder for this preprint (which was not certified by peer review) is the author/funder, who has granted bioRxiv a license to display the preprint in perpetuity. It is made available under aCC-BY-ND 4.0 International license.

Figure legends

Figure 1: *In vitro* expansion of primary ECs leads to changes in expression profiles.

Principal component analysis of expression profiles obtained from heart and kidney EC samples immediately after isolation (day 0) identified 4783 differentially expressed genes (FDR<10%) between tissue origins. *In vitro* expansion for 3 days resulted in significant shifts in expression programs, with the number of differentially expressed genes being reduced to 2397 between heart versus kidney ECs, indicating phenotypic drift occurring in the absence of a native microenvironment; n=3 biologic replicates per condition.

Figure 2: I*n vivo* targeting of *Tek*-positive cells to determine tissue-specific EC content.

(A-D) Histologic analysis of *Rosa*$^{mT/mG}$*,Tek-Cre*$^{+/0}$ brain (A), heart (B), kidney (C) and liver (D); *Tek*-positive cells are identified by the expression of membrane-bound green fluorescent protein, while *Tek*-negative cells express membrane-bound Tomato red fluorescent protein; scale bar = 25 µm. (E) Percentage of *Tek*-positive cells, as a proxy for EC content in each tissue, as determined by high-throughput DNA sequencing of *Rpl22* isoforms in tissues from *Rpl22*$^{fl/fl}$*, Tek-Cre*$^{+/0}$ animals; n=5 biologic replicates (mean ± SD).

Figure 3: Evaluation of transcriptome versus translatome data after (EC) TRAP.

(A) Mice expressing HA-tagged *Rpl22* in all cells show only minor differences between tissue-specific transcriptomes and translatomes from brain, heart, kidney, liver and lung by genome-wide principal component analysis. (B) EC translatomes obtained after TRAP are highly distinct from the unselected tissue transcriptomes, with the exception of lung. n=3 biologic replicates per tissue.

Figure 4: Identification of enriched transcripts after EC-TRAP.

bioRxiv preprint doi: https://doi.org/10.1101/708701; this version posted July 19, 2019. The copyright holder for this preprint (which was not certified by peer review) is the author/funder, who has granted bioRxiv a license to display the preprint in perpetuity. It is made available under aCC-BY-ND 4.0 International license.

(A) Of the putative EC-enriched genes in each tissue (FDR<10%), GO analysis of the 500 top-ranked genes with the highest enrichment scores shows overrepresentation of transcripts involved in vascular-related processes. (B) Unsupervised hierarchical clustering of EC-enriched genes (log_2 fold change >2 in at least 1 tissue) shows distinct, highly heterogeneous vascular bed-specific EC expression patterns. (C) Comparison of the top 500 most enriched genes per tissue identifies a group of pan-endothelial and subsets of tissue-specific EC-enriched genes. Data based on n=3 biologic replicates per tissue.

Figure 5: Single-molecule *in situ* hybridization validates EC-enriched transcripts identified by TRAP.

(A-B) Colocalization of *Bvht* and *Eva1b*, both identified as pan-EC markers by EC-TRAP, with *Tek* by *in situ* hybridization in kidney, brain and liver. (C-D) *3110099E03Rik* and *Wnt9b* were identified as kidney- and liver-specific EC markers, respectively and were only present in the corresponding tissues, where they also colocalized with *Tek,* confirming their EC origin. Dotted lines in the insets outline the cell nuclei as indicated by DAPI. Scale bars are 10 µm in overviews (left column in each panel), and 2.5 µm in insets (remaining columns).

Figure 6: Dissociation-induced changes in EC gene expression programs.

(A) PCA analysis of EC translatomes obtained from TRAP samples after cycloheximide perfusion and mechanical dissociation versus samples following enzymatic tissue dissociation without cycloheximide perfusion in brain, liver and kidney. (B) mRNA abundance presented as log_2(TPM) shows clustering of brain and liver EC translatomes by preparation method (black: mechanical, red: enzymatic) rather than by tissue type. Data from n=3 biologic replicates per tissue.

Figure 7: *In vivo* LPS-induced changes uncovered by EC-TRAP.

(A-B) Volcano plots indicate significantly affected genes by LPS treatment (red), either for tissue transcriptomes (A) or in the EC translatome identified by EC-TRAP (B). The horizontal dotted lines

bioRxiv preprint doi: https://doi.org/10.1101/708701; this version posted July 19, 2019. The copyright holder for this preprint (which was not certified by peer review) is the author/funder, who has granted bioRxiv a license to display the preprint in perpetuity. It is made available under aCC-BY-ND 4.0 International license.

mark an FDR cut-off <10%, with the vertical dotted lines denoting $\log_2$ fold changes of >1 or <-1. Data averaged from n=3 biologic replicates per tissue.

Figure 1

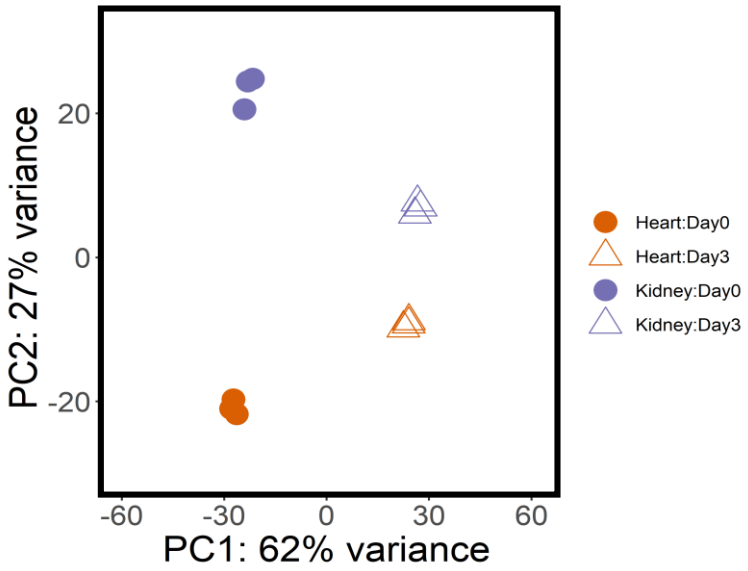
PC2: 27% variance
20
0
-20
-60
-30
0
30
60
PC1: 62% variance
Heart:Day0
Heart:Day3
Kidney:Day0
Kidney:Day3

Figure 2

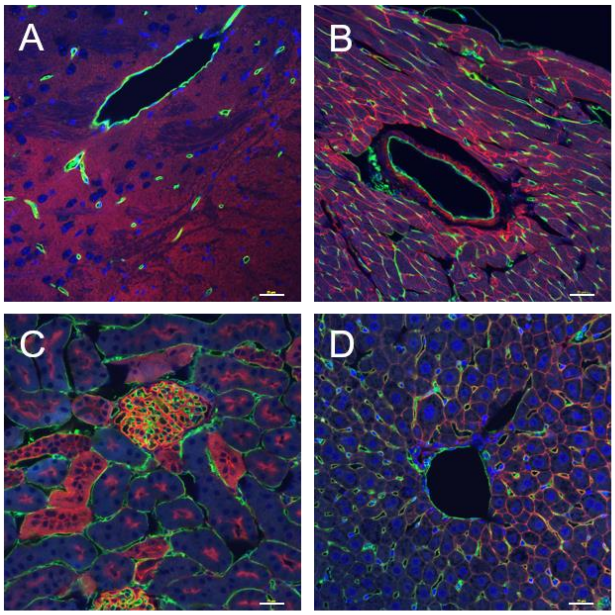
A
B
C
D

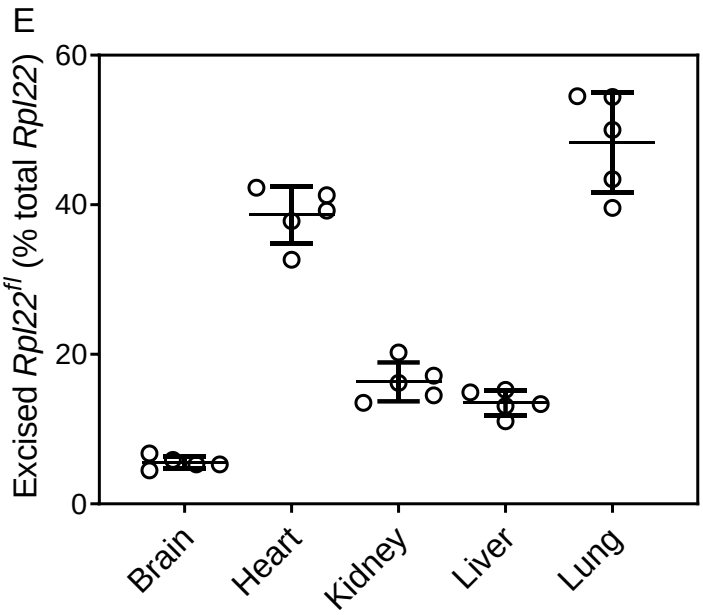
E
Excised Rpl22fl (% total Rpl22)
60
40
20
0
Brain
Heart
Kidney
Liver
Lung

Figure 3

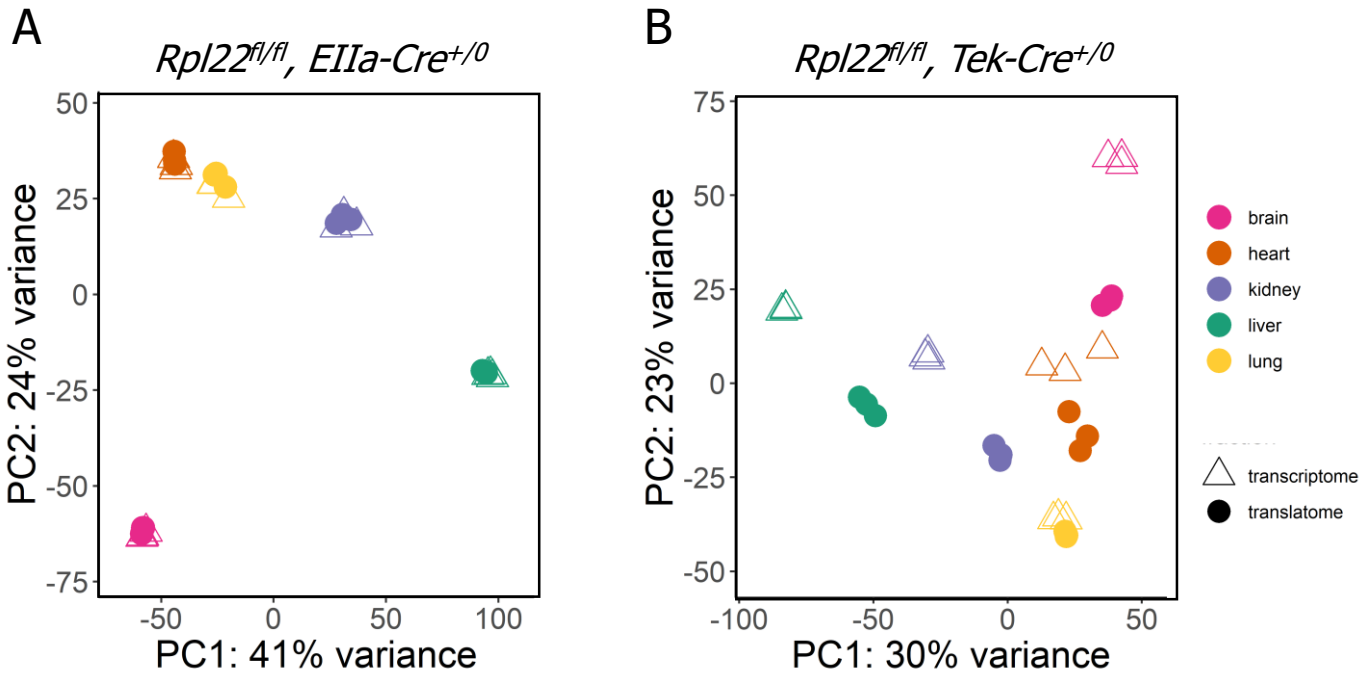
A
Rpl22fl/fl, EIIa-Cre+/0
PC2: 24% variance
PC1: 41% variance
50
25
0
-25
-50
-75
-50
0
50
100
B
Rpl22fl/fl, Tek-Cre+/0
PC2: 23% variance
PC1: 30% variance
75
50
25
0
-25
-50
-100
-50
0
50
brain
heart
kidney
liver
lung
transcriptome
translatome

Figure 4

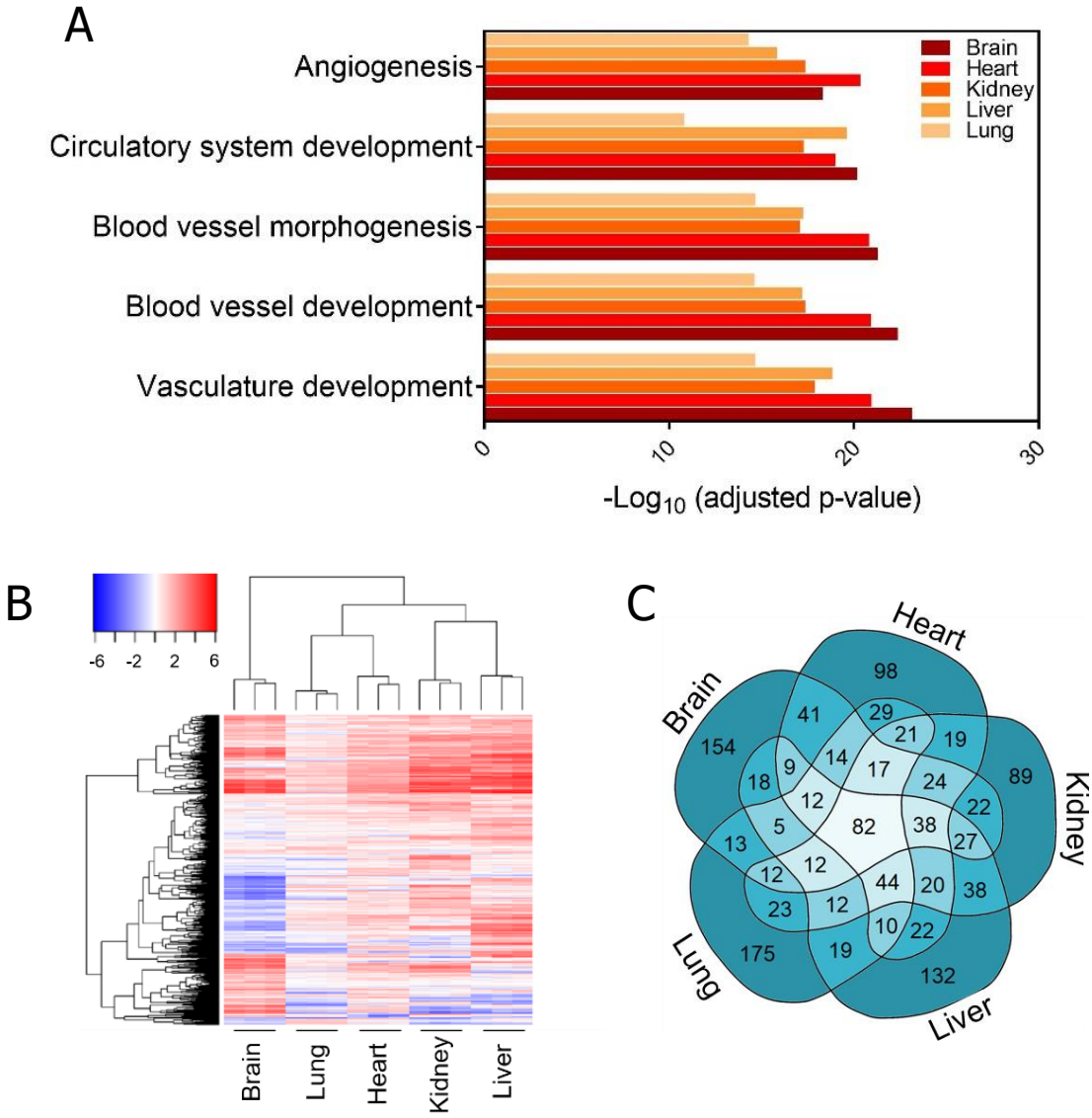
A
Angiogenesis
Circulatory system development
Blood vessel morphogenesis
Blood vessel development
Vasculature development
Brain
Heart
Kidney
Liver
Lung
0
10
20
30
-Log10 (adjusted p-value)
B
-6
-2
2
6
Brain
Lung
Heart
Kidney
Liver
C
Heart
Brain
Kidney
Lung
Liver
98
154
89
175
132
41
29
21
19
14
17
24
18
9
12
22
5
82
38
27
13
12
12
44
20
38
23
12
10
22
19

Figure 5

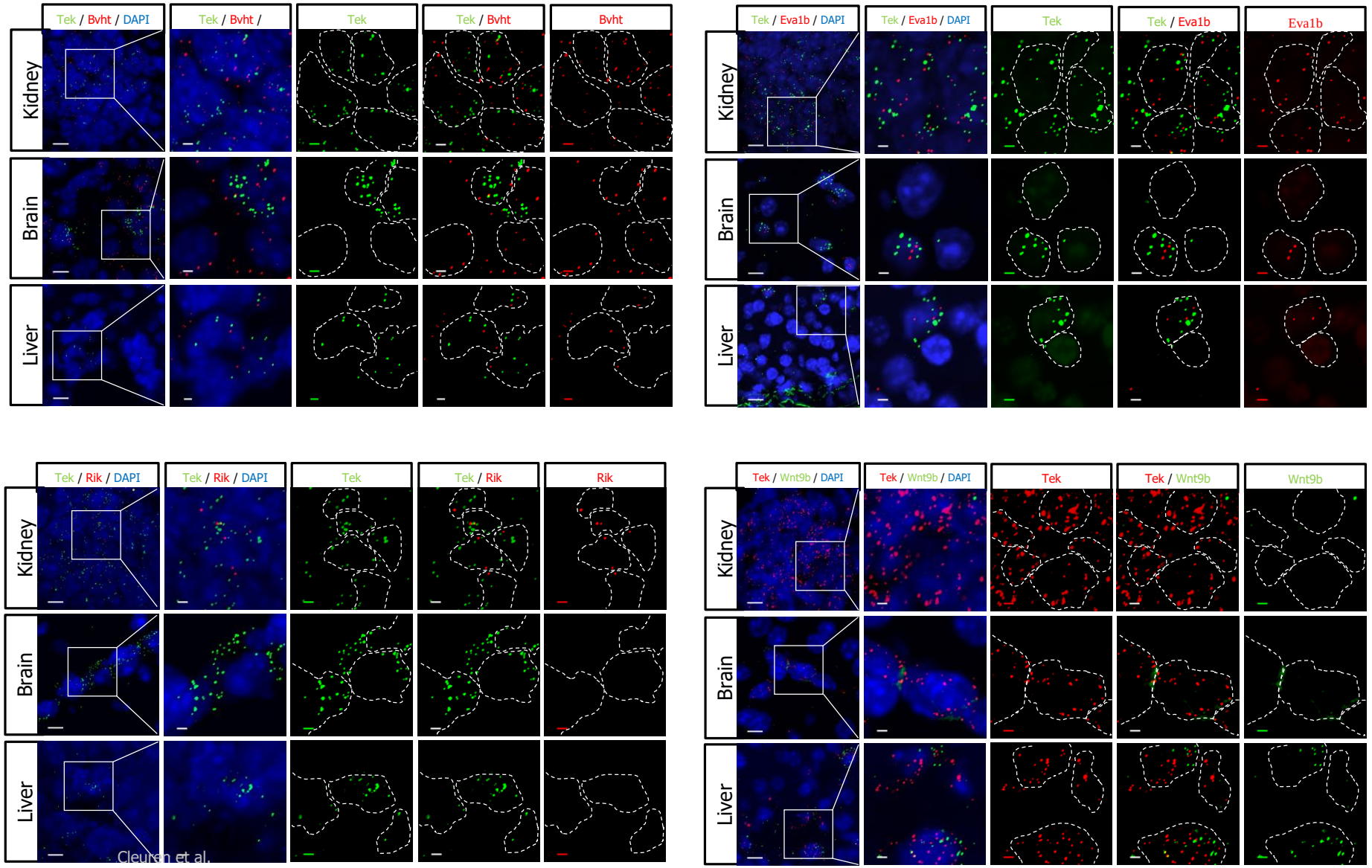
Tek / Bvht / DAPI
Tek / Bvht /
Tek
Tek / Bvht
Bvht
Tek / Eva1b / DAPI
Tek / Eva1b / DAPI
Tek
Tek / Eva1b
Eva1b
Tek / Rik / DAPI
Tek / Rik / DAPI
Tek
Tek / Rik
Rik
Tek / Wnt9b / DAPI
Tek / Wnt9b / DAPI
Tek
Tek / Wnt9b
Wnt9b
Kidney
Brain
Liver

Figure 6

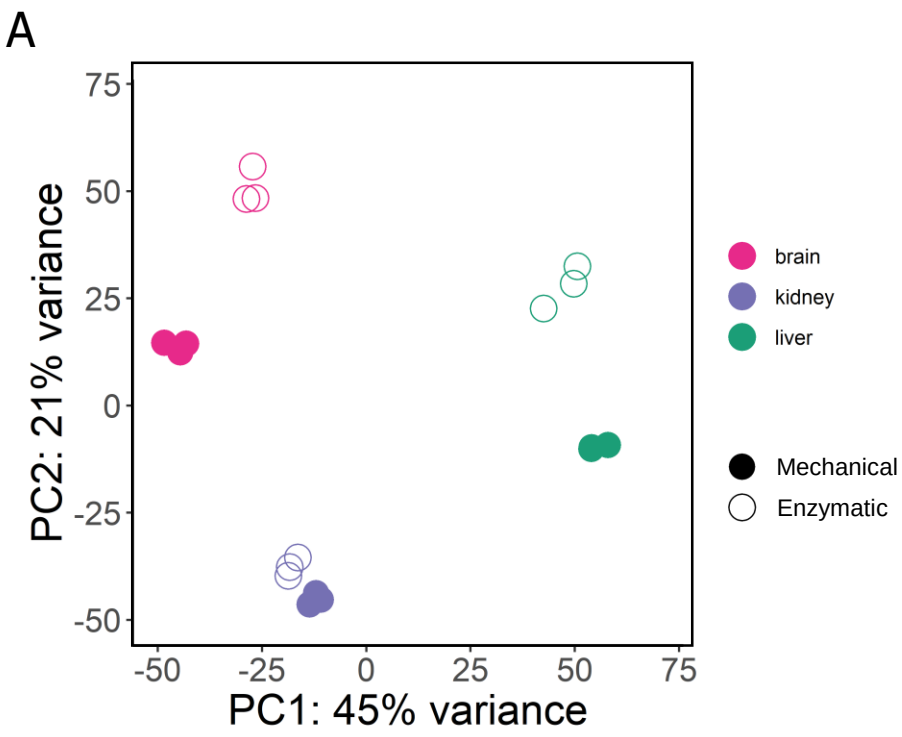
A
75
50
25
0
-25
-50
PC2: 21% variance
-50
-25
0
25
50
75
PC1: 45% variance
brain
kidney
liver
Mechanical
Enzymatic

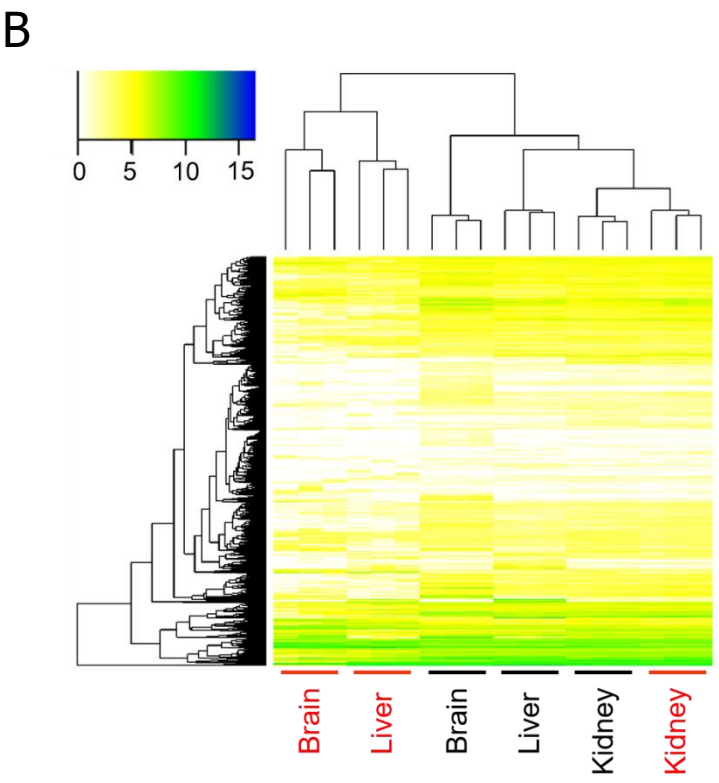
B
0
5
10
15
Brain
Liver
Brain
Liver
Kidney
Kidney

Figure 7

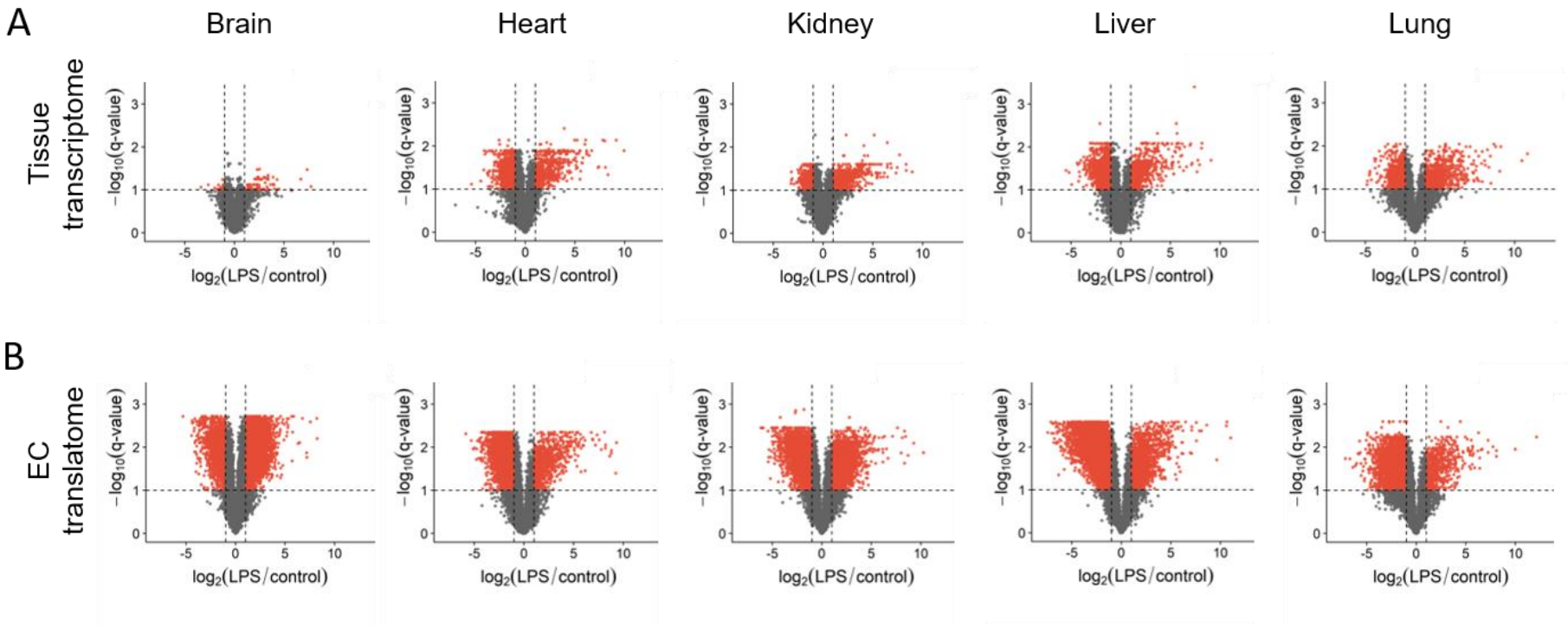
A
Brain
Heart
Kidney
Liver
Lung
Tissue transcriptome
B
EC translatome
$-\log_{10}$(q-value)
$\log_2$(LPS/control)

Table 1: 82 pan-endothelial genes present in all 5 tissues after EC-TRAP

bioRxiv preprint doi: https://doi.org/10.1101/708701; this version posted July 19, 2019. The copyright holder for this preprint (which was not certified by peer review) is the author/funder, who has granted bioRxiv a license to display the preprint in perpetuity. It is made available under aCC-BY-NC-ND 4.0 International license.

	Brain	Heart	Kidney	Liver	Lung
Adcy4	3.79	2.10	2.85	3.88	0.97
Apol10b	3.65	2.78	3.81	2.29	1.15
Arhgap19	3.03	1.66	1.81	3.44	1.00
Arhgef15	1.88	2.66	4.25	4.52	1.59
B3gnt3	3.33	2.68	3.38	4.14	1.14
B4galt4	2.27	2.00	2.65	3.85	1.55
Bcl2l1	1.79	2.19	1.94	2.14	1.26
C1qc	5.26	2.98	5.18	5.70	1.96
Caskin2	2.82	2.35	2.67	3.10	1.22
Ccl12	4.82	2.33	4.56	3.83	1.85
Ccl24	3.96	2.61	3.06	5.17	1.24
Ccl7	3.52	1.75	3.40	3.45	1.60
Ccl8	4.83	2.76	4.78	4.95	2.32
Ccm2l	2.99	1.64	3.32	2.71	0.79
Cd300lg	2.31	2.68	4.58	4.75	1.56
Cd34	3.40	2.01	4.58	3.81	1.16
Cdh5	3.87	2.65	3.93	4.14	1.02
Cldn5	4.46	2.79	3.18	5.02	1.78
Clec14a	4.23	2.56	4.32	4.75	1.34
Clec1a	2.45	2.24	3.92	3.99	1.47
Cyyr1	4.47	2.41	4.16	4.30	1.13
Dll4	3.25	2.52	3.87	3.67	1.22
Ecscr	4.75	2.69	4.91	5.05	1.60
Efcab4a	4.01	2.96	4.31	4.92	1.93
Egfl7	4.04	2.48	4.71	4.95	1.87
Eltd1	4.69	2.41	4.28	4.21	1.16
Emcn	4.56	2.71	4.61	4.59	1.41
Eng	4.74	2.77	4.15	4.66	1.31
Ephb4	3.43	2.28	2.82	3.12	1.14
Erg	3.23	2.40	4.06	3.67	1.47
Esm1	2.37	2.26	4.72	2.72	1.65
Etl4	1.87	1.84	2.08	3.30	0.83
Eva1b	2.18	2.06	3.21	3.99	1.07
Fcgr1	4.47	2.73	3.35	4.44	1.57
Fgd5	3.23	2.02	3.84	3.80	1.01
Flt1	4.69	2.32	3.82	3.73	1.14
Flt4	3.23	2.05	3.89	4.13	1.03
Folr2	4.53	2.91	4.25	5.42	1.48
Gja4	3.04	1.80	3.82	4.48	1.06
Gm13056	3.12	2.56	3.79	3.08	1.31
Gm14207	2.78	2.78	2.68	3.84	2.03
Gm20748	3.79	2.44	4.32	4.29	2.03
Gpr4	3.16	2.48	3.59	3.40	1.24
Gpx7	1.46	1.24	2.86	2.05	0.81
Grasp	1.48	1.58	2.89	2.51	1.18
Hspa12b	3.74	2.65	3.43	2.96	1.52
Kif26a	2.97	1.92	2.87	2.85	0.94
Kifc3	1.40	1.36	2.83	4.23	1.45
Kitl	2.03	2.27	3.84	3.76	1.06
Lbx2	2.43	2.06	2.52	3.49	1.82

bioRxiv preprint doi: https://doi.org/10.1101/708701; this version posted July 19, 2019. The copyright holder for this preprint (which was not certified by peer review) is the author/funder, who has granted bioRxiv a license to display the preprint in perpetuity. It is made available under aCC-BY-NC-ND 4.0 International license.

Ltc4s	4.06	2.52	2.10	5.59	1.96
Meox1	3.10	2.14	4.84	2.14	1.35
Mmrn2	4.45	2.54	4.32	4.62	1.11
Nos3	3.66	2.08	2.92	2.57	1.04
Pcdh12	1.52	2.07	2.92	3.54	1.13
Pdgfb	2.46	2.92	3.56	3.04	1.60
Pkn3	3.69	2.54	3.07	2.30	1.10
Plscr4	2.59	1.89	2.20	2.42	0.89
Podxl	4.46	2.86	3.23	3.60	1.25
Ramp2	3.97	2.84	4.37	5.12	2.13
Rasip1	1.50	1.96	4.04	4.35	1.49
Robo4	4.54	2.28	4.50	4.40	1.48
She	4.01	2.46	3.80	3.45	1.55
Slc9a3r2	3.85	3.04	4.75	4.23	1.67
Smad6	1.90	1.69	2.14	3.22	1.75
Sorbs3	2.74	2.51	3.15	3.16	1.02
Sox18	3.87	2.89	4.44	4.05	1.76
Sox7	3.61	2.68	3.62	3.04	1.18
Tek	4.59	2.14	4.44	4.30	1.23
Thsd1	3.88	2.59	3.35	2.16	1.26
Tinagl1	3.96	2.38	3.38	4.86	1.07
Tlr2	3.29	1.98	3.20	3.51	1.21
Tmem204	4.48	2.91	4.85	4.97	1.56
Trim47	4.33	2.59	1.75	4.09	1.09
Uaca	3.54	1.55	2.04	2.84	0.85
Ube2c	1.59	2.31	2.48	3.20	1.52
Ushbp1	4.52	2.81	4.75	4.87	1.51
Vegfc	2.82	2.22	2.47	2.28	1.03
Zmynd15	1.44	2.21	2.05	3.70	1.00
1810011O10Rik	2.42	2.17	3.60	2.49	1.07
2610203C22Rik	3.52	2.12	2.55	2.78	1.76
6030455H03Rik	3.09	2.25	2.46	3.81	1.80

The 82 genes listed here include all genes that are significantly enriched (FDR<10%) and present within the 500 top-ranked genes with the highest enrichment scores within all 5 tissues. The values in each column represent log2 fold changes (average of 3 biologic replicates).

bioRxiv preprint doi: https://doi.org/10.1101/708701; this version posted July 19, 2019. The copyright holder for this preprint (which was not certified by peer review) is the author/funder, who has granted bioRxiv a license to display the preprint in perpetuity. It is made available under aCC-BY-ND 4.0 International license.

Table 2: Tissue-specific, EC restricted transcripts identified by EC-TRAP

Brain	*Cldn13, Dyrk4, Edn3, Ermap, Fcnb, Foxl2, Foxq1, Gal3st4, Gm10384, Gm11378, Gm12708, Gm 13291, Gm15998, Gm24867, Gm694, Gm9946, Gm9999, Lao1, Magel2, Ndnf, Rad54b, Slc19a3, Slco1c1, Sox15, Tmem8c, Zic3, 1700009J07Rik, 6030468B19Rik*
Heart	*A2m, Gm13154, Gm16565, Gm17234, Itgbl1*
Kidney	*Calca, E130006D01Rik, Fam101a, Gata5, Krtdap, Lgr5, U90926, 3110099E03Rik*
Liver	*Adamdec1, Gm13994, Il13ra2, Serpina3i, Smc1b, Sprr2b, Tmem132e, Ush1g, Wnt9b, 6030498E09Rik*
Lung	*Aard, Abca14, Ankrd63, B3gnt7, Ear1, Fignl2, Glp1r, Gm26878, Gm6116, Gm830, Hic2, Krt79, Mkrn3, Nr6a1, Pnpla5, Prdm8, Prr18, Prss12, Rnase1, Rnase1, Rprml, Rufy4, Speer4f, Tekt3, Tepp, Trgj1, Trim29, 4930452B06Rik*

Transcripts that are significantly enriched (FDR<10%) and present within a specific vascular bed while no expression was observed in the transcriptomes of other tissues.

bioRxiv preprint doi: https://doi.org/10.1101/708701; this version posted July 19, 2019. The copyright holder for this preprint (which was not certified by peer review) is the author/funder, who has granted bioRxiv a license to display the preprint in perpetuity. It is made available under aCC-BY-ND 4.0 International license.

Supplementary Information for

The *in vivo* endothelial cell translatome is highly heterogeneous across vascular beds

Audrey C.A. Cleuren, Martijn A. van der Ent, Hui Jiang, Kristina L. Hunker, Andrew Yee, David R. Siemieniak, Grietje Molema, William C. Aird, Santhi K. Ganesh and David Ginsburg[§]

[§]Corresponding author email ginsburg@umich.edu

This PDF includes:

Supplementary Material and Methods

Figures S1 to S6

Tables S1 to S6

Supplementary references

bioRxiv preprint doi: https://doi.org/10.1101/708701; this version posted July 19, 2019. The copyright holder for this preprint (which was not certified by peer review) is the author/funder, who has granted bioRxiv a license to display the preprint in perpetuity. It is made available under aCC-BY-ND 4.0 International license.

Supplementary Material and Methods

Mice

All mice were housed under standard conditions according to the University of Michigan's Unit of Laboratory Animal Medicine guidelines. Mice were originally obtained from The Jackson Laboratory and bred to C57BL/6 for at least 5 generations, either by the donating institute or The Jackson Laboratory. Upon arrival, colonies were subsequently maintained on a C57BL/6J background, with experimental animals being backcrossed for at least 3 additional generations. Genotyping was performed on DNA isolated from tail clips using the PCR primers listed in Supplemental Table S5.

RiboTag mice (1) (*Rpl22*$^{fl/fl}$; stock 011029: B6N.129-*Rpl22*$^{tm1.1Psam}$/J) carrying a conditional hemagglutinin (HA)-epitope tagged ribosomal protein *Rpl22* gene were crossed to *Tek-Cre* recombinase transgenes (2, 3) (stock 004128: B6.Cg-Tg(Tek-cre)12Flv/J) to generate animals with HA-tagged polysomes in endothelial and hematopoietic cells, while other cell types are expected to express only the wildtype RPL22. However, *Tek-Cre* has previously also been described to target *loxP*-flanked sequences in germ cells (2). As this occurs at a lower frequency in males than in females, only *Tek-Cre*$^{+/0}$ males were used for matings, and the efficiency and specificity of the *Tek-Cre* recombinase was evaluated by breeding *Tek-Cre*$^{+/0}$ to *Rosa*$^{mT/mG}$ reporter mice (4) (stock 007676: B6.129(Cg)-*Gt(ROSA)26Sor*$^{tm4(ACTB-tdTomato,-EGFP)Luo}$/J).

Rpl22$^{fl/fl}$ mice were also bred to *Pf4-Cre* recombinase males (5) (stock 008535:C57BL/6-Tg(Pf4-icre)Q3Rsko/J) or *EIIa-Cre* transgenes (6) (stock 003724: B6.FVB-Tg(EIIa-cre)C5379Lmgd/J) to determine megakaryocyte/platelet specific transcripts, or to generate animals with ubiquitously expressed HA-tagged RPL22, respectively.

Blood and tissue collection

Ten-week-old *Rpl22*$^{fl/fl}$, *Tek-Cre*$^{+/0}$ males were anesthetized with 50 µg pentobarbital/g body weight and blood was drawn via cardiac puncture into a 9:1 sodium citrate solution (Sigma-Aldrich) containing cycloheximide (Sigma-Aldrich) to a final concentration of 100 µg/mL. Following the blood draw, intracardiac perfusion with 12 mL 100 µg/mL cycloheximide in phosphate

bioRxiv preprint doi: https://doi.org/10.1101/708701; this version posted July 19, 2019. The copyright holder for this preprint (which was not certified by peer review) is the author/funder, who has granted bioRxiv a license to display the preprint in perpetuity. It is made available under aCC-BY-ND 4.0 International license.

buffered saline (PBS) was performed to lock the ribosome onto the mRNA (7) and limit blood contamination of tissue samples. After perfusion, organs were harvested, snap frozen in liquid nitrogen and stored at -80°C until further processing. Blood samples were immediately processed and treated with ammonium-chloride-potassium (ACK) lysis buffer (Thermo Fisher Scientific) according to the manufacturer's protocol to remove red blood cells. The resulting cell pellet was resuspended in polysome buffer (50 mM Tris pH 7.5, 100 mM KCl, 12 mM $MgCl_2$, 1% Igepal CA-630 (Sigma-Aldrich), 1 mM dithiothreitol, 200 U/mL RNaseOUT (Invitrogen), 1 mg/mL heparin sodium salt (Sigma-Aldrich), 100 µg/mL cycloheximide and an EDTA-free protease inhibitor cocktail (Roche)) followed by immunoprecipitation.

To study the platelet transcriptome, blood samples from five 10 week old *Rpl22*$^{fl/fl}$, *Pf4-Cre*$^{+/0}$ males were pooled and centrifuged at 100 x g for 5 minutes to obtain platelet rich plasma and platelets were subsequently pelleted by centrifugation at 800 x g for 10 minutes and resuspended in polysome buffer.

Lipopolysaccharide treatment

For the LPS-induced endotoxemia model, *Rpl22*$^{fl/fl}$,*Tek-Cre*$^{+/0}$ mice were injected intraperitoneally with LPS (*E.Coli* 026:B6 from Sigma-Aldrich) at 1 µg/g body weight 4 hours before blood draw, cycloheximide perfusion and tissue collection.

Enzymatic tissue dissociation

To study the effects of enzymatic tissue dissociation on the EC expression program, tissues were collected after exsanguination by cardiac puncture and intracardiac perfusion with 12 mL PBS. Brain, kidney and liver samples were harvested and immediately minced and incubated with Collagenase A (25 mg/mL; Roche), Dispase II (25 mg/mL; Roche) and DNase I (250 µg/mL; Roche) at 37°C for 30 minutes (8). The subsequent cell suspension was filtered through a 70 µm cell strainer and cells were washed twice with ice-cold PBS before adding polysome buffer and being directly subjected to TRAP.

bioRxiv preprint doi: https://doi.org/10.1101/708701; this version posted July 19, 2019. The copyright holder for this preprint (which was not certified by peer review) is the author/funder, who has granted bioRxiv a license to display the preprint in perpetuity. It is made available under aCC-BY-ND 4.0 International license.

Bone marrow transplantation

Bone marrow was harvested from 8-week old *Rpl22*$^{fl/fl}$*,Tek-Cre*$^{+/0}$ or *Rpl22*$^{fl/fl}$*,Tek-Cre*$^{-}$ donors and 5-10 million donor cells were injected into recipient *Rpl22*$^{fl/fl}$*,Tek-Cre*$^{+/0}$ mice via the tail vein as previously described (9). Eight weeks after transplantation, mice were anesthetized and perfused with cycloheximide/PBS after which tissues were harvested, snap frozen in liquid nitrogen and stored at -80° until further processing.

Translating Ribosome Affinity Purification (TRAP) and RNA isolation

Frozen tissues (25-100 mg) were pulverized using a spring-loaded hammer and added to polysome buffer. Tissue homogenates were subsequently centrifuged to remove cellular debris and clear lysates were incubated with a purified mouse monoclonal antibody against the HA epitope tag (HA.11 clone 16B12, BioLegend; 3µg/400µl lysate) for 1 hour at 4°C after which magnetic protein G beads (New England BioLabs; 100µl/400µl lysate) equilibrated in polysome buffer were added for an additional 30 minute incubation. The magnetic beads were subsequently washed 3 times with high salt buffer (50 mM Tris (pH 7.5), 300 mM KCl, 12 mM $MgCl_2$, 1% Igepal CA-630, 1 mM dithiothreitol and 100 µg/mL cycloheximide). RLT buffer (RNeasy Mini Kit, Qiagen) supplemented with 2-mercapto-ethanol (1% vol/vol) was added to the beads and vigorously vortexed to dissociate the mRNA from the HA-tagged polysomes. Total RNA from tissue lysates and TRAP polysomal complexes was isolated using the Qiagen RNeasy Mini Kit, including an on-column DNase digestion step, and quantified with the Quant-iT RiboGreen RNA assay (Thermo Fisher Scientific).

cDNA conversion and RNASeq library preparation

RNA from total tissue lysates (5 ng) or TRAP-selected polysomes (10 ng) was converted into cDNA using the SMARTer Ultra Low Input kit, followed by amplification with the accompanying Advantage 2 PCR kit (Clontech) according to the manufacturer's protocol. The resulting cDNA was bead-purified (Agencourt AMPure XP beads, Beckman Coulter) and mechanically sheared to a 200-250 base pair range (Bioruptor, Diagenode). End repair with T4 DNA polymerase was followed by dA-tailing using Klenow 3' to 5' exonuclease (New England BioLabs) and adenosine

bioRxiv preprint doi: https://doi.org/10.1101/708701; this version posted July 19, 2019. The copyright holder for this preprint (which was not certified by peer review) is the author/funder, who has granted bioRxiv a license to display the preprint in perpetuity. It is made available under aCC-BY-ND 4.0 International license.

triphosphate to create a 3' adenosine overhang to promote adapter ligation (NEXTflex multiplex adapters, Bioo Scientific). After purification (MinElute Reaction Cleanup kit, Qiagen), samples were linearized by PCR before being size-selected in a range of 300-350 bp using Invitrogen's E-Gel system. Final enrichment of the adapter-modified cDNA fragments was performed by PCR using Phusion High-Fidelity DNA Polymerase (New England BioLabs). Quality of the final libraries was assessed on the Agilent BioAnalyzer and quantified using the Kapa Library quantification kit (Kapa Biosystems). Flow cells were prepared with 8 samples being multiplexed per lane and sequenced as 50 nucleotide reads on the Illumina HiSeq 2500.

RNASeq data analysis

Demultiplexed fastq files were aligned against the mouse Gencode reference (GRCm38.p2, Wellcome Trust Sanger Institute) (10) using Bowtie2 (11) and quantified with rSeq(12). Given their separate translational machinery (13), genes encoded by mitochondrial DNA are not associated with HA-tagged RPL22-containing polysomes, which was confirmed by reduced abundance of these genes after TRAP (Supplemental Figure S5). Thus, to avoid a biased inflation of the TRAP-selected transcripts, mitochondrial genes were excluded from analysis. Quantified sequencing reads were normalized to transcripts per million mapped reads (TPM) and transcripts with an average TPM >1 after TRAP were used for further analyses. Differential gene expression analysis to calculate enrichment scores ($\log_2$ fold changes) based on transcript abundance in the total tissue lysate and HA-selected fraction, or between experimental conditions, were performed in R (version 3.5.2) where *p*-values were calculated using a Welch's t-test and adjusted *p*-values were determined based on the Benjamini-Hochberg method, with a false discovery rate (FDR) <10% considered to be significant. Significant differentially expressed transcripts were subjected to gene ontology (GO) (14, 15) analyses using the online STRING (Search Tool for the Retrieval of Interacting Genes/Proteins) biological database version 11.0 (16).

Classification of gene enrichment categories and EC translatomes

Transcripts significantly depleted (enrichment score <0) after TRAP were classified as parenchymal genes, whereas transcripts significantly more abundant (enrichment score >0) were

bioRxiv preprint doi: https://doi.org/10.1101/708701; this version posted July 19, 2019. The copyright holder for this preprint (which was not certified by peer review) is the author/funder, who has granted bioRxiv a license to display the preprint in perpetuity. It is made available under aCC-BY-ND 4.0 International license.

labeled as *Tek*-enriched (Supplemental Figure 6A). However, *Tek* is also transiently expressed in hematopoietic cells, which may lead to the identification of false positives due to blood contamination of tissues. Therefore, *Tek*-enriched genes were additionally filtered based on data obtained from EC-TRAP on tissues collected from an *Rpl22*$^{fl/fl}$, *Tek-Cre*$^{+/0}$ recipient following bone marrow transplantation using a *Rpl22*$^{fl/fl}$, *Tek-Cre*$^{-}$ donor, as well as TRAP performed on peripheral blood samples from *Rpl22*$^{fl/fl}$, *Tek-Cre*$^{+/0}$ to identify genes that were enriched in the EC compartment only (Supplemental Figure 6A). Of note, this stringent filtering approach removes a number of established EC markers known to be expressed by megakaryocytes/platelets (17), which were also identified by TRAP on platelets from *Rpl22*$^{fl/fl}$, *Pf4Cre*$^{+/0}$ mice (Supplemental Table S6).

Translatome profiles of *Tek*$^{+}$ cells are defined as all mRNAs with an averaged TPM value >1 after TRAP, excluding significantly depleted parenchymal genes per tissue. Additional exclusion of genes primarily originating from hematopoietic cells identified by the bone marrow transplant data resulted in the identification of tissue-specific EC translatomes (Supplemental Figure S6b).

Primary EC isolation and microarray analysis

ECs from heart capillaries and kidney cortex peritubular capillaries were isolated as previously described (18). In summary, tissues from 4-6 C57BL/6 mice (2-4 weeks old) were pooled, minced and digested with type I collagenase at 37°C for 30 minutes, followed by separation through a 70 µm cell strainer. Cells were washed and incubated with rat anti-mouse CD31 antibody (BD Pharmingen) and CD31-positive cells were collected and either immediately processed for microarray analysis, or cultured in DMEM containing 15% fetal bovine serum and endothelial mitogen BT-203 (Biomedical Technologies) for 3 days before RNA isolation for microarray analysis using the Illumina MouseRef-8 Expression BeadChip. Quantile normalization was performed using the GeneSpring GX software (version 11.5.1; Agilent) and additional processing and differential expression analyses were performed using the R packages lumi (19) (version 2.34.0) and limma (20) (version 3.38.3). Adjusted *p*-values were determined based on the Benjamini-Hochberg method where an FDR <10% for differentially expressed genes was considered to be significant.

bioRxiv preprint doi: https://doi.org/10.1101/708701; this version posted July 19, 2019. The copyright holder for this preprint (which was not certified by peer review) is the author/funder, who has granted bioRxiv a license to display the preprint in perpetuity. It is made available under aCC-BY-ND 4.0 International license.

Tissue specific endothelial cell content

High throughput DNA sequencing of floxed and *Cre*-excised *Rpl22* isoforms was performed to determine the *Tek*-positive cell content within multiple tissues. *Rpl22*$^{fl/fl}$*,Tek-Cre*$^{+/0}$ males were perfused with PBS and tissues were harvested, followed by DNA isolation (DNeasy Blood and Tissue kit, Qiagen). Intron 3 of *Rpl22*, spanning either the LoxP site for the floxed allele or the combined LoxP/FRT site for the *Cre*-excised allele (1) was PCR amplified using the following primers: 5′-CACCTGTGCGGTCTTTCTCT-3′ and 5′ GCAAGCAAGCGTCTATCACA-3′ (Figure S7). After PCR purification (QIAquick PCR purification kit, Qiagen) libraries were prepared for multiplexed high throughput sequencing as above and sequenced on the Illumina MiSeq as 75 nucleotide paired-end reads. Raw reads were aligned to the genomic *Rpl22* isoforms and the fraction *Cre*-excised sequences of the total number of *Rpl22* reads, indicating the *Tek*-positive cell content, was used as a proxy for the fraction of ECs assuming excision occurred in both alleles per cell.

Histology

Rosa$^{mT/mG}$*,Tek-Cre*$^{+/0}$ mice were anesthetized and perfused with 4% paraformaldehyde in PBS. Tissues were isolated and post-fixed overnight at 4°C in 4% paraformaldehyde, followed by overnight cryoprotection in 30% sucrose (4°C) and embedded in optimal cutting temperature medium (OCT, Sakura). Ten micron cryosections were mounted with Prolong Gold antifade reagent including DAPI (4′,6-diamidino-2-phenylindole; Thermo Fischer Scientific) and imaged on a Nikon A1 Confocal microscope using the accompanying Elements Viewer software.

Single-molecule fluorescent in situ RNA hybridization

Mice were perfused with 12 ml PBS and tissues were immediately embedded in OCT compound. Twelve micron sections were mounted on SuperFrost Plus slides (Thermo Fisher) and dried overnight at -20°C. After fixing and dehydration, slides were subjected to the RNAscope technology (Advanced Cell Diagnostics) for multiplexed fluorescent *in situ* RNA hybridization, which allows visualization of single mRNA transcripts (21). Sections were treated with Protease IV for 30 minutes at room temperature followed by probe hybridization, followed by signal amplification and counterstaining according to the manufacturer's protocol. In order to determine

bioRxiv preprint doi: https://doi.org/10.1101/708701; this version posted July 19, 2019. The copyright holder for this preprint (which was not certified by peer review) is the author/funder, who has granted bioRxiv a license to display the preprint in perpetuity. It is made available under aCC-BY-ND 4.0 International license.

endothelial localization, probes were multiplexed with *Tek* (Mm-*Tek*-C1) in either channel 2 (Mm-*Eva1b*-C2, Mm-*3110099E03Rik*-C2 and Mm-*Wnt9b*-C2) or channel 3 (Mm-*Bvht*-C3). Slides were imaged on a Nikon A1 Confocal microscope and analyzed using the Elements Viewer software.

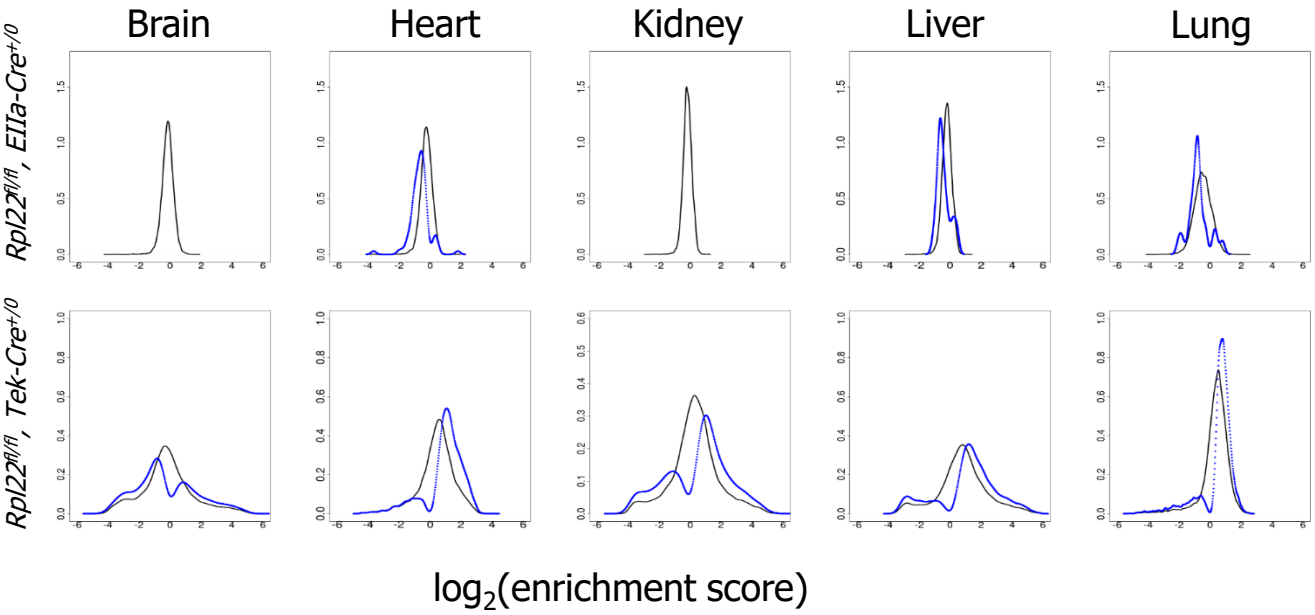

Supplemental Figure S1: Density plots of enrichment scores for TRAP performed on mice with HA-tagged RPL22 in all cells (*Rpl22$^{fl/fl}$, EIIa-Cre$^{+/0}$*; top panel) show an overall limited dynamic range in the distribution of enrichment scores in tissues (black lines), with few significant differences between the transcriptome and translatome (blue lines, enrichment scores with FDR<10%). EC-TRAP (*Rpl22$^{fl/fl}$, Tek-Cre$^{+/0}$*; bottom panel) identifies genes enriched in ECs (blue line, $\log_2$ fold change >0) as well as parenchymal genes ($\log_2$ fold change <0).

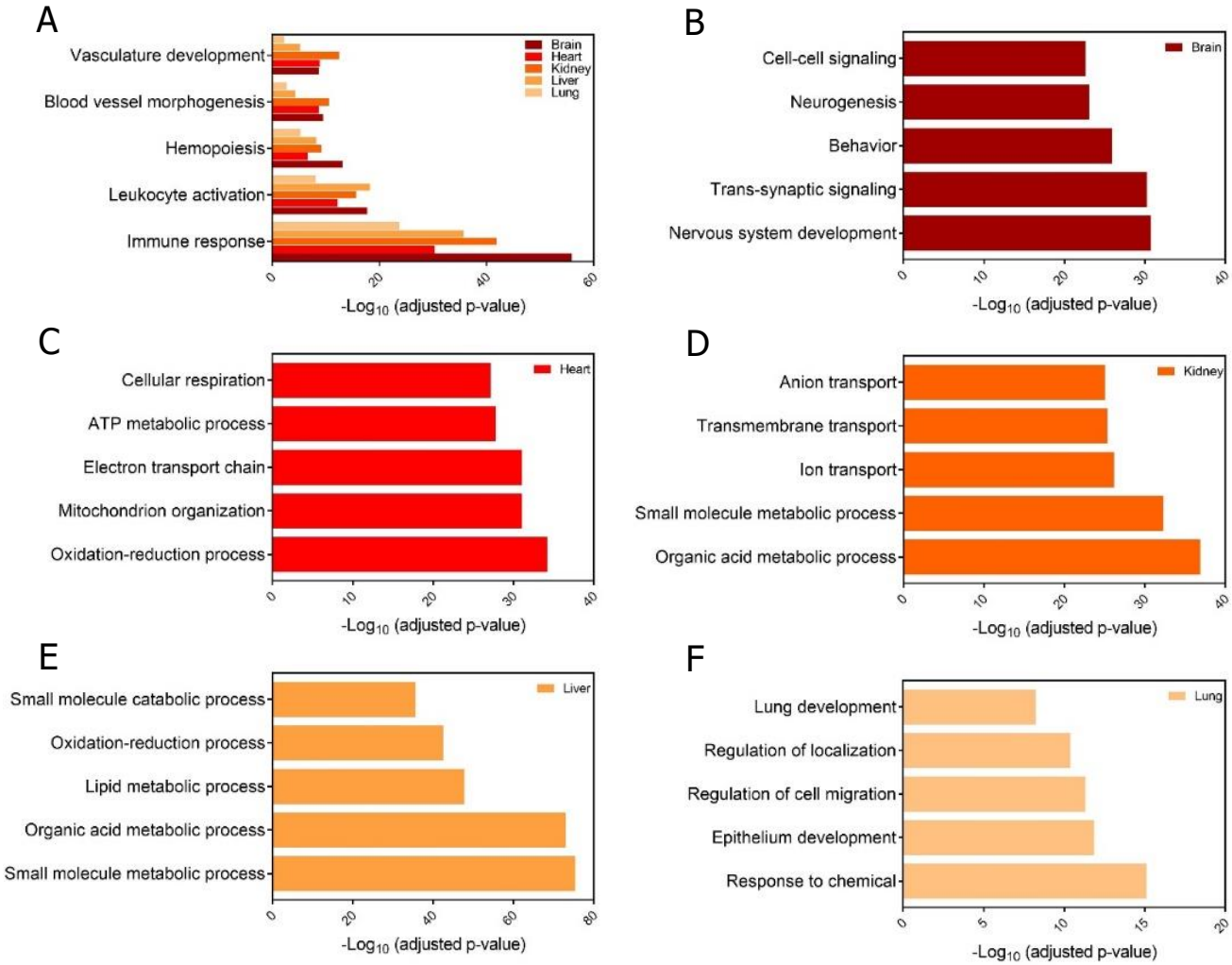

Supplemental Figure S2: Gene ontology analysis of significantly enriched and depleted genes after TRAP. (A) Top 500 enriched genes after TRAP (FDR<10%, ranked based on enrichment scores) were subjected to GO analysis which identified processes associated with vascular and hematopoietic cells, consistent with the known expression of *Tek*. (B-F) GO analysis on the top 500 most depleted transcripts per tissue identified processes expected to be associated with tissue-specific parenchymal cells, consistent with efficient removal of non-EC mRNAs by the TRAP procedure.

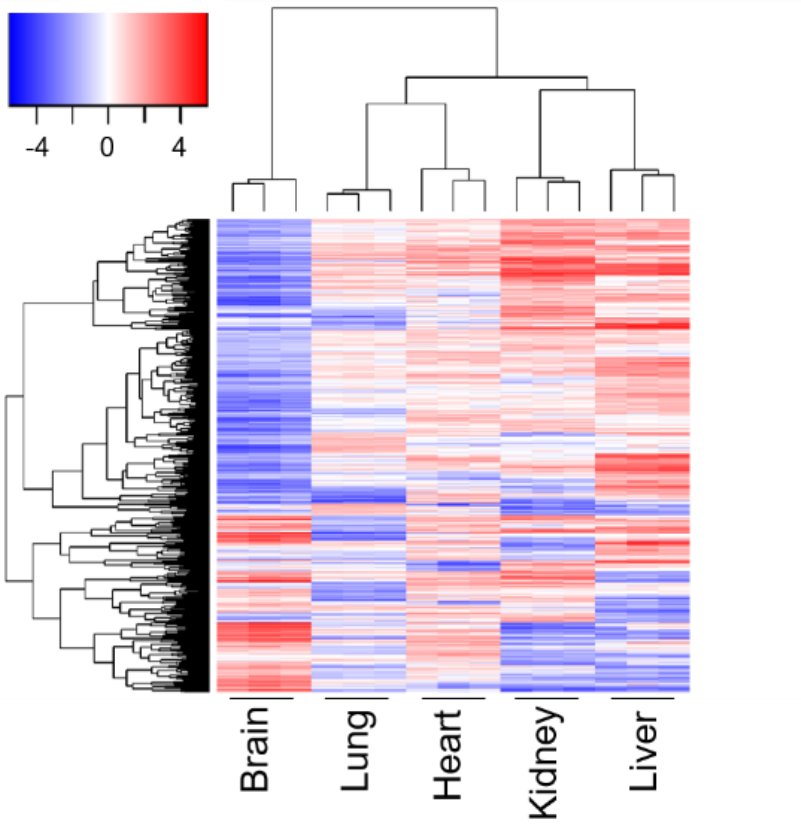

Supplemental Figure S3: Hierarchical clustering of transcripts identified as EC-enriched in at least 1 tissue (log_2 fold change >1), while primarily parenchymal-specific in at least 1 other tissue (log_2 fold change <1). See Supplemental Table S2 for the full gene list and accompanying enrichment scores.

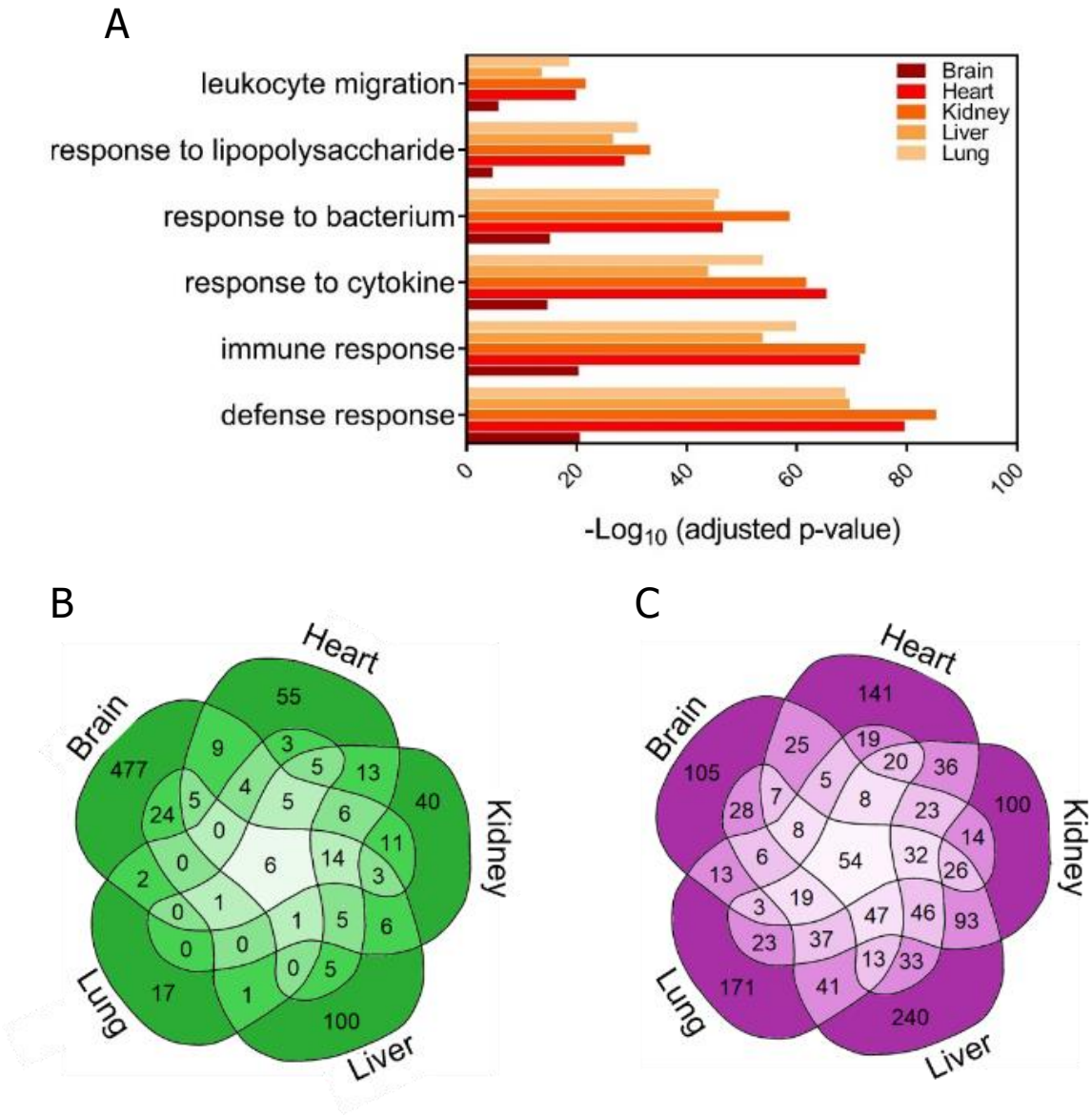

Supplemental Figure S4: Tissue-specific changes in expression profiles upon LPS exposure. (A) GO analysis of organ-wide transcriptomes following LPS exposure shows upregulation of genes involved in the defense response. (B-C) Venn diagram showing the overlap between EC-enriched genes significantly upregulated (log_2 fold change >1; C) versus downregulated (log_2 fold change <-1; D) across tissues after LPS exposure.

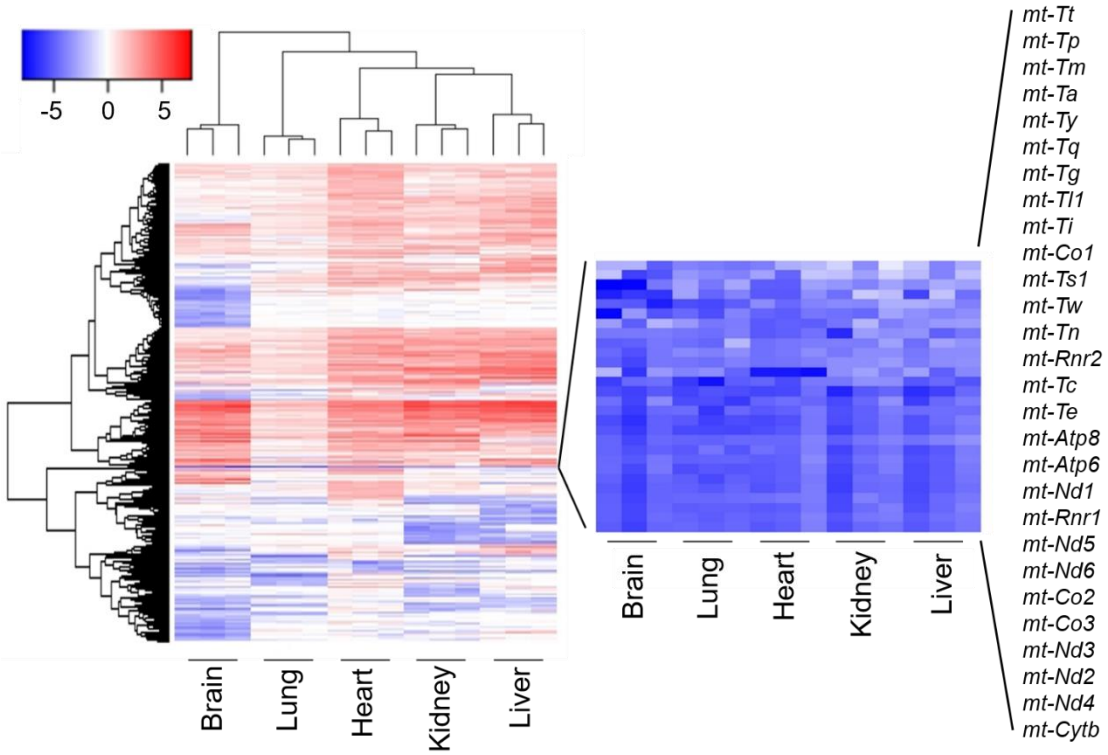

Figure S5: Unsupervised clustering of enrichment scores after EC-TRAP indicates a general and expected depletion of mitochondrial genes as these are not associated with RPL22-containing ribosomes. To avoid bias and inflation of enrichment scores, mitochondrial genes were therefore excluded before performing differential expression analysis after TRAP.

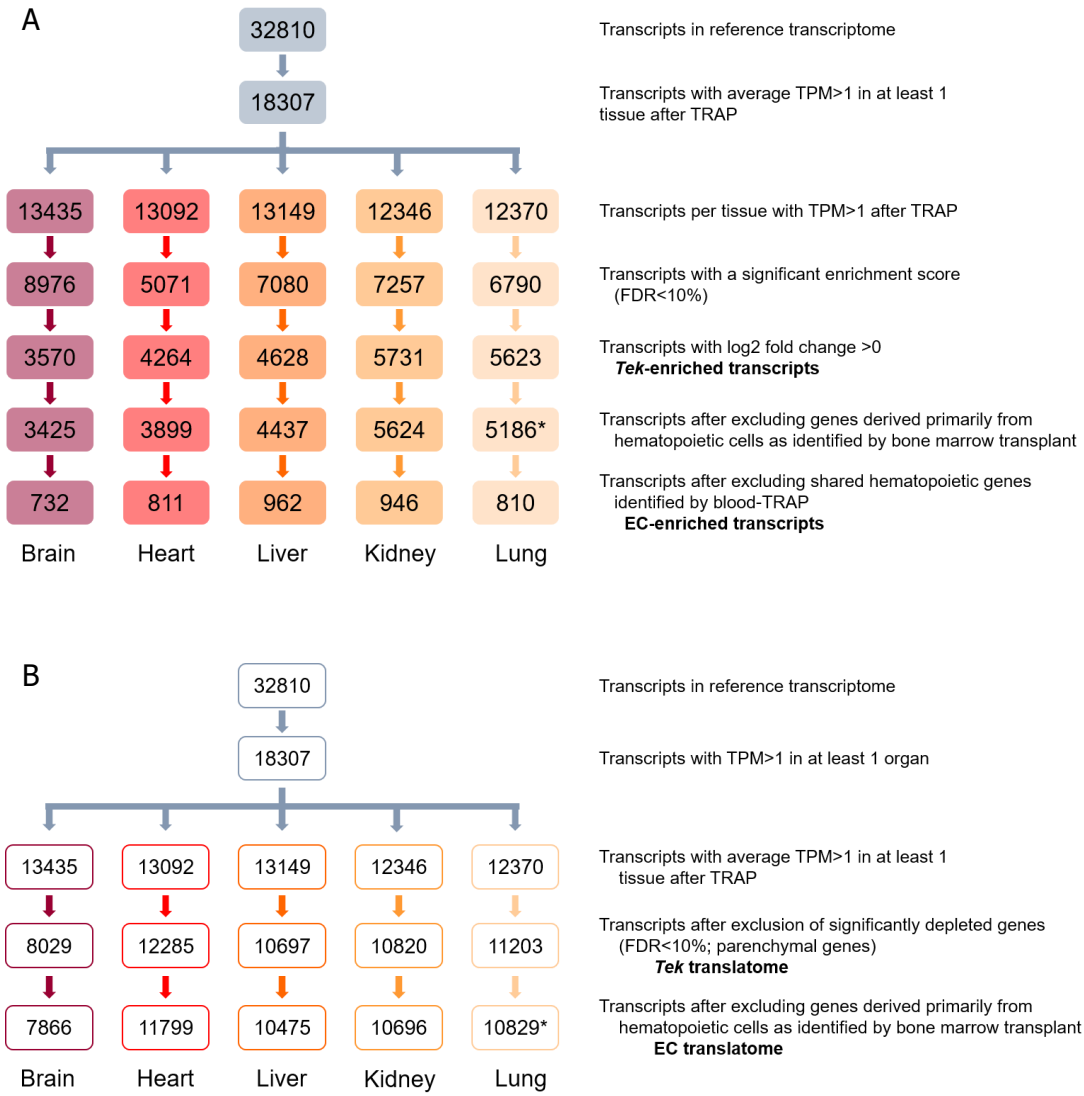

Figure S6: Classification of gene enrichment categories and cell-specific expression profiles

(A) Number of transcripts present after filtering RNASeq data to identify genes that are specifically enriched in ECs, thus excluding genes that are commonly shared with other cell types. (B) Number of all transcripts identified in EC translatomes, which include housekeeping genes as well as transcripts shared, but not primarily derived from, hematopoietic cells.

*Due to suboptimal sequencing quality of lung samples obtained from the *Rpl22*$^{fl/fl}$, *Tek-Cre*$^{+/0}$ mouse receiving *Rpl22*$^{fl/fl}$, *Tek-Cre*$^{-}$ bone marrow, hematopoietic transcripts were defined based on the sum of hematopoietic genes identified in brain, heart, kidney and liver.

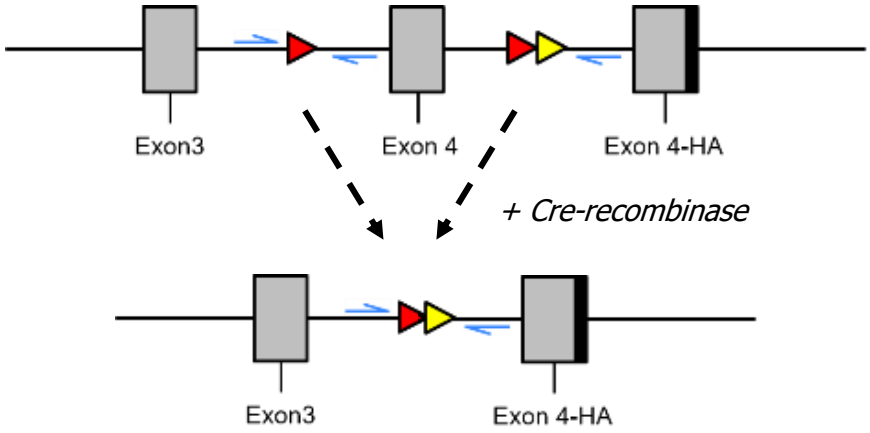

Figure S7: Primer design to identify the tissue-specific EC content based on genomic *Rpl22* isoforms. PCR primers in the floxed allele span the LoxP site (▶) resulting in a 157 basepair amplicon whereas after *Cre-recombinase* and excision of the wildtype exon 4, primers will span both the loxP and FRT site (▷) leading to a 240 basepair amplicon. Amplicons were sequenced as paired-end 75 nucleotide reads, allowing the discrimination of the HA-expressing allele from the total amplicons sequenced.

Supplemental Table S1: Enrichment scores of genes significantly enriched or depleted in mice ubiquitously expression HA-tagged Rpl22

Heart

	Log2Fold change	adjusted p-value		Log2Fold change	adjusted p-value
Bcor	1.795	0.0540	*Zmym2*	-0.628	0.0980
Pcmp	0.494	0.0980	*Akap11*	-0.646	0.0910
Coq7	0.460	0.0980	*Mrpl30*	-0.682	0.0910
Swi5	0.387	0.0980	*Naa15*	-0.688	0.0663
Mrpl46	0.348	0.0910	*Xrn2*	-0.699	0.0910
Limd2	0.303	0.0980	*Ankrd12*	-0.717	0.0087
Atp6v1g1	0.223	0.0980	*Lmf2*	-0.737	0.0910
Oard1	0.194	0.0661	*Stt3b*	-0.741	0.0910
Ahcyl2	-0.206	0.0577	*Gls*	-0.754	0.0980
Rnf144a	-0.211	0.0980	*Pcbp2*	-0.759	0.0910
Tmem123	-0.235	0.0980	*Ttc3*	-0.774	0.0980
Pgam5	-0.244	0.0910	*Nkain4*	-0.806	0.0910
5730507C01Rik	-0.256	0.0980	*Slc12a7*	-0.814	0.0663
Phyh	-0.259	0.0980	*Eif5b*	-0.824	0.0910
Cyp39a1	-0.287	0.0910	*Ewsr1*	-0.830	0.0661
Ngdn	-0.288	0.0992	*Tdrd3*	-0.844	0.0910
Atp6v0c	-0.291	0.0661	*Kansl1l*	-0.856	0.0910
Naprt1	-0.325	0.0910	*Dnm3*	-0.876	0.0980
Psmd11	-0.340	0.0980	*Tmem82*	-0.932	0.0980
Egln1	-0.354	0.0910	*Eef1d*	-0.943	0.0980
Coq6	-0.380	0.0058	*9430015G10Rik*	-0.952	0.0910
Fam46a	-0.385	0.0980	*Plcg1*	-0.993	0.0682
Vdac3	-0.394	0.0663	*Itch*	-0.997	0.0847
Srp72	-0.399	0.0910	*Atf7ip*	-1.000	0.0980
Tmem170b	-0.401	0.0058	*Lamb1*	-1.012	0.0910
Nr1d1	-0.411	0.0980	*Sf3b1*	-1.013	0.0910
Ptpn6	-0.469	0.0910	*Pfkfb2*	-1.025	0.0980
Ddx31	-0.473	0.0430	*Gm4631*	-1.043	0.0661
Ppap2b	-0.498	0.0910	*Pank4*	-1.060	0.0980
Dnajc16	-0.505	0.0910	*Gdpd1*	-1.113	0.0663
Zfp277	-0.508	0.0385	*Gm17066*	-1.123	0.0910
4921531C22Rik	-0.521	0.0577	*Abce1*	-1.135	0.0661
Stx4a	-0.538	0.0430	*Zc3h7a*	-1.213	0.0663
Zfp91	-0.541	0.0910	*Srek1*	-1.228	0.0910
Morf4l2	-0.543	0.0682	*Nox4*	-1.282	0.0663
Ccdc6	-0.567	0.0980	*Myoz2*	-1.328	0.0910
4930506M07Rik	-0.567	0.0661	*Chchd3*	-1.431	0.0682
Enc1	-0.569	0.0577	*Prpf8*	-1.469	0.0910
Hspa5	-0.571	0.0980	*Zcchc7*	-1.516	0.0385
Ppp1r11	-0.579	0.0910	*Myh6*	-1.771	0.0142
Nol11	-0.585	0.0980	*Gid4*	-2.006	0.0663
Sclt1	-0.594	0.0910	*Neat1*	-3.633	0.0980
Cyb5r1	-0.611	0.0663			

Liver

	Log2Fold change	adjusted p-value		Log2Fold change	adjusted p-value
Fam25c	0.461	0.0994	*Hsd3b5*	-0.575	0.0994
Nedd8	0.460	0.1000	*Copb1*	-0.598	0.0994
Ndufs6	0.425	0.0975	*Txnip*	-0.611	0.0657
S100a10	0.323	0.0967	*Acsl1*	-0.613	0.0282
Urad	0.202	0.0994	*Reln*	-0.624	0.0967

bioRxiv preprint doi: https://doi.org/10.1101/708701; this version posted July 19, 2019. The copyright holder for this preprint (which was not certified by peer review) is the author/funder, who has granted bioRxiv a license to display the preprint in perpetuity. It is made available under aCC-BY-ND 4.0 International license.

Fcf1	0.185	0.0908	*Dmgdh*	-0.625	0.0967
Cst3	0.174	0.0994	*Slc17a1*	-0.626	0.0975
Ndufs8	0.106	0.0967	*Slc10a1*	-0.640	0.0967
Decr1	-0.107	0.0922	*Scaf8*	-0.673	0.0967
H2-Q1	-0.142	0.0967	*Slc38a3*	-0.674	0.0967
Etf1	-0.146	0.0967	*Tulp4*	-0.680	0.0922
Kdsr	-0.232	0.0967	*Rps20*	-0.682	0.0967
Cyp2d26	-0.324	0.1000	*Dll1*	-0.695	0.0282
Cyp2j5	-0.326	0.0994	*Ap3m1*	-0.727	0.0967
Itih3	-0.368	0.0967	*Abcb4*	-0.743	0.0496
Sypl	-0.383	0.0967	*Slco1a1*	-0.779	0.0797
Chuk	-0.407	0.0967	*Sec31a*	-0.799	0.0967
Zmynd8	-0.431	0.0967	*Maf*	-0.840	0.0967
Ppil4	-0.447	0.0994	*Kdm5a*	-0.928	0.0994
Cnot7	-0.476	0.0967	*Kdr*	-0.953	0.0967
Man1b1	-0.485	0.0994	*Rpl32*	-0.997	0.0975
Klkb1	-0.555	0.0967	*Wsb1*	-1.119	0.0657

bioRxiv preprint doi: https://doi.org/10.1101/708701; this version posted July 19, 2019. The copyright holder for this preprint (which was not certified by peer review) is the author/funder, who has granted bioRxiv a license to display the preprint in perpetuity. It is made available under aCC-BY-ND 4.0 International license.

Lung

	Log2Fold change	adjusted p-value		Log2Fold change	adjusted p-value
Scgb3a1	0.798	0.0872	*Arhgap5*	-0.831	0.0490
Bud31	0.363	0.0948	*Ctc1*	-0.864	0.0490
Abracl	0.257	0.0965	*Sgip1*	-0.921	0.0839
Sar1a	-0.313	0.0948	*Itpr3*	-0.953	0.0839
Tln2	-0.337	0.0839	*Sorl1*	-1.077	0.0839
Dtx3	-0.643	0.0798	*Msn*	-1.169	0.0490
Ep400	-0.672	0.0839	*Usp9x*	-1.230	0.0839
Cog4	-0.733	0.0839	*Man1a*	-1.367	0.0839
Ascc2	-0.772	0.0839	*Macf1*	-1.802	0.0839
Ddx58	-0.792	0.0839	*Gid4*	-2.013	0.0651
Bclaf1	-0.825	0.0490			

Note: for brain and kidney there were no genes significantly enriched/depleted after TRAP

bioRxiv preprint doi: https://doi.org/10.1101/708701; this version posted July 19, 2019. The copyright holder for this preprint (which was not certified by peer review) is the author/funder, who has granted bioRxiv a license to display the preprint in perpetuity. It is made available under aCC-BY-ND 4.0 International license.

Supplemental Table S2: EC genes significantly enriched (log2 fold change >1) in at least 1 organ while also being significantly depleted (log2 fold change <-1) in at least 1 other organ.

	Brain	Heart	Kidney	Liver	Lung
A2m	-2.58	**1.92**	-0.46	0.83	-0.02
A4galt	**3.43**	**1.45**	**-1.32**	0.74	**1.27**
A530016L24Rik	0.99	**-2.33**	**1.23**	0.30	-0.60
A630076J17Rik	-0.02	**1.20**	**-2.21**	-1.61	0.00
A830019P07Rik	-1.94	0.37	**1.41**	1.82	0.08
Aard	-1.65	-0.26	0.00	-0.41	**1.79**
Aatk	**-2.16**	0.08	**1.49**	2.09	0.72
Abcc6	**2.25**	0.03	-1.50	**-2.48**	-0.01
Abcg2	**3.50**	**1.45**	**-1.87**	**-1.43**	**1.24**
Abhd15	**2.06**	0.33	0.52	**-1.33**	0.62
Ablim3	**-1.86**	**2.31**	1.07	-1.77	**-2.04**
Acaa1b	0.04	-0.37	**-2.54**	**-2.38**	**1.03**
Acacb	**1.39**	-1.20	-0.12	**-1.67**	0.10
Acap3	**-1.58**	0.90	**1.71**	2.14	0.43
Adam23	**-3.18**	0.40	0.86	4.24	0.80
Adam3	**2.37**	**1.04**	-0.01	0.00	-1.14
Adamdec1	0.00	-0.08	0.41	4.22	-1.33
Adamts4	**-3.06**	0.52	0.21	1.39	-0.07
Add2	**-2.93**	0.39	**2.86**	0.01	0.18
Adh7	**1.03**	-0.41	0.82	**-1.43**	-2.15
Adtrp	**1.98**	-1.67	**-3.30**	**-3.04**	-0.23
Aebp1	**-3.07**	0.49	**-1.51**	1.42	**-2.63**
Agap1	**-1.35**	0.74	**-1.04**	1.36	0.66
Agmo	**1.35**	0.92	-0.27	**-1.88**	**-1.24**
AI836003	**-2.73**	-0.19	1.31	0.14	**1.85**
Aif1l	**1.50**	0.59	**-2.91**	-0.84	-0.75
Ajuba	**1.01**	**1.03**	-0.59	0.52	**-1.02**
Akr1b8	-1.11	0.37	0.63	5.09	**-2.10**
Akr1c14	**4.09**	**2.38**	**-2.96**	**-3.17**	**-3.72**
Alpl	**2.70**	0.51	**-1.76**	**-2.62**	-0.83
Amigo2	**-1.36**	1.85	**1.62**	1.89	**1.02**
Ang	**4.59**	1.52	1.44	**-2.72**	**-2.39**
Angptl4	**2.76**	0.64	**-1.63**	**-2.21**	**-1.55**
Ankrd29	**-1.54**	1.12	0.92	3.15	-0.04
Ankrd63	-1.70	-0.46	0.00	0.00	**1.61**
Aoah	**3.07**	1.82	**-1.99**	**2.98**	0.22
Apba1	**-1.81**	**1.07**	0.90	0.90	0.37
Aplp1	**-3.48**	0.06	**1.20**	1.67	0.14
Apol9a	1.53	0.08	**3.44**	**-2.58**	0.75
Aqp11	**2.26**	0.37	**-1.98**	**-2.44**	**1.25**
Arhgap8	**2.33**	1.72	-0.91	0.84	**-1.55**
Arhgef26	**-2.19**	0.93	**2.21**	**-1.70**	0.04
Arhgef28	-0.60	**1.11**	**-1.05**	-0.05	-1.94

bioRxiv preprint doi: https://doi.org/10.1101/708701; this version posted July 19, 2019. The copyright holder for this preprint (which was not certified by peer review) is the author/funder, who has granted bioRxiv a license to display the preprint in perpetuity. It is made available under aCC-BY-ND 4.0 International license.

Arhgef39	0.24	**1.58**	**-1.51**	1.29	0.29
Armcx4	-1.41	0.10	0.99	2.36	0.95
Arsb	0.53	**1.12**	**-1.67**	-0.09	0.16
Art3	-0.94	-1.54	**2.15**	3.15	**-2.77**
Asgr2	**1.82**	0.63	0.96	**-3.00**	0.35
Atl1	**-3.39**	0.91	**1.05**	1.75	-0.21
Atp6v0d2	0.44	0.83	**-3.34**	-1.10	**1.41**
Atp6v0e2	**-2.86**	0.22	**-1.77**	1.60	**1.47**
Atp6v1g2	**-3.79**	-1.09	0.71	2.19	0.00
B230110C06Rik	-1.39	**-1.76**	**1.54**	-0.04	0.03
B3galnt1	**-1.61**	**1.83**	-0.23	2.42	-0.46
B4galt6	**-1.71**	0.62	0.26	2.24	0.48
B930041F14Rik	**-1.56**	0.16	0.46	1.41	0.15
B9d1	**-1.32**	0.90	-0.63	2.14	**-1.10**
BC030867	-1.05	1.02	**1.16**	0.90	0.59
Bche	**1.41**	-1.98	0.06	**-3.01**	-0.75
Bend6	**-1.38**	0.93	**1.81**	1.38	0.51
Bex4	**-3.29**	**1.67**	**-3.30**	-0.47	**-4.14**
Bhlhe22	-2.24	0.04	**1.09**	0.29	-0.12
Bmper	-2.10	0.54	**1.35**	1.61	-1.74
Boc	**-1.38**	0.97	**2.48**	0.03	-1.00
Bok	**-1.48**	**2.14**	0.59	2.35	**-1.05**
Btbd3	**-1.88**	**1.74**	**1.42**	1.92	**1.18**
C130074G19Rik	**3.19**	**2.42**	-0.10	**-1.37**	**1.66**
C1qtnf1	**-1.17**	**1.39**	0.35	3.85	**-1.36**
C1qtnf2	-1.86	**1.44**	**1.98**	1.46	0.78
C1qtnf7	-1.43	0.46	**1.02**	1.25	**-2.17**
C1ra	**1.79**	1.12	0.52	**-1.60**	-0.75
C1rl	**1.78**	0.18	**-2.54**	**-2.55**	-1.15
C2cd2l	**-1.48**	**1.34**	-0.52	0.89	0.85
C4b	**1.70**	1.22	0.66	**-1.32**	**-2.62**
Cacnb3	**-2.89**	0.55	0.01	1.24	0.07
Cadm1	**-1.11**	1.40	1.18	2.07	-0.43
Calca	-3.49	0.16	**2.84**	0.04	-1.72
Camkk1	**-2.46**	-0.16	0.96	1.23	-1.30
Capsl	**-2.87**	-0.05	**2.20**	0.09	-2.69
Car14	0.39	-3.81	**-3.26**	**-2.93**	**1.55**
Car5a	**3.40**	-0.02	**-2.57**	**-2.77**	0.08
Car8	**-2.77**	**2.66**	**3.42**	**1.01**	**-1.31**
Car9	-0.41	0.63	**-2.21**	2.29	0.17
Cbr2	**4.84**	2.29	**3.38**	3.34	**-4.60**
Ccdc106	**-2.18**	**2.02**	-0.20	3.33	0.30
Ccdc141	**2.67**	-2.39	**-1.78**	-1.68	-0.90
Ccdc148	**-2.86**	0.12	**-1.20**	3.40	-0.27
Ccdc160	**-1.69**	0.56	-2.15	2.77	0.96
Ccdc19	-1.25	**1.24**	0.62	1.30	**-1.20**
Ccdc68	-0.42	0.43	**-2.30**	-0.13	**1.16**

bioRxiv preprint doi: https://doi.org/10.1101/708701; this version posted July 19, 2019. The copyright holder for this preprint (which was not certified by peer review) is the author/funder, who has granted bioRxiv a license to display the preprint in perpetuity. It is made available under aCC-BY-ND 4.0 International license.

Ccl19	**1.11**	0.56	-1.18	-1.01	-0.64
Cdh11	**-2.68**	**1.81**	-1.01	0.12	-2.35
Cdh13	**-1.72**	0.29	**2.56**	4.64	-0.48
Cdh4	**-2.74**	0.18	0.19	2.19	0.08
Cdk14	**-2.61**	0.66	0.72	1.46	0.93
Cdkn1c	**1.08**	**2.25**	**1.04**	2.65	**-1.20**
Celf4	**-3.68**	-0.17	1.01	1.87	0.25
Cep112	0.21	**-1.49**	0.79	1.05	-0.46
Ces2e	**1.29**	**2.01**	**2.59**	**-1.97**	**1.29**
Cfh	**3.44**	**1.62**	-0.87	**-1.63**	**-1.79**
Cgnl1	**1.34**	**1.50**	-0.99	0.06	**-1.23**
Chst1	**-2.79**	0.94	0.50	0.39	**1.34**
Chst2	**-2.65**	0.39	**4.10**	3.72	**1.48**
Chst8	**-1.36**	-0.14	**2.42**	0.42	-0.93
Cldn15	0.22	0.78	**3.95**	1.57	**-1.58**
Cnrip1	**-2.52**	**1.51**	**2.85**	3.58	0.90
Cntfr	**-3.46**	0.26	-0.70	2.19	-0.43
Col13a1	0.24	0.15	1.21	3.66	-1.50
Col14a1	**1.04**	0.32	-0.17	**-1.15**	-0.75
Col23a1	-1.27	**1.74**	0.46	1.73	**-2.32**
Col8a1	-0.39	**1.21**	-0.27	2.66	-1.24
Coro2b	**-1.68**	**1.63**	**2.53**	2.33	**1.15**
Cox4i2	**-1.94**	**1.18**	-0.06	0.42	**-4.22**
Cp	**2.77**	0.58	-0.75	**-3.20**	**-3.02**
Cped1	-0.94	0.78	**1.30**	**-1.75**	**-1.90**
Cplx2	**-3.32**	1.26	0.15	2.58	0.30
Cpne5	**-3.15**	-0.80	-0.14	0.62	**1.40**
Cpt1c	**-3.49**	0.54	**1.14**	0.86	-1.02
Creb5	**-1.34**	**1.22**	**2.16**	0.73	0.64
Crmp1	**-3.16**	0.56	**1.44**	0.78	0.49
Cryba4	**4.26**	**-1.85**	1.54	**3.87**	0.99
Ctgf	0.76	0.51	0.04	1.67	**-1.06**
Ctnnd2	**-2.33**	0.57	**1.44**	0.64	-0.61
Cutal	**3.59**	-0.09	**-3.81**	**-2.92**	-1.69
Cx3cl1	**-2.22**	**1.83**	**1.19**	0.26	**1.67**
Cxcl12	**3.07**	**2.39**	**-2.07**	**-2.41**	**1.25**
Cxcl14	**-2.99**	0.92	-1.43	1.25	**-3.41**
Cxxc4	**-2.80**	0.40	**1.07**	0.68	0.28
Cyp26b1	-1.52	0.13	0.97	2.18	0.90
Cyp27a1	**1.12**	0.47	-0.77	**-2.65**	**-1.03**
Cyp2d22	1.07	**1.29**	**1.80**	**-1.91**	0.36
Cyr61	**1.87**	0.92	0.12	-0.30	**-1.48**
D630036G22Rik	**1.02**	0.55	-0.05	**-1.40**	**1.30**
Dab2	**3.19**	**2.02**	**-1.23**	3.75	0.82
Dapk2	-0.84	**1.53**	**3.08**	2.71	**-2.69**
Dbndd2	**-2.88**	1.19	**1.61**	1.49	**1.04**
Ddah1	**-1.07**	0.09	**-3.47**	**-1.69**	**1.81**

bioRxiv preprint doi: https://doi.org/10.1101/708701; this version posted July 19, 2019. The copyright holder for this preprint (which was not certified by peer review) is the author/funder, who has granted bioRxiv a license to display the preprint in perpetuity. It is made available under aCC-BY-ND 4.0 International license.

Degs2	**4.82**	**2.28**	**-3.42**	-0.74	0.21
Depdc7	0.85	0.56	**-3.06**	-1.77	**1.04**
Dkk3	**-3.98**	-0.74	**-2.23**	2.92	**-2.32**
Dlk1	-2.30	0.06	**1.21**	0.02	-0.07
Dmkn	**-2.76**	-0.44	**1.49**	0.19	**-3.13**
Dmpk	-0.84	-2.04	-0.40	3.94	-1.34
Dnaic1	**-3.16**	-0.32	**2.76**	0.66	**1.50**
Dnajb5	**-1.72**	-1.53	**1.59**	2.02	0.61
Dok5	**-3.68**	-0.73	**1.55**	0.13	-0.11
Dpysl3	**-3.24**	0.82	**1.45**	3.18	0.56
Dpysl5	**-2.77**	-0.11	-0.11	0.00	**1.03**
Dusp26	**-3.34**	0.29	**2.91**	0.03	0.43
Dync2li1	**-1.76**	**1.23**	**-1.75**	0.94	**-1.78**
E130006D01Rik	-1.29	-0.01	**1.81**	0.00	-0.09
Ecm2	**1.25**	**1.06**	**1.51**	**1.19**	**-1.03**
Edil3	**-3.67**	-0.09	**2.62**	0.27	0.89
Edn3	**3.69**	-0.63	-2.16	-0.16	-2.85
Ednrb	**-1.92**	**2.05**	**3.82**	3.07	0.66
Elp6	**-1.28**	**1.15**	0.71	0.81	0.74
Enho	**-3.42**	0.08	**2.89**	0.14	**1.87**
Enpp3	0.25	**1.29**	**-2.00**	**-2.35**	-0.08
Enpp6	**-2.04**	**1.84**	**-2.62**	0.63	0.53
Epb4.1l3	**-3.03**	-0.91	**-2.39**	3.44	-0.90
Epha4	**-1.90**	0.07	**1.97**	0.44	0.15
Ephb1	**-2.64**	**1.01**	**2.77**	0.22	-0.15
Eps8	0.79	**1.80**	**-2.45**	-0.35	-0.74
Eps8l2	**2.07**	**1.30**	**-2.04**	**-2.56**	**-2.10**
Eva1a	0.34	**2.76**	**-2.25**	**-2.15**	0.23
F7	0.25	0.04	-0.30	**-3.29**	**1.21**
F9	**1.75**	-0.04	0.14	**-3.23**	0.10
Fabp1	-0.93	-2.63	-1.55	**-2.06**	**2.53**
Fam115a	**-1.98**	1.26	0.79	1.63	-0.20
Fam124a	**-1.93**	**1.01**	**1.80**	4.05	0.80
Fam189a2	-0.33	-0.17	**2.28**	3.14	**-1.27**
Fam20a	**-1.19**	0.93	**1.14**	-0.37	-0.66
Fam212b	**-3.40**	-0.15	**1.26**	0.41	-1.11
Fam84a	**-3.43**	-0.66	**-1.82**	1.37	-1.23
Fbln5	**2.49**	**1.40**	-0.15	**1.50**	**-1.20**
Fez1	**-3.50**	1.51	**1.16**	0.13	-0.42
Fibin	**-2.21**	**1.04**	**2.74**	-0.13	**1.53**
Flrt3	**-3.11**	-0.11	**3.46**	0.72	**-1.78**
Flywch1	**-2.66**	0.99	0.61	2.36	0.92
Flywch2	**-3.44**	**1.28**	0.71	1.67	**-1.27**
Fmo2	**3.93**	**1.25**	**-3.09**	0.84	**-1.13**
Fndc4	**-2.88**	0.19	**1.01**	**-2.00**	0.77
Foxf2	**3.47**	0.19	0.00	0.00	**-2.11**
Fstl1	**-1.02**	**1.09**	**2.77**	2.46	0.06

bioRxiv preprint doi: https://doi.org/10.1101/708701; this version posted July 19, 2019. The copyright holder for this preprint (which was not certified by peer review) is the author/funder, who has granted bioRxiv a license to display the preprint in perpetuity. It is made available under aCC-BY-ND 4.0 International license.

Fxyd6	**-2.36**	**2.08**	**3.42**	3.28	-0.03
Gal	**-3.52**	-0.01	-0.34	0.87	**2.33**
Gamt	-0.41	0.76	-0.15	**-2.47**	**1.05**
Gas6	**1.60**	**1.65**	**1.97**	2.63	**-1.79**
Gch1	**2.68**	1.11	**2.62**	**-2.18**	0.61
Gdpd1	**-2.03**	-0.98	0.65	3.02	-0.88
Gfpt2	**-2.14**	0.47	**2.70**	1.23	0.02
Gfra2	**-2.89**	0.75	0.92	2.78	-0.86
Gja1	**-2.06**	-1.28	**3.60**	3.63	**-1.47**
Gldc	-1.54	0.80	**-2.40**	**-2.29**	**1.17**
Gm10687	-1.05	0.84	**1.20**	2.17	0.37
Gm11716	0.13	**-3.58**	**2.71**	0.95	-0.29
Gm13716	-2.32	0.68	**1.43**	0.06	0.00
Gm13889	-1.92	0.68	**3.02**	3.53	**1.74**
Gm14097	**2.84**	-1.49	-0.10	**-2.48**	**1.25**
Gm14290	**-2.22**	0.24	**2.44**	2.33	0.09
Gm14964	**-2.07**	0.19	-1.50	1.63	**-2.29**
Gm15564	0.82	**1.24**	**-1.34**	**-1.62**	**1.33**
Gm15972	-0.59	-1.32	**-2.12**	1.66	-0.07
Gm1673	**-2.38**	1.23	0.83	2.25	-0.05
Gm27030	-1.10	0.14	0.64	1.05	0.11
Gm4876	**-1.16**	0.96	**1.14**	-0.43	0.59
Gm684	**2.40**	0.58	**2.44**	0.25	**-1.55**
Gpr125	0.17	0.53	**-1.33**	-0.58	**1.11**
Gpr68	**-1.99**	0.29	**1.96**	1.56	0.60
Gprc5a	**1.43**	1.07	0.16	1.28	**-2.89**
Gprc5b	**-2.91**	**1.40**	0.80	0.69	-1.02
Grp	**-2.19**	0.00	0.00	0.00	**1.61**
Grtp1	-1.42	-1.04	**-3.19**	**-3.03**	**1.73**
Gstt3	**1.10**	**1.86**	**-1.73**	-1.84	**-1.56**
Hagh	**-1.15**	-0.54	**-1.82**	**-1.97**	**1.02**
Hbegf	-0.17	-0.81	0.33	2.57	**-1.67**
Hebp1	-0.24	0.25	**-2.22**	**-2.05**	**1.03**
Hecw2	-1.79	1.16	**2.11**	2.20	0.87
Hist3h2ba	**-3.17**	**1.80**	1.20	1.25	1.25
Hmgcs2	**2.70**	-0.52	**-2.67**	**-2.96**	-2.28
Hoxb5	-1.23	1.16	**2.36**	3.61	**1.55**
Hpcal4	**-3.87**	-0.84	-0.43	-0.02	**1.07**
Hrct1	**3.47**	**2.27**	**3.18**	**1.35**	**-1.92**
Hspa12a	**-2.90**	-0.46	-0.50	1.61	0.74
Hspb8	0.51	-2.75	**1.84**	**-2.50**	-0.73
Hspg2	**2.57**	1.77	**2.93**	3.44	-1.92
Ido1	-1.23	0.76	**1.58**	0.00	**1.05**
Ift122	**-1.90**	**2.14**	0.19	2.39	-0.26
Ift57	**-1.59**	0.07	0.02	1.58	0.69
Ift74	**-1.31**	0.22	-0.36	1.10	-0.18
Igf2	**-3.12**	**2.11**	**1.93**	0.77	0.49

bioRxiv preprint doi: https://doi.org/10.1101/708701; this version posted July 19, 2019. The copyright holder for this preprint (which was not certified by peer review) is the author/funder, who has granted bioRxiv a license to display the preprint in perpetuity. It is made available under aCC-BY-ND 4.0 International license.

Igfbp3	**1.74**	**1.74**	**2.70**	-0.38	**-2.24**
Igfbp5	**-3.35**	1.00	**2.36**	0.63	**-1.57**
Igsf3	**-1.96**	0.72	-0.45	3.50	-0.40
Igsf5	**3.63**	-0.43	**-3.40**	**-3.21**	**-1.86**
Il13ra2	-1.17	0.13	0.03	3.72	-0.03
Il20rb	**-1.02**	0.58	**1.38**	0.56	0.89
Il33	**-4.03**	0.67	**2.94**	2.83	**-2.38**
Irf6	**2.93**	**2.06**	**-2.86**	**-2.30**	**-1.69**
Irx3	-0.17	-0.42	**1.66**	-0.09	**-1.51**
Irx5	-0.25	-0.41	**2.27**	0.04	**-1.67**
Ism1	**1.29**	0.92	-0.18	0.30	**-2.90**
Itga8	-0.52	-0.10	0.61	2.00	**-2.29**
Itgbl1	-2.34	**1.35**	-0.25	-0.29	-1.17
Itih5	**2.72**	0.47	**-1.23**	-1.33	-0.99
Kazn	**-2.42**	0.64	**-1.82**	1.82	**1.07**
Kcnb1	**-2.27**	0.12	**2.30**	2.49	0.23
Kcng2	-0.74	**-2.21**	-0.03	1.01	0.00
Kcnj10	**-3.07**	-0.14	**-1.78**	1.97	0.05
Kcnj5	-1.02	-2.62	**1.74**	-0.02	-0.13
Kcns3	-2.15	-0.17	-0.63	1.23	-0.93
Kcp	**1.06**	0.06	-1.06	0.41	-0.06
Kctd13	**-2.38**	0.13	0.45	1.73	0.04
Kctd17	**-2.05**	**2.27**	**1.11**	2.61	0.88
Khdrbs3	**-1.91**	**-1.53**	0.82	1.84	-1.92
Kif3a	**-2.47**	0.15	0.35	2.20	0.09
Kit	**-2.85**	**1.60**	0.84	3.66	0.91
Krt8	-1.11	-0.32	**-3.47**	1.27	**-3.67**
Lama4	**1.78**	0.71	**2.28**	3.06	**-1.51**
Lancl2	**-2.22**	0.64	0.53	1.16	0.33
Large	**-1.19**	-0.95	0.65	1.47	-0.04
Lbp	**-1.08**	1.42	**3.29**	0.06	0.20
Ldb2	**-1.96**	**2.16**	**3.45**	3.68	**1.34**
Ldlr	-0.54	**1.08**	0.97	**-2.23**	**-1.42**
Leprel1	**1.73**	0.99	**-2.84**	0.75	-0.55
Limch1	-0.63	-0.42	**2.14**	1.78	**-2.51**
Liph	**3.17**	0.29	-0.38	0.47	**-2.55**
Lrrc3	**2.77**	-0.10	**-1.18**	**-1.91**	0.25
Lrrc3b	**-3.03**	-0.41	**3.95**	0.46	0.45
Lrrc55	**-2.87**	1.06	**1.96**	0.13	0.03
Lrrn4cl	-1.94	0.86	**2.42**	1.75	-0.16
Lsamp	**-3.56**	**1.92**	0.10	0.06	-0.23
Lsr	**3.83**	**1.09**	-0.60	**-2.29**	-0.33
Lurap1l	**-1.58**	**1.21**	0.87	**-1.59**	0.33
Lysmd2	**-1.73**	**1.48**	**2.18**	0.70	**1.73**
Macrod2	**-1.74**	-0.32	**-2.37**	-0.07	**1.09**
Mag	**-2.48**	0.88	**1.84**	2.90	0.75
Mamld1	**-1.20**	0.58	1.94	2.01	0.26

bioRxiv preprint doi: https://doi.org/10.1101/708701; this version posted July 19, 2019. The copyright holder for this preprint (which was not certified by peer review) is the author/funder, who has granted bioRxiv a license to display the preprint in perpetuity. It is made available under aCC-BY-ND 4.0 International license.

Map1b	**-3.26**	0.31	**2.23**	0.84	-0.13
Map6	**-1.34**	**1.26**	0.97	0.08	**-1.57**
Matk	**-1.59**	1.77	**2.64**	3.32	0.53
Mb21d2	**-1.97**	0.48	-1.27	1.21	-0.04
Mdk	**-3.35**	**1.66**	**-3.26**	-1.13	-2.91
Me3	**-2.28**	-3.03	**-2.97**	0.12	**1.00**
Mecom	**3.44**	**1.88**	-0.29	**2.76**	**-1.10**
Megf8	**-1.01**	0.48	0.82	1.35	-0.03
Meis2	**-3.18**	0.02	**3.63**	3.72	0.68
Meox2	0.05	**2.43**	1.07	0.10	-1.38
Mettl24	-1.25	-0.37	**1.11**	0.15	0.56
Mfap5	-0.95	0.88	**2.04**	-0.28	**-2.14**
Mfsd2a	**2.57**	-0.34	**-3.29**	**-2.14**	-1.73
Mfsd7c	**3.61**	-0.91	**-1.04**	-0.91	0.46
Mid2	**-1.36**	0.42	0.73	1.10	0.75
Mlf1	**-1.04**	-3.69	2.06	2.48	**-2.54**
Mlxipl	**3.46**	-1.13	**-2.31**	**-2.21**	-0.65
Mmp15	-0.45	0.48	**2.47**	**-2.27**	**-1.11**
Mmp17	**-2.71**	**1.07**	**1.77**	-0.07	0.10
Mmp2	**1.21**	0.88	0.61	-0.44	**-1.70**
Mn1	**-1.38**	0.92	**3.54**	-0.31	-0.19
Mogat2	**1.34**	-0.64	**-2.82**	-0.87	0.04
Morn1	**-1.04**	**1.05**	-1.19	0.23	-0.57
Mpped2	**-2.32**	**-2.00**	-0.68	-0.21	**1.37**
Ms4a4d	0.55	0.51	**1.55**	-1.16	**-3.64**
Myo1b	0.46	1.08	**1.16**	**-3.10**	**-2.32**
Nat2	**1.36**	0.94	**-2.34**	-0.58	0.28
Ncald	**-4.00**	0.25	-0.22	-0.99	**1.19**
Nckap5	-0.39	-1.00	-1.04	0.21	**1.05**
Ndn	**-3.70**	0.66	**1.43**	0.77	-0.01
Ndnf	**1.54**	-0.34	0.18	-0.01	-2.27
Ndufa4l2	**-2.35**	**1.09**	**-1.87**	**-1.51**	**-4.25**
Neurl1b	**-1.36**	**1.42**	**1.24**	0.73	**1.03**
Nexn	**-1.28**	-2.84	**1.53**	3.02	-0.83
Nhlrc1	**-1.07**	-0.15	-0.25	-0.17	**1.39**
Nipa1	**-1.75**	-0.20	0.05	1.01	-0.94
Nlgn1	**-3.27**	-0.17	**1.10**	0.00	-0.04
Notum	**1.89**	-0.08	-1.59	**-1.75**	-1.37
Nov	**-2.73**	0.86	**1.47**	0.13	-1.04
Npl	**2.46**	**2.60**	**-2.14**	4.77	0.85
Npr2	-0.91	**1.02**	0.80	0.01	**-2.39**
Nptxr	**-3.29**	1.03	**1.38**	0.98	-0.47
Nr1h3	0.15	0.68	**-1.37**	1.37	**-1.15**
Nr2f1	**-2.74**	0.22	0.40	1.39	-0.25
Nrep	**-2.33**	**1.21**	**1.93**	-1.31	-0.71
Nrg1	**-2.93**	**1.39**	-1.00	**1.01**	-0.59
Nsg1	**-3.22**	**2.04**	**3.81**	2.36	**1.81**

bioRxiv preprint doi: https://doi.org/10.1101/708701; this version posted July 19, 2019. The copyright holder for this preprint (which was not certified by peer review) is the author/funder, who has granted bioRxiv a license to display the preprint in perpetuity. It is made available under aCC-BY-ND 4.0 International license.

Ntf3	**-2.37**	**2.16**	**3.31**	2.21	-1.30
Nts	**-3.50**	**2.30**	0.72	2.44	0.45
Nudt17	**-1.06**	0.05	**1.29**	0.24	**1.00**
Oaf	0.10	**1.21**	**-1.16**	**-2.39**	-0.24
Ocln	**3.70**	**1.62**	**-3.06**	**-2.36**	0.23
Olfm1	**-3.25**	0.69	**1.69**	3.66	**1.10**
Olfm2	**-3.92**	0.00	**2.08**	-0.44	**1.77**
Olfml2b	-0.20	-0.64	**1.97**	-0.14	-1.79
Olfml3	**4.02**	**1.09**	**-1.47**	0.52	**-2.95**
Palmd	**3.08**	**1.41**	**3.60**	**-2.25**	**1.34**
Paqr5	**4.40**	-0.32	**-3.29**	0.05	-0.47
Paqr8	**-3.07**	0.82	1.52	1.41	-0.22
Pawr	-0.15	**1.40**	**-1.86**	-0.78	0.89
Pcbp3	**-2.72**	**1.70**	0.01	1.65	**1.58**
Pcdh1	**1.15**	**2.17**	0.58	**-1.98**	**1.25**
Pcdh17	**-2.60**	**1.83**	**2.07**	2.28	**1.20**
Pcdha2	**-3.39**	0.00	0.21	0.35	**1.34**
Pcdhb14	-1.42	1.25	0.68	1.13	0.36
Pcdhb15	-1.15	0.68	**1.05**	0.41	0.11
Pcdhb17	**-1.03**	0.92	1.32	1.00	-0.02
Pcdhb7	**-1.36**	0.47	**1.59**	0.79	0.33
Pcolce	**-2.84**	0.83	**-1.47**	1.69	**-2.74**
Pcolce2	-1.52	0.22	0.23	4.05	**-2.35**
Pde10a	**-2.62**	0.55	0.42	1.33	-0.04
Pde9a	**-2.64**	0.97	**-1.69**	**-2.21**	**1.40**
Pdgfc	-0.97	**1.23**	**-1.96**	1.94	0.15
Pdgfrl	-1.20	**1.06**	-0.33	0.62	-1.59
Pgf	**-2.12**	0.98	**1.63**	1.25	-0.23
Phlda1	**-2.04**	-0.88	**1.39**	-2.21	**-1.39**
Pianp	**-3.22**	0.06	**1.47**	2.37	0.55
Pigz	**-2.20**	1.08	0.20	2.33	-0.06
Pir	**2.28**	**1.33**	**1.68**	**-1.81**	-0.07
Pknox2	**-2.06**	-0.45	-0.39	0.59	**1.20**
Pla2r1	-0.14	-0.60	0.88	1.36	-1.45
Plagl1	-1.79	**1.48**	-1.06	0.97	**-1.36**
Plcb1	**-1.35**	**1.59**	0.61	0.12	0.94
Plcb4	**-1.21**	0.96	**1.42**	2.68	0.38
Plekhm2	**-1.11**	-0.83	-0.77	1.50	0.05
Plk3	0.41	**1.59**	-0.05	**-1.53**	1.08
Pllp	-0.03	0.64	**-2.19**	-2.26	**1.77**
Plxdc2	**2.39**	0.55	**-1.60**	1.11	**-2.87**
Postn	0.30	**1.08**	0.24	-0.97	**-3.73**
Ppap2c	0.65	**1.68**	**-1.35**	-0.98	**-1.04**
Ppapdc3	**-1.92**	-1.09	0.34	1.68	-0.04
Ppfia2	**-3.16**	0.12	0.17	1.02	-0.13
Prdm8	-1.52	0.04	0.00	0.03	**1.00**
Prelp	**-3.09**	0.98	0.64	1.13	**-2.02**

bioRxiv preprint doi: https://doi.org/10.1101/708701; this version posted July 19, 2019. The copyright holder for this preprint (which was not certified by peer review) is the author/funder, who has granted bioRxiv a license to display the preprint in perpetuity. It is made available under aCC-BY-ND 4.0 International license.

Prickle2	**-2.42**	**1.00**	**2.11**	1.35	**1.14**
Prr15	1.58	**2.63**	**-1.23**	0.24	-0.28
Prrg3	**-2.20**	**1.52**	**1.11**	1.78	**-1.80**
Prss12	-1.78	0.13	-0.67	-0.11	**1.40**
Prune2	**-1.60**	0.30	**2.60**	2.68	0.58
Ptgis	**2.37**	**1.16**	-0.80	2.92	**-1.45**
Ptgr1	**1.36**	**1.57**	**-1.84**	0.23	**-1.95**
Ptk7	-0.48	1.35	**1.43**	1.06	-1.65
Ptpru	**-1.31**	0.17	**3.53**	0.30	**1.50**
Pvrl4	0.40	1.60	0.61	2.03	**-1.19**
Pxdn	**-1.00**	**1.69**	**1.99**	2.76	0.83
Qpct	**-1.85**	0.73	**2.79**	-0.05	0.12
Rab3a	**-3.82**	-0.34	-0.37	1.81	0.18
Rab42	**-1.21**	0.36	-0.20	2.54	0.68
Rac3	**-1.17**	1.69	0.20	1.26	**-2.59**
Ramp3	**-1.49**	**2.70**	**4.28**	3.52	**1.73**
Rapsn	**2.68**	**-2.33**	**-1.38**	0.52	-0.38
Rarb	**-2.74**	-0.73	**1.82**	2.51	-0.55
Raver2	**-1.57**	-0.40	-0.30	1.45	0.77
Rbfox2	**-1.75**	-0.36	**1.85**	1.05	0.64
Rbfox3	**-3.30**	-0.40	**1.31**	2.76	**1.71**
Rbp1	-0.34	**1.90**	**2.24**	0.49	**-2.55**
Reck	**3.02**	**1.42**	**1.56**	0.67	**-1.49**
Reep1	**-2.56**	-1.66	**1.03**	1.66	**1.34**
Rerg	**-3.24**	0.53	-0.99	2.23	**-1.91**
Rgs7bp	**-3.03**	0.41	0.62	2.06	-0.35
Rilpl1	-0.10	**-2.21**	**2.03**	3.47	0.23
Rims3	**-2.75**	0.16	0.28	2.60	0.47
Rnf157	**-2.45**	0.27	**2.71**	2.90	0.64
RP24-390G17.1	**-1.11**	-0.04	0.34	1.16	0.03
Rprml	-2.91	0.00	0.14	0.11	**1.98**
Rps6ka2	**-1.65**	**1.81**	**2.13**	2.74	**1.16**
Rps6kl1	**-2.67**	**2.19**	**2.82**	1.10	0.13
Rspo3	**-1.91**	1.22	0.12	3.85	**1.13**
Rtn1	**-3.78**	0.76	**1.72**	2.20	0.33
Rtp3	**2.14**	**1.63**	**2.88**	**-2.27**	**1.36**
Saa3	1.54	**2.65**	2.99	**-1.96**	-0.73
Sall1	**2.73**	**1.67**	-2.63	-1.49	0.64
Samd11	-1.45	0.31	0.77	1.08	0.42
Samd4	**-1.56**	-0.48	**1.30**	0.77	-0.52
Scgb3a1	**3.89**	-0.94	0.04	1.03	**-3.65**
Scn1b	**-2.43**	0.78	**2.51**	3.51	0.01
Scn3b	**-3.05**	0.80	0.79	0.67	**1.33**
Sdk2	-1.07	0.48	**1.55**	-0.05	-0.29
Sema3c	**2.42**	-0.72	**-2.21**	0.37	0.58
Sema3d	-1.45	0.31	**2.99**	1.13	-0.78
Sema5b	-1.40	-0.11	**1.08**	-0.24	0.00

bioRxiv preprint doi: https://doi.org/10.1101/708701; this version posted July 19, 2019. The copyright holder for this preprint (which was not certified by peer review) is the author/funder, who has granted bioRxiv a license to display the preprint in perpetuity. It is made available under aCC-BY-ND 4.0 International license.

Sept8	**-2.37**	0.97	0.85	2.65	-0.29
Serpinb1b	**-2.53**	-0.16	0.10	1.22	-0.54
Serpinf1	0.29	1.00	**1.69**	**-2.92**	**-2.25**
Sertad4	**-1.91**	**1.57**	0.74	0.35	-0.30
Sez6l2	**-3.56**	**1.60**	0.69	0.05	-0.27
Sfrp2	-1.76	**1.10**	-0.47	-0.13	-0.91
Sgcb	**-1.73**	-1.09	1.05	2.31	-0.56
Sgsm3	**-1.31**	0.56	**1.37**	1.51	-0.42
Slc12a5	**-2.57**	0.32	**1.50**	2.04	0.55
Slc16a13	**1.03**	**1.43**	**-1.84**	1.00	0.61
Slc16a2	**1.59**	0.80	**-2.39**	-1.37	-0.27
Slc16a4	**3.60**	0.61	**-3.87**	-1.09	-0.66
Slc16a9	**1.36**	-0.05	**-3.15**	1.59	0.88
Slc19a3	**3.69**	0.07	-2.48	-0.30	-0.91
Slc22a17	**-3.04**	0.09	-0.92	2.28	-0.36
Slc22a8	**3.49**	-0.23	**-3.65**	-1.01	-0.01
Slc38a3	**1.42**	-2.13	**-3.02**	**-3.21**	-0.11
Slc38a5	**4.54**	0.20	-0.03	0.00	**-2.82**
Slc39a8	**3.42**	-0.12	**-2.23**	**1.57**	**-3.70**
Slc45a3	-1.12	1.34	-1.19	1.77	-0.82
Slc46a1	**1.24**	0.33	**-2.96**	-1.13	-1.22
Slc7a8	0.89	1.55	**-2.80**	3.47	0.61
Slco1a4	**4.25**	1.03	**1.71**	**-3.04**	-0.03
Slco2b1	**4.37**	**1.44**	0.76	**-2.59**	-0.26
Smoc1	**-1.53**	**1.93**	-0.24	**-2.57**	-0.27
Smpd3	**-2.41**	0.99	**1.08**	-0.40	-0.17
Smyd2	**-1.16**	-0.90	**1.64**	0.88	0.63
Sncg	**-1.47**	**1.82**	**4.52**	4.31	1.06
Snx22	**-1.43**	0.30	**1.82**	1.31	-0.50
Snx24	-0.47	0.62	**-1.03**	1.23	-0.54
Sorbs2	**1.33**	-1.99	0.54	**-1.78**	0.12
Sparcl1	-0.96	**1.90**	**3.13**	-0.02	**-1.78**
Spats2l	**-1.60**	0.87	0.77	2.52	0.17
Sphk1	**-1.68**	**1.43**	**-1.85**	0.06	**-3.32**
Spint1	**3.18**	-0.03	**-2.76**	0.23	**-1.23**
Spock2	**1.46**	0.59	0.10	0.35	**-2.85**
Spry2	**-2.26**	0.22	**1.69**	3.34	0.22
Sspn	0.25	**-1.99**	1.43	1.73	0.26
St6galnac2	**3.74**	**1.30**	**-2.24**	-0.09	0.23
Stac2	**-3.08**	0.13	0.47	1.25	0.57
Steap3	**1.37**	0.13	-0.60	**-1.71**	**-1.26**
Stk39	**-2.66**	**-2.16**	**-1.64**	1.53	-0.29
Stmn2	**-2.98**	**2.10**	**3.73**	1.89	**1.92**
Stox2	**-1.71**	0.25	0.58	1.49	0.23
Stra6	**2.59**	1.37	-1.38	-0.04	0.06
Stxbp1	**-2.94**	**1.32**	**3.14**	3.47	**1.29**
Stxbp6	**-1.30**	**1.60**	-0.56	-0.83	**1.26**

bioRxiv preprint doi: https://doi.org/10.1101/708701; this version posted July 19, 2019. The copyright holder for this preprint (which was not certified by peer review) is the author/funder, who has granted bioRxiv a license to display the preprint in perpetuity. It is made available under aCC-BY-ND 4.0 International license.

Sulf2	**-1.21**	0.21	**1.95**	0.19	0.03
Sult1a1	**2.95**	**2.04**	**3.10**	**-1.02**	0.72
Sult5a1	**2.33**	0.73	0.27	**-2.61**	**-2.03**
Sybu	**-2.91**	0.55	**1.38**	-0.11	-1.13
Syn1	**-3.15**	0.12	0.15	1.39	0.50
Synpo	**-2.60**	-0.74	**1.53**	0.81	-0.58
Syt7	**-2.00**	0.35	**1.17**	1.63	0.19
Tbc1d9	**-1.08**	**1.47**	0.92	2.32	0.71
Tbx3	**2.71**	1.13	**1.81**	-1.56	**1.42**
Tbx4	**1.58**	0.07	0.29	0.25	**-2.10**
Tceal1	**-1.24**	-0.15	**1.01**	2.08	0.36
Tctex1d4	-1.21	0.22	0.83	2.02	**-2.89**
Tctn2	**-1.31**	0.76	-0.73	1.03	-0.12
Tdrkh	**-1.50**	0.85	0.65	0.98	**1.28**
Tfec	**1.64**	**1.14**	**-2.73**	3.73	**1.22**
Tgfa	0.89	**1.25**	0.37	-0.97	-1.33
Tgfb2	**1.26**	0.22	**1.46**	**1.45**	**-1.09**
Thbs2	**-1.26**	0.74	**2.36**	0.44	-0.36
Thrsp	0.12	-0.46	**1.88**	**-2.00**	-0.47
Thsd7a	-1.79	0.90	**1.06**	1.05	0.54
Timp1	-0.36	0.89	**1.92**	0.84	**-1.28**
Timp4	**-2.77**	**3.11**	**4.83**	0.13	0.32
Tlcd2	**1.86**	**1.29**	-0.42	**-1.82**	0.23
Tm6sf2	**2.40**	0.73	**-1.54**	**-2.52**	-0.20
Tmeff2	**-3.74**	0.43	0.00	-0.69	**1.81**
Tmem119	**4.85**	**1.05**	**2.41**	1.32	**-1.71**
Tmem132a	**-2.51**	0.67	0.99	2.20	0.43
Tmem132e	-1.37	0.12	0.26	3.30	-0.02
Tmem150a	**1.10**	-0.68	**-1.62**	**-1.49**	-0.85
Tmem181a	**-1.71**	0.04	0.64	1.51	0.16
Tmem182	-0.32	**-3.07**	**2.52**	0.00	-0.19
Tmem255a	**-3.41**	**1.09**	0.85	0.26	-0.03
Tmem47	**-3.10**	0.57	**2.20**	2.38	0.63
Tmem65	-0.97	**-1.41**	-0.05	1.86	0.26
Tnfrsf11b	-1.90	-0.29	**2.63**	-1.78	0.91
Tnfrsf19	**1.21**	-0.94	**1.08**	-1.14	-2.18
Tox2	**-3.04**	**1.55**	**1.12**	1.25	**1.56**
Tppp	**-2.57**	**1.19**	0.35	-0.21	0.78
Tram1l1	**-3.20**	0.18	0.19	0.40	**1.31**
Trim3	**-1.85**	1.16	**1.61**	1.60	-0.26
Trim32	**-2.45**	0.82	0.26	1.47	0.75
Trim62	**-1.77**	0.76	**1.95**	1.29	0.19
Trip6	**1.44**	**1.30**	0.55	0.49	**-1.64**
Trpc3	**-1.95**	-0.28	**1.40**	0.44	-0.36
Trpv4	**1.62**	**1.71**	**-2.40**	1.38	0.41
Tshz3	**-1.73**	0.16	**1.13**	1.13	-0.08
Tspan11	-1.75	**1.42**	0.77	0.79	**-3.06**

bioRxiv preprint doi: https://doi.org/10.1101/708701; this version posted July 19, 2019. The copyright holder for this preprint (which was not certified by peer review) is the author/funder, who has granted bioRxiv a license to display the preprint in perpetuity. It is made available under aCC-BY-ND 4.0 International license.

Tspan15	**-1.72**	**1.83**	**2.78**	3.62	-0.25
Tspan6	**-1.17**	**2.35**	**1.11**	2.61	0.92
Ttc9	**-1.37**	**2.32**	**1.87**	0.10	**-1.36**
Ttll7	**-1.75**	0.43	0.96	2.40	0.98
Uchl1	**-3.62**	0.31	**4.47**	1.18	**1.54**
Ucma	**-2.16**	**1.48**	0.00	0.00	0.11
Unc5a	**-2.20**	**1.15**	1.28	2.28	0.26
Upk1b	**3.49**	-0.43	**-1.85**	-0.77	**-3.52**
Ust	**-2.02**	0.19	0.24	1.34	-1.01
Vil1	**3.28**	0.70	**-3.39**	-0.60	0.46
Vnn3	**1.50**	-0.01	0.82	**-2.77**	-1.57
Vstm4	-1.98	-0.31	-1.28	2.30	**-1.86**
Vstm5	**-2.80**	**1.61**	-0.96	2.00	0.60
Wnt2	-2.10	**1.39**	**3.21**	4.94	-2.01
Wscd1	**-1.42**	**2.65**	**3.11**	2.97	**1.56**
Wt1	-0.21	**1.29**	-1.47	-0.30	-1.13
Zc2hc1a	**-2.53**	0.25	-0.43	1.76	-0.56
Zdhhc14	**-1.16**	0.76	0.91	1.86	0.15
Zfp13	**-1.53**	1.06	0.74	2.22	0.30
Zfp37	**-1.53**	0.89	1.32	2.11	0.09
Zfp382	**-1.43**	0.98	**1.80**	1.71	0.30
0610040B09Rik	-0.10	0.19	**-2.49**	2.00	0.57
1110018N20Rik	-2.25	-0.44	**2.64**	2.69	0.22
1110032F04Rik	-1.39	**1.11**	-0.22	-0.03	0.28
1500009L16Rik	**-3.37**	0.29	-0.47	-0.14	**1.10**
1600029D21Rik	-0.37	-0.43	**-3.66**	-1.69	**1.06**
2010001M06Rik	**-1.91**	1.12	**-2.18**	4.08	**-1.91**
2010012P19Rik	-0.17	0.35	-0.35	2.29	**-1.03**
2700033N17Rik	-1.62	-0.50	**2.24**	1.84	0.81
2810468N07Rik	**-2.92**	0.31	**1.69**	0.61	**1.25**
4631405J19Rik	-0.22	-2.55	**1.18**	0.00	0.27
4833424O15Rik	-2.85	-0.07	0.20	1.38	-0.03
4930506M07Rik	**-1.33**	**1.83**	0.84	0.29	0.46
4933436C20Rik	-0.58	**-1.01**	**2.50**	0.07	-1.68
5033430I15Rik	**-1.78**	-1.83	-0.59	1.06	0.22
5430416O09Rik	**2.39**	**1.71**	**2.93**	0.50	-1.21
5730409E04Rik	**-1.55**	0.79	**1.94**	1.80	**1.16**
9330179D12Rik	-2.59	-0.92	**1.13**	0.34	-0.24

Values represent enrichment scores (log2 fold changes) based on 3 biologic replicates. Bold font indicates significant scores (FDR<10%)

Supplemental Table S3: Comparison of high and low abundant EC-enriched genes identified by TRAP versus EC genes identified by single cell data RNASeq

	Transcripts overlapping between EC-TRAP and single cell RNASeq analysis		Total transcripts identified in single cell RNASeq analysis	
	Low abundant	High abundant		Reference
Brain	14	29	1798	Vanlandewijck et al. (27)
Heart	24	50	1294	Lother et al. (26)
Kidney	1	28	553	Han et al. (25)
Liver	0	28	216	Han et al. (25)
	11	67	2700	Tabula Muris (29)
	3	52	851	Tabula Muris (29)
Lung	1	44	349	Han et al. (25)
	2	77	1013	Tabula Muris (29)
	1	68	867	Tabula Muris (29)

bioRxiv preprint doi: https://doi.org/10.1101/708701; this version posted July 19, 2019. The copyright holder for this preprint (which was not certified by peer review) is the author/funder, who has granted bioRxiv a license to display the preprint in perpetuity. It is made available under aCC-BY-ND 4.0 International license.

Supplemental Table S4: Selected genes previously identified to be affected in endotoxemia

bioRxiv preprint doi: https://doi.org/10.1101/708701; this version posted July 18, 2019. The copyright holder for this preprint (which was not certified by peer review) is the author/funder, who has granted bioRxiv a license to display the preprint in perpetuity. It is made available under a CC-BY-ND 4.0 International license.

		Brain	Heart	Kidney	Liver	Lung
Adhesion	*Selp*	**2.84**	**5.69**	**3.96**	**2.53**	**1.80**
	Vcam1	0.88	**3.02**	**2.23**	-0.62	**3.20**
	Selp	**4.78**	**6.91**	**4.81**	**2.25**	**3.56**
	Sell	1.58	2.54	**1.42**	0.26	0.73
	Icam1	**1.65**	**4.60**	**2.22**	0.72	-0.03
Barrier function	*Cdh5*	**-1.55**	**-1.63**	**-0.98**	**-2.40**	**-1.89**
	Ctnna1	**-1.70**	-0.52	**-1.22**	**-2.16**	**-1.29**
	Ctnnb1	**-0.81**	**-1.39**	**-1.22**	-0.74	-1.91
	Ctnnd1	**-1.20**	**-1.52**	**-1.00**	**-1.36**	**-3.34**
	Gja1	0.96	-0.08	-1.24	-0.53	-0.67
	Gja4	**-0.89**	0.76	**-2.27**	**-2.02**	**-1.92**
	Gja5	**-3.84**	**-4.18**	**-4.73**	**-5.04**	**-2.70**
	Cldn5	**-3.99**	-1.08	**-1.73**	**-4.26**	0.14
	F11r	**-1.69**	0.26	**-0.96**	**-0.99**	-0.09
	Jam2	**-1.66**	**-0.70**	**-0.85**	**-2.55**	**-1.27**
	Jam3	1.29	**-1.96**	**-2.29**	**-2.20**	-1.31
	Ocln	**-3.14**	**-2.20**	2.59	-0.32	**-2.54**
	Tjp1	-0.07	**-1.99**	**-1.24**	-0.87	**-2.96**
	Tjp2	**-0.63**	**-1.51**	**-1.02**	**-2.18**	**-0.90**
Coagulation	*Thbd*	**-2.03**	**-2.57**	**-1.96**	**-0.98**	**-5.65**
	Tfpi	**-2.07**	-1.27	**-2.60**	**-4.55**	**-2.37**
	Procr	**-1.75**	**-0.51**	**-1.12**	**0.96**	**0.93**
	Serpine1	**0.58**	**4.43**	**4.55**	**4.90**	**5.47**
	Vwf	**-3.61**	**2.51**	**-2.40**	**-4.01**	-1.70
	F2r	-0.13	**-1.49**	**-2.04**	**-2.49**	-0.32
	Plau	**-2.90**	**-1.59**	-0.75	**-1.93**	1.02
	Plat	-0.37	-0.49	0.08	**-1.22**	1.04
	Plaur	**2.38**	**2.22**	**-0.63**	0.43	-0.25

Values represent log2 fold changes where positive values indicate upregulation and negative values indicate downregulation after LPS exposure. Bold font indicates significant scores (FDR<10%)

Supplemental Table S6: Genotyping primers and expected amplicon sizes.

Gene	Forward primer (5'-3')	Reverse primer (5'-3')	product sizes
Rpl22	GGGAGGCTTGCTGGATATG	TTTCCAGACACAGGCTAAGTACAC	290 bp (flox) 342 bp (null)
Tek (endogenous)	CCCTGTGCTCAGACAGAAATGAGA	TAAGCCGGCTAAAGAGTCCA	200 bp
Tek-Cre	CCCTGTGCTCAGACAGAAATGAGA	CGCATAACCAGTGAAACAGCATTG	579 bp
Rosa (endogenous)	CTCTGCTGCCTCCTGGCTTCT	CGAGGCGGATCACAAGCAATA	310 bp
Rosa^{mTmG}	CTCTGCTGCCTCCTGGCTTCT	TCAATGGGCGGGGGTCGCT	260 bp
EIIa-Cre	CCGCTGGAGATGACGTAGTT	CGCATAACCAGTGAAACAGCATTG	450 bp
Pf4-Cre	CCAAGTCCTACTGTTTCTCACTC	TGCACAGTCAGCAGGTT	390 bp

bioRxiv preprint doi: https://doi.org/10.1101/687201; this version posted July 19, 2019. The copyright holder for this preprint (which was not certified by peer review) is the author/funder, who has granted bioRxiv a license to display the preprint in perpetuity. It is made available under CC-BY-ND 4.0 International license.

bioRxiv preprint doi: https://doi.org/10.1101/708701; this version posted July 19, 2019. The copyright holder for this preprint (which was not certified by peer review) is the author/funder, who has granted bioRxiv a license to display the preprint in perpetuity. It is made available under aCC-BY-ND 4.0 International license.

Supplemental Table S6: Tek-enriched genes also enriched in platelet TRAP of Rpl22<fl/fl>, Pf4-Cre<+/0> mice

Brain				
A130010J15Rik	*Cyb5*	*Irf3*	*Pofut1*	*Stag2*
Aaed1	*Cyb561a3*	*Isg15*	*Polr2a*	*Stam2*
Aagab	*Cyb5r3*	*Itfg3*	*Polr2d*	*Stard3*
Abcb4	*Cyba*	*Itga6*	*Polr2e*	*Stard3nl*
Abcc3	*Cyth3*	*Itgal*	*Polr3gl*	*Stat3*
Abcc4	*D17H6S56E-5*	*Itgb1*	*Ppcdc*	*Stat5b*
Abhd2	*D8Ertd738e*	*Itgb2*	*Ppib*	*Stat6*
Acadm	*Dapp1*	*Itgb3*	*Ppp1ca*	*Stk24*
Acads	*Dcaf12*	*Itgb5*	*Ppp1r12c*	*Stk3*
Acer2	*Dctpp1*	*Itpkb*	*Ppp1r18*	*Stk40*
Actb	*Ddah2*	*Itsn2*	*Ppp2r1b*	*Stom*
Actg1	*Ddc*	*Jak2*	*Ppp2r5a*	*Stra13*
Actn4	*Ddi2*	*Katna1*	*Ppp6r1*	*Strip1*
Actr3	*Ddrgk1*	*Kdr*	*Ppp6r3*	*Stx2*
Acy3	*Dennd2c*	*Khk*	*Ppt2*	*Stx5a*
Adam10	*Dennd2d*	*Klc4*	*Pqlc1*	*Stx7*
Adam17	*Dennd6a*	*Klhl6*	*Prcp*	*Stxbp2*
Adh1	*Dera*	*Kpnb1*	*Prex1*	*Stxbp3a*
Adipor1	*Dhrs3*	*Krcc1*	*Prkab1*	*Sumf1*
Adipor2	*Dnajc1*	*Lamc1*	*Prkcd*	*Supt4a*
Adora3	*Dnajc10*	*Lamp1*	*Prorsd1*	*Surf4*
Afap1l1	*Dnajc17*	*Lamtor1*	*Proser2*	*Susd3*
Aga	*Dnajc3*	*Laptm4a*	*Prr13*	*Syf2*
Agtrap	*Dnase1l1*	*Laptm5*	*Prrg2*	*Syk*
Ak2	*Dnm2*	*Lasp1*	*Psma7*	*Syngr2*
Akap13	*Dock11*	*Lat*	*Psme1*	*Tab2*
Akr1a1	*Dok1*	*Layn*	*Ptbp1*	*Tacc1*
Akr1b10	*Dok2*	*Lcn2*	*Ptbp3*	*Taf12*
Aldh9a1	*Dpf2*	*Ldlrap1*	*Ptgs1*	*Tagln2*
Alg14	*Dscr3*	*Lefty1*	*Ptplad2*	*Tal1*
Alkbh5	*Dusp16*	*Leprot*	*Ptpn1*	*Taldo1*
Alox12	*Dusp23*	*Lgals3bp*	*Ptpn18*	*Tapbp*
Alox5ap	*Dusp3*	*Lgals9*	*Ptpn22*	*Tapbpl*
Amdhd2	*Ech1*	*Limd1*	*Ptprj*	*Tax1bp3*
Anapc11	*Ecm1*	*Lims1*	*Ptrf*	*Tbc1d14*
Angptl7	*Edem1*	*Lmf2*	*Pttg1*	*Tbc1d22a*
Ankrd13a	*Eef2k*	*Lmo2*	*Pttg1ip*	*Tbxas1*
Ano6	*Ehbp1l1*	*Lpcat3*	*Pxdc1*	*Tcn2*
Anxa5	*Ehd4*	*Lpp*	*Pxk*	*Tex261*
Anxa7	*Eif4e2*	*Lrp10*	*Pxmp4*	*Tfe3*
Ap1s2	*Eif4ebp3*	*Lrp8*	*Pycard*	*Tgfb1*
Ap3b1	*Eif4g3*	*Lrrc25*	*Pygl*	*Tgm2*
Aph1a	*Elf2*	*Lrrc32*	*Qsox1*	*Tie1*
Apold1	*Elovl1*	*Lrrc8a*	*Rab13*	*Timm17b*
Arap1	*Epb4.1*	*Lrrc8c*	*Rab27a*	*Timp3*

bioRxiv preprint doi: https://doi.org/10.1101/708701; this version posted July 19, 2019. The copyright holder for this preprint (which was not certified by peer review) is the author/funder, who has granted bioRxiv a license to display the preprint in perpetuity. It is made available under aCC-BY-ND 4.0 International license.

Arf6
Arhgap10
Arhgap18
Arhgap31
Arhgdia
Arhgdib
Arpc1b
Arpc2
Arpc3
Arpc4
Arpc5
Arrb2
Arrdc1
As3mt
Asf1b
Atl3
Atox1
Atp1b3
Atp6v0a2
Atp6v1g1
Aup1
B230378P21Rik
B4galt1
Bach1
Bak1
Bax
Bbc3
BC004004
BC017643
BC026585
Bcat2
Bckdk
Bcl10
Bid
Bin1
Bin2
Bin3
Bloc1s5
Blvrb
Bmp2
Bmp2k
Bri3
Bsg
Bst2
Btbd7
Calr
Calu
Camk1
Cap1
Epb4.1l2
Erp29
Esam
Etfb
Etv6
Evi2a
F11r
Fadd
Fam102b
Fam105b
Fam114a2
Fam126a
Fam212a
Fam219b
Fam43a
Fam63a
Fam63b
Fam76a
Fam78a
Fam89b
Fam96a
Fancg
Fas
Fbxw2
Fcer1g
Fermt3
Fez2
Fgd3
Fhl3
Fhod1
Fli1
Flii
Flna
Fmo5
Fnta
Frmd8
Fuca1
Furin
Fyco1
Gab2
Gabarap
Galk1
Galnt1
Gata2
Gatad2a
Gcnt1
Gcnt2
Ggh
Gimap6
Lrrfip1
Lrrk1
Lyl1
Lyn
Lyve1
Lyz1
Lyz2
M6pr
Mad2l2
Magt1
Maml2
Man1a
Man2b1
Map2k2
Map4k4
Mapk14
Mapk3
Mapkapk2
Mapkapk3
Mapre1
Marcks
Mavs
Mbd2
Mbd6
Mcl1
Mcur1
Med10
Med11
Med20
Mepce
Mesdc2
Mfap3
Mfng
Mgat1
Mgme1
Mgmt
Micu2
Mill2
Mis18a
Mknk1
Mknk2
Mlec
Mob1a
Mob2
Mob3a
Mocs1
Mpp1
Mprip
Mrpl44
Rab31
Rab32
Rab35
Rab3d
Rab43
Rab7l1
Rac1
Ralb
Rap1a
Rap1b
Rarg
Rb1
Rbm17
Rbm38
Rbms1
Rbpj
Rbpms
Rcan1
Rcbtb2
Rcor1
Rfk
Rgs10
Rgs12
Rhbdf2
Rhoa
Rhob
Rhoc
Rhog
Rhoj
Ric8
Rin3
Rit1
Rnaseh2c
Rnf114
Rnf125
Rnf144b
Rnf166
Rnf185
Rnpepl1
RP24-176F12.14
Rpain
Rpn2
Rps27l
Rps6kb2
Rragc
Rras
Rsu1
Rtfdc1
S100a13
Tjp2
Tk2
Tln1
Tlr12
Tm4sf1
Tm9sf2
Tmbim1
Tmbim6
Tmc6
Tmcc3
Tmco1
Tmed10
Tmed2
Tmed3
Tmed7
Tmem109
Tmem123
Tmem140
Tmem14c
Tmem159
Tmem198b
Tmem219
Tmem223
Tmem234
Tmem248
Tmem43
Tmem50a
Tmem59
Tmem86a
Tmod3
Tnfaip8l2
Tnfrsf21
Topbp1
Tor1aip1
Tor4a
Tpcn1
Tpd52
Tpm3
Tpm4
Tpp1
Trabd
Traf7
Trafd1
Tram2
Trappc6a
Trem1
Treml2
Trim24
Trim5

bioRxiv preprint doi: https://doi.org/10.1101/708701; this version posted July 19, 2019. The copyright holder for this preprint (which was not certified by peer review) is the author/funder, who has granted bioRxiv a license to display the preprint in perpetuity. It is made available under aCC-BY-ND 4.0 International license.

Capn2
Capns1
Capza1
Capzb
Casp3
Casp6
Cass4
Cat
Ccdc115
Ccdc12
Ccdc50
Ccl3
Ccnd1
Ccnd3
Ccng2
Ccs
Ccser2
Cd151
Cd1d1
Cd200r1
Cd274
Cd63
Cd81
Cd84
Cd93
Cd97
Cdc26
Cdc42
Cdc42ep4
Cdh23
Cdk19
Cdk2ap2
Cdk6
Cdk9
Cdkn1a
Cebpa
Cebpb
Cebpg
Cenpb
Cenpo
Cers2
Chi3l7
Chmp2a
Chmp3
Chrac1
Chsy1
Cib1
Clic1
Clic4
Ginm1
Git2
Glb1
Gltp
Gm12942
Gm13476
Gm13840
Gm15503
Gm16266
Gm20492
Gm26510
Gm26880
Gm4070
Gm5617
Gna12
Gna13
Gnai2
Gnai3
Golph3l
Gp9
Gpbp1l1
Gpcpd1
Gpr108
Gpr146
Gpr56
Gpr97
Gpsm3
Gpx1
Grn
Gsap
Gtf3c6
Gucd1
H2-D1
H2-K1
H2-T22
H2-T23
H2-T24
H3f3a
H3f3b
Hadha
Hcls1
Hcst
Hdac7
Heca
Herpud1
Hexa
Hgsnat
Hhex
Hipk1
Msn
Msrb2
Mtdh
Mtfr1l
Mthfs
Mtmr14
Mtus1
Mvp
Mxd4
Myd88
Myh9
Myl6
Mylk
Mylpf
Myo9b
Myom1
Naga
Ncf1
Ncoa3
Ncstn
Nde1
Ndrg1
Ndufa7
Necap2
Nek7
Nek9
Neurl3
Nfe2
Ninj1
Nkiras2
Nosip
Nqo2
Nras
Nrbp1
Nubp2
Nucb1
Nudt7
Numb
Nxt1
Oard1
Oas3
Ogfr
Ogg1
Orai1
Orai3
Oraov1
Ostc
Ostf1
P2rx1
S1pr2
Sat1
Sav1
Sbno2
Scamp2
Scarb1
Scarf1
Scp2
Sdcbp
Sdf4
Sdpr
Sec11a
Sec13
Sec24b
Sec61a1
Sec61b
Sema4d
Sept2
Sept15
Serf2
Serhl
Serinc3
Serp1
Serpinb9
Sertad1
Sertad2
Sft2d1
Sgce
Sh2b3
Sh3glb1
Shc1
Shfm1
Sin3b
Skap2
Ski
Skil
Sla
Slain2
Slc16a10
Slc16a3
Slc25a1
Slc25a20
Slc25a24
Slc30a1
Slc35a3
Slc35a4
Slc35b2
Slc39a1
Slc39a11
Trim56
Triobp
Trp53inp1
Trpv2
Tsc22d1
Tsc22d3
Tspan14
Tspan31
Tspan32
Tspan9
Tspo
Ttc23
Ttc28
Ttc7
Tuba1c
Twf1
Twf2
Uba7
Ubald2
Ube2g2
Ube2i
Ube2q1
Ubiad1
Ubn1
Ubxn1
Ulk2
Unc119b
Unc50
Usp12
Usp25
Vamp5
Vamp8
Vasp
Vav1
Vkorc1
Vps25
Vps37b
Vps72
Vwf
Was
Wasf2
Wdr1
Wdsub1
Wipf1
Wnk1
Xbp1
Yap1
Yif1b
Ykt6

bioRxiv preprint doi: https://doi.org/10.1101/708701; this version posted July 19, 2019. The copyright holder for this preprint (which was not certified by peer review) is the author/funder, who has granted bioRxiv a license to display the preprint in perpetuity. It is made available under aCC-BY-ND 4.0 International license.

Clint1	*Hipk3*	*P2ry13*	*Slc3a2*	*Zbtb42*
Clk3	*Hmgcl*	*Pacsin2*	*Slc44a2*	*Zcchc2*
Cln5	*Hmha1*	*Palm*	*Slc6a6*	*Zdhhc18*
Cmtm3	*Hnrnpab*	*Pan3*	*Slc7a5*	*Zdhhc7*
Cmtm6	*Hnrnpf*	*Paqr7*	*Slc9a9*	*Zfand2b*
Cnbp	*Hnrnpm*	*Parvb*	*Slpi*	*Zfp362*
Cndp2	*Hnrnpul1*	*Pcbp2*	*Smagp*	*Zfp36l2*
Cnn2	*Hpgd*	*Pcif1*	*Smap2*	*Zfp422*
Cnot6	*Hpn*	*Pcp4l1*	*Smarcd2*	*Zfp646*
Cnot8	*Hps1*	*Pcsk7*	*Smox*	*Zfp652*
Cnppd1	*Hps4*	*Pdcd6ip*	*Smtn*	*Zfp710*
Cnpy3	*Hpse*	*Pdk1*	*Smurf1*	*Zfp746*
Cnr2	*Hs1bp3*	*Pear1*	*Smurf2*	*Zfp830*
Commd1	*Hsd3b7*	*Pecam1*	*Snrpc*	*Zfyve21*
Commd6	*Hspa5*	*Pfkfb3*	*Snx1*	*Znrf2*
Commd7	*Htatip2*	*Pfkfb4*	*Snx17*	*Zyx*
Coro1b	*I830012O16Rik*	*Pggt1b*	*Snx4*	*0610010K14Rik*
Cpne3	*Iah1*	*Pgm1*	*Snx5*	*0610031J06Rik*
Cpt1a	*Ifi27*	*Pgpep1*	*Sord*	*1110001A16Rik*
Cpt2	*Ifit3*	*Phc1*	*Sp3*	*1110007C09Rik*
Cr1l	*Ifitm2*	*Phc2*	*Sphk2*	*1600012H06Rik*
Cradd	*Ifitm3*	*Pigc*	*Sppl2a*	*1700017B05Rik*
Crtap	*Ifnar1*	*Pip4k2a*	*Spsb2*	*1700034P13Rik*
Csk	*Ifrd2*	*Pla2g16*	*Sptlc2*	*1810009A15Rik*
Csnk1e	*Igtp*	*Pla2g4a*	*Srd5a3*	*2200002D01Rik*
Ctbs	*Ikbkb*	*Plek*	*Srgap2*	*2210404O07Rik*
Ctdsp1	*Il21r*	*Plekha2*	*Srgn*	*2310011J03Rik*
Ctdsp2	*Il27ra*	*Plekhm1*	*Sri*	*2510039O18Rik*
Ctnna1	*Ilk*	*Plekho1*	*Srp68*	*2610001J05Rik*
Ctnnb1	*Ing1*	*Plscr1*	*Srpr*	*2900026A02Rik*
Ctsa	*Inpp5b*	*Pmm2*	*Srsf9*	*4931406C07Rik*
Ctsd	*Inpp5d*	*Pmp22*	*Ss18*	*4931406P16Rik*
Ctsw	*Inpp5k*	*Pnkp*	*Ssr4*	*5031425E22Rik*
Ctsz	*Irak3*	*Pnpla2*	*St3gal1*	*5031439G07Rik*
Cuta	*Irak4*	*Pnrc1*	*St6galnac3*	

Heart

Aagab	*Ctnnb1*	*Il27ra*	*Ppap2b*	*St3gal1*
Abcc4	*Ctps2*	*Ilk*	*Ppib*	*St3gal2*
Abhd16a	*Ctsa*	*Incenp*	*Ppm1g*	*St6galnac3*
Abhd17a	*Ctsz*	*Inf2*	*Ppp1ca*	*Stag2*
Abhd4	*Cttn*	*Ing1*	*Ppp1cc*	*Stam2*
Abi1	*Cuedc1*	*Inpp4a*	*Ppp1r12c*	*Stard3nl*
Acd	*Cuedc2*	*Inpp5b*	*Ppp1r13b*	*Stard4*
Acer2	*Cul4b*	*Inpp5d*	*Ppp1r15b*	*Stim2*
Actb	*Cuta*	*Inpp5f*	*Ppp1r16b*	*Stk16*
Actg1	*Cyb5r3*	*Inpp5k*	*Ppp1r18*	*Stk19*
Actn1	*Cyba*	*Ipo11*	*Ppp1r2*	*Stk24*

bioRxiv preprint doi: https://doi.org/10.1101/708701; this version posted July 19, 2019. The copyright holder for this preprint (which was not certified by peer review) is the author/funder, who has granted bioRxiv a license to display the preprint in perpetuity. It is made available under aCC-BY-ND 4.0 International license.

Actn4
Actr3
Adam10
Adam17
Adam9
Adarb1
Add3
Adh1
Adprh
Aebp2
Afap1l1
Aftph
Agap3
Agpat5
AI837181
Aip
Akap5
Akr1a1
Aldh18a1
Aldh9a1
Alg14
Alkbh6
Amdhd2
Anapc11
Anapc16
Anapc2
Ankfy1
Ankrd13a
Ano6
Anxa5
Anxa7
Ap1g1
Ap1m1
Ap1s1
Ap2m1
Ap2s1
Aplp2
Apold1
Aqp1
Arcn1
Arf1
Arf3
Arf6
Arfgap3
Arhgap1
Arhgap10
Arhgap18
Arhgap23
Arhgap28
Cyth1
Cyth3
D17H6S56E-5
Dcaf12
Dck
Dcp1b
Dctn5
Dda1
Ddah2
Ddi2
Ddit3
Ddrgk1
Ddx47
Ddx5
Degs1
Dennd2c
Dennd5a
Dera
Dgkd
Dgkz
Dhrs3
Dhx38
Dlgap4
Dnajb11
Dnajc3
Dnajc7
Dnase1l1
Dok1
Dok2
Dpy19l1
Drg1
Dscr3
Dusp16
Dusp3
Dxo
Dync1i2
Dync1li2
Dynlt1a
Ecm1
Edc3
Edem1
Efcab14
Egln2
Ehd3
Ehmt2
Eif1a
Eif1ad
Eif4e2
Eif4ebp3
Irak4
Isg15
Itga6
Itgb1
Itm2b
Itpkb
Itsn2
Izumo4
Jak2
Josd1
Jup
Katna1
Kctd20
Kctd7
Kdm2a
Kdr
Khk
Klc1
Klf9
Klhdc4
Klhl6
Kmt2e
Knop1
Kpnb1
Lamp1
Lamtor2
Laptm4a
Lasp1
Layn
Lcn2
Ldlrap1
Lefty1
Leprot
Lgals3bp
Lgals9
Lman2
Lmf2
Lpin2
Lrp10
Lrpap1
Lrrc25
Lrrc29
Lrrc32
Lrrc59
Lrrc8a
Lrrc8b
Lrrc8c
Lrrc8d
Lrrfip1
Ppp1r9b
Ppp2ca
Ppp2cb
Ppp2r4
Ppp2r5a
Ppp3ca
Ppt1
Pqlc1
Prcp
Prdm4
Prelid1
Prex1
Prkaa1
Prkacb
Prkcd
Prkcdbp
Prkce
Prmt2
Prr13
Prr24
Prrc2b
Prrg2
Psen1
Psmb4
Psmd4
Psmd9
Psme1
Ptbp1
Ptbp3
Ptgs1
Ptk2
Ptms
Ptplad2
Ptpn1
Ptpn12
Ptpn18
Ptpra
Ptpre
Ptrf
Pttg1ip
Pum2
Pxdc1
Pxk
Qpctl
Qsox1
Rab1
Rab13
Rab18
Rab27a
Stk25
Stk3
Stk4
Strn4
Stx12
Stx18
Stx2
Stx4a
Stx5a
Stx6
Stx7
Sumo3
Supt4a
Surf1
Surf2
Susd1
Suv420h1
Syf2
Tab2
Tacc1
Tada3
Tagln2
Tal1
Taok3
Tapbp
Tapbpl
Tax1bp3
Tbc1d14
Tbc1d20
Tbc1d22a
Tbc1d9b
Tbcb
Tbl1x
Tcf25
Tcn2
Tdrd7
Ten1
Tex261
Tfe3
Tgfb1
Thap7
Tie1
Timm17b
Timp3
Tinf2
Tjp2
Tln1
Tm2d2
Tm2d3

bioRxiv preprint doi: https://doi.org/10.1101/708701; this version posted July 19, 2019. The copyright holder for this preprint (which was not certified by peer review) is the author/funder, who has granted bioRxiv a license to display the preprint in perpetuity. It is made available under aCC-BY-ND 4.0 International license.

Arhgap31
Arhgdia
Arhgdib
Arhgef12
Arid1a
Arid2
Armcx6
Arpc1b
Arpc2
Arpc3
Arpc4
Arpc5
Arrb1
Arrb2
Arrdc1
Arsa
Asap1
Asf1b
Asl
Atf5
Atg4b
Atg7
Atic
Atox1
Atp1b3
Atp2a3
Atp6v0b
Atp6v0d1
Atp6v1a
Atxn7l3b
Aup1
Bad
Bak1
Bax
Bbc3
BC005624
BC017643
BC029214
Bcl10
Bcl2
Bcl7b
Bcr
Becn1
Bet1l
Bicd2
Bid
Bin1
Bin3
Blmh
Eif4g3
Elf2
Elovl1
Emc10
Emilin1
Eno1
Ensa
Epor
Eps15
Erbb2ip
Ercc3
Ergic1
Ergic3
Erp29
Esam
Etnk1
Etv6
Exoc5
Ezh1
F11r
F2r
F2rl3
Fam102b
Fam104a
Fam105b
Fam107b
Fam134a
Fam13b
Fam168b
Fam172a
Fam175b
Fam192a
Fam195b
Fam212a
Fam219b
Fam222b
Fam32a
Fam3c
Fam43a
Fam53b
Fam53c
Fam57b
Fam63a
Fam76a
Fam89b
Fancg
Fas
Fbxl2
Fbxo46
Lrrk1
Lsm1
Lsm14a
Ly6g6d
Lyl1
Lyn
Lypla2
Lyve1
Lyz2
M6pr
Mad1l1
Mad2l2
Madd
Maml2
Man1a
Man1a2
Man1b1
Man2b1
Manbal
Manf
Map2k1
Map2k5
Mapk1
Mapk3
Mapre1
Marcks
Mark2
Marveld1
Mbd2
Mcf2l
Mcl1
Mea1
Med11
Med13l
Med4
Mepce
Mesdc2
Mest
Mfap3
Mfng
Mfsd4
Mfsd6
Mgat1
Mgll
Micu1
Mill2
Mis18a
Mknk1
Mob1a
Rab31
Rab32
Rab35
Rab3d
Rab43
Rab4b
Rab5a
Rab5c
Rab7
Rab7l1
Rab9
Rabif
Rac1
Rad21
Rad9a
Ralb
Ralbp1
Rap1b
Rap1gds1
Rap2a
Rap2b
Rarg
Rasa3
Rbck1
Rbm17
Rbms1
Rcbtb2
Rcc2
Rce1
Reep2
Rer1
Rffl
Rgs10
Rgs12
Rhbdf2
Rhoa
Rhob
Rhoc
Rhog
Rhoj
Ric8
Rin3
Rit1
Rlim
Rnaseh2c
Rnf125
Rnf141
Rnf144a
Rnf167
Tm4sf1
Tm7sf3
Tmbim1
Tmbim6
Tmc6
Tmcc2
Tmcc3
Tmed10
Tmed3
Tmem115
Tmem140
Tmem158
Tmem159
Tmem175
Tmem189
Tmem198b
Tmem219
Tmem222
Tmem234
Tmem241
Tmem248
Tmem29
Tmem50a
Tmem59
Tmem63a
Tmem68
Tmem9
Tmod3
Tmppe
Tnfaip8l2
Tnfrsf21
Tnks2
Tollip
Topbp1
Tor1a
Tor4a
Tox4
Tpcn1
Tpd52
Tpm3
Tpm4
Tpst2
Trabd
Traf7
Tram2
Trappc3
Trappc6a
Trim37
Trim39

bioRxiv preprint doi: https://doi.org/10.1101/708701; this version posted July 19, 2019. The copyright holder for this preprint (which was not certified by peer review) is the author/funder, who has granted bioRxiv a license to display the preprint in perpetuity. It is made available under aCC-BY-ND 4.0 International license.

Bloc1s5
Blvrb
Bmp2k
Brap
Brd9
Brox
Bst2
Btbd2
Btbd7
C1galt1c1
C230081A13Rik
Cald1
Calm1
Calr
Camk1
Cant1
Cap1
Capn2
Capns1
Capza1
Capzb
Car7
Casp6
Ccdc115
Ccdc12
Ccdc124
Ccdc50
Ccdc71
Ccdc9
Ccnd1
Ccnd3
Ccndbp1
Ccng2
Ccny
Ccs
Cd274
Cd2bp2
Cd44
Cd55
Cd63
Cd81
Cd93
Cd97
Cdc42
Cdc42ep2
Cdc42ep4
Cdc42se2
Cdca8
Cdh23
Fbxo7
Fcer1g
Fchsd1
Fez2
Fhod1
Fis1
Fkbp2
Fkbp8
Fli1
Foxj2
Frmd8
Fuca1
Furin
Fxyd2
Fyn
G3bp2
G6pdx
Gab2
Gabarapl1
Gak
Galk1
Galk2
Gars
Gata2
Gatad2a
Gcnt1
Gcnt2
Gga1
Ggh
Ggnbp2
Gimap6
Gipc1
Git1
Git2
Gle1
Glipr2
Glod4
Gls
Gltp
Gltpd1
Gm12942
Gm16286
Gm20492
Gm26880
Gna12
Gnai2
Gnai3
Gnaq
Gnas
Mob2
Mob3a
Mon1b
Morf4l2
Mospd3
Mpp1
Mprip
Mras
Msn
Mtch1
Mtf1
Mthfd1l
Mthfs
Mtmr12
Mtmr6
Mtss1l
Mvp
Mxd4
Myd88
Myl6
Mylk
Mylpf
Mysm1
Naa60
Naaa
Naga
Nav1
Ncaph2
Nck2
Ncoa3
Ncstn
Nde1
Ndel1
Ndrg1
Necap2
Nedd8
Nelfe
Neurl3
Ngfrap1
Ninj1
Nkap
Nmb
Nosip
Nr1h2
Nras
Nsfl1c
Nub1
Nubp2
Nudcd3
Rnf185
Rnf187
Rnf38
Rnf41
Rnf44
Rpain
Rpn2
Rqcd1
Rragc
Rras
Rrp7a
Rsu1
Rtf1
Rtfdc1
Rtn3
Rybp
S100a10
S100a13
S1pr2
Samd1
Samd4b
Sat1
Scamp2
Scarb1
Scarf1
Sdcbp
Sdf4
Sdpr
Sec11a
Sec13
Sec14l1
Sec22b
Sec24b
Sec61a1
Sec61b
Sec62
Secisbp2l
Seh1l
Sel1l
Selm
Selt
Sept2
Sept9
Sept11
Sept15
Sepw1
Serf2
Serinc3
Serp1
Trim5
Trim56
Triobp
Trpv2
Tsc22d3
Tsg101
Tspan14
Tspan17
Tspan18
Tspan31
Tspan9
Tspo
Ttc23
Ttc28
Ttc5
Ttyh3
Tuba1a
Tubb2a
Tubb2b
Twf1
Txndc15
Txnrd1
U2af1
Uba7
Ubald1
Ubb
Ube2h
Ube2i
Ube2j1
Ube2j2
Ube2q1
Ube2s
Ube2z
Ubfd1
Ubn1
Ubxn1
Ubxn2b
Ubxn8
Uhmk1
Unc119b
Upp1
Uso1
Usp22
Usp6nl
Vamp5
Vamp8
Vasp
Vill
Vipas39

bioRxiv preprint doi: https://doi.org/10.1101/708701; this version posted July 19, 2019. The copyright holder for this preprint (which was not certified by peer review) is the author/funder, who has granted bioRxiv a license to display the preprint in perpetuity. It is made available under aCC-BY-ND 4.0 International license.

Cdipt
Cdk19
Cdk2ap2
Cdk6
Cdk9
Cdkn1a
Cdkn2aipnl
Cdkn2d
Cebpg
Cenpb
Cenpo
Cep170
Cep72
Cerk
Cers2
Cfl1
Cggbp1
Chek2
Chmp1a
Chmp2a
Chmp2b
Chmp3
Chmp6
Chmp7
Chst11
Chst12
Chsy1
Cib1
Cinp
Ckap4
Clec4d
Clic1
Clic4
Cmip
Cmtm3
Cmtm6
Cnbp
Cndp2
Cnep1r1
Cnn2
Cnot8
Cnp
Cnppd1
Cnpy3
Cnr2
Colec12
Commd7
Comtd1
Cops7a
Gnb1
Gnb2
Gng12
Gnpda2
Gnptg
Golga7
Gorasp2
Gpr56
Gpr97
Gpsm3
Gpx1
Grk5
Grk6
Grn
Gsap
Gsk3a
Gskip
Gsr
Gstt1
Gtf2e2
Gypc
H2afz
H2-D1
H2-K1
H2-T22
H2-T23
H2-T24
H3f3a
H3f3b
Hcls1
Hcst
Hdac5
Hdac7
Hexa
Hexdc
Hexim1
Hgsnat
Hipk1
Hivep2
Hmg20a
Hnrnpc
Hnrnpf
Hnrnph2
Hnrnpk
Hnrnpm
Hnrnpu
Homer3
Hp1bp3
Hpcal1
Nudt9
Numb
Nup50
Nup62
Nxt1
Oaz2
Ogfr
Orai3
Oraov1
Os9
Ostc
Ostf1
Ostm1
Otub1
P2ry13
Pacs1
Pafah1b2
Pagr1a
Palm
Pan3
Panx1
Papss2
Parvb
Pbx2
Pcbp1
Pcbp2
Pcif1
Pck2
Pdcd6
Pdcd6ip
Pde2a
Pdia3
Pdlim1
Pdzd8
Pea15a
Pear1
Pecam1
Pef1
Peg12
Pex14
Pfkfb3
Pfn1
Pgam1
Pgm1
Pgm2l1
Phc2
Phf1
Phf23
Pip4k2c
Serpinb9
Sertad1
Sft2d1
Sgce
Sh2b3
Sh3gl1
Sh3glb2
Shc1
Sigmar1
Sin3b
Sirt7
Skap2
Ski
Skil
Slc12a6
Slc16a3
Slc25a24
Slc25a25
Slc30a1
Slc35a4
Slc38a6
Slc39a11
Slc39a4
Slc39a6
Slc39a9
Slc3a2
Slc44a1
Slc44a2
Slc6a6
Slc9a3r1
Slpi
Slu7
Smagp
Smap1
Smarcd2
Smc1a
Smg6
Smg7
Smox
Smu1
Smurf2
Snap29
Snd1
Snf8
Snrnp25
Snrpc
Snw1
Snx1
Snx11
Vkorc1
Vps25
Vps28
Vps29
Vps33a
Vps4b
Vps51
Vps53
Vwf
Wasf2
Wbscr27
Wdfy1
Wdr1
Wdr26
Wdsub1
Whamm
Wipf1
Wrap73
Wwox
Wwp2
Ypel3
Ywhab
Ywhah
Zc3h4
Zcchc10
Zcchc2
Zcchc6
Zdhhc16
Zdhhc18
Zdhhc20
Zdhhc7
Zfand2b
Zfand3
Zfp281
Zfp362
Zfp414
Zfp422
Zfp426
Zfp652
Zfp664
Zfp715
Zfp746
Zfp830
Zfyve20
Zmiz2
Zmynd11
Znhit1
Zyx
0610010K14Rik

bioRxiv preprint doi: https://doi.org/10.1101/708701; this version posted July 19, 2019. The copyright holder for this preprint (which was not certified by peer review) is the author/funder, who has granted bioRxiv a license to display the preprint in perpetuity. It is made available under aCC-BY-ND 4.0 International license.

Copz1	*Hpgd*	*Pip5k1c*	*Snx17*	*0610031J06Rik*
Coro1b	*Hps1*	*Pitpnm2*	*Snx3*	*1500011B03Rik*
Coro1c	*Hs1bp3*	*Pkp4*	*Snx4*	*1600012H06Rik*
Cox6a1	*Hsd17b12*	*Pla2g4a*	*Specc1*	*1700017B05Rik*
Cpe	*Hsd3b7*	*Plek*	*Spin1*	*1700037C18Rik*
Cpne3	*Hsdl1*	*Plekha2*	*Spire1*	*1810009A15Rik*
Cpne8	*Hsp90b1*	*Plekhm1*	*Sppl2a*	*2200002D01Rik*
Cr1l	*Hspa2*	*Plekho1*	*Sppl2b*	*2310011J03Rik*
Crcp	*Htra2*	*Plekho2*	*Sppl3*	*2310036O22Rik*
Creb3l1	*I830012O16Rik*	*Plscr1*	*Spred2*	*2310047M10Rik*
Crebbp	*Iah1*	*Plvap*	*Spsb2*	*2510039O18Rik*
Crk	*Ica1*	*Plxna4*	*Sptlc2*	*2610524H06Rik*
Crkl	*Ifi27*	*Pmm2*	*Spty2d1*	*2700012I20Rik*
Crlf2	*Ifit3*	*Pmp22*	*Srd5a3*	*2900026A02Rik*
Crtap	*Ifitm10*	*Pnkp*	*Srgap2*	*3110082I17Rik*
Csk	*Ifitm2*	*Pofut1*	*Srgn*	*4931406P16Rik*
Csnk1d	*Ifitm3*	*Poldip3*	*Sri*	*5031425E22Rik*
Csnk1e	*Ifnar1*	*Pole3*	*Srsf9*	*5031439G07Rik*
Csrp1	*Ift20*	*Polr2d*	*Ss18*	*8430427H17Rik*
Ctdsp2	*Ift27*	*Polr2e*	*Ssbp3*	*9130401M01Rik*
Ctdspl	*Igtp*	*Polr3gl*	*Ssna1*	*9430023L20Rik*
Ctif	*Ikbkb*	*Pop7*	*Ssu72*	*9530082P21Rik*

Kidney

Aagab	*Dck*	*Itga6*	*Pofut1*	*Ss18*
Aar2	*Dclk2*	*Itgal*	*Poldip3*	*Ssna1*
Abca7	*Dcp1b*	*Itgb1*	*Polg*	*Ssu72*
Abcc3	*Dctn3*	*Itgb2*	*Polr2d*	*St3gal1*
Abcc4	*Dctn4*	*Itgb3*	*Polr3gl*	*St3gal2*
Abhd12	*Dctn5*	*Itgb4*	*Pop7*	*St3gal4*
Abhd17a	*Dctn6*	*Itgb5*	*Ppap2b*	*St3gal5*
Abi1	*Dcun1d5*	*Itm2b*	*Ppib*	*St6galnac3*
Acbd3	*Dda1*	*Itpkb*	*Ppil1*	*Stat3*
Acd	*Ddah2*	*Itsn1*	*Ppm1g*	*Stat5b*
Acer2	*Ddit3*	*Jak1*	*Ppme1*	*Stat6*
Actb	*Ddx47*	*Josd2*	*Ppp1ca*	*Stim1*
Actg1	*Dennd2c*	*Jup*	*Ppp1r12c*	*Stim2*
Actn4	*Dennd4a*	*Kansl2*	*Ppp1r13b*	*Stk11*
Actr1a	*Dennd5a*	*Kctd20*	*Ppp1r16b*	*Stk19*
Actr3	*Dffa*	*Kdm2a*	*Ppp1r18*	*Stk4*
Adam10	*Dgkz*	*Kdr*	*Ppp1r2*	*Stom*
Adam17	*Dhps*	*Khsrp*	*Ppp1r3d*	*Strn*
Adarb1	*Dhx38*	*Kif3c*	*Ppp1r9b*	*Strn4*
Add1	*Dlgap4*	*Klc1*	*Ppp2ca*	*Stub1*
Adipor1	*Dnajc10*	*Klhl6*	*Ppp2cb*	*Stx12*
Adora3	*Dnajc17*	*Kmt2e*	*Ppp2r1a*	*Stx2*
Adprh	*Dnajc7*	*Kpnb1*	*Ppp2r4*	*Stx4a*
Afap1l1	*Dnase1l1*	*Lamc1*	*Ppp2r5a*	*Stx5a*

bioRxiv preprint doi: https://doi.org/10.1101/708701; this version posted July 19, 2019. The copyright holder for this preprint (which was not certified by peer review) is the author/funder, who has granted bioRxiv a license to display the preprint in perpetuity. It is made available under aCC-BY-ND 4.0 International license.

Agap3
Ahsa1
AI597468
AI837181
Aip
Akap13
Akt3
Aldh18a1
Alg14
Alox12
Alox5ap
Anapc11
Anapc2
Ank
Ankfy1
Ankrd13a
Anp32a
Anxa5
Anxa7
Ap1m1
Ap1s2
Ap2s1
Ap3d1
Apbb1
Aplp2
Apold1
Arap1
Arf5
Arfgap1
Arhgap1
Arhgap10
Arhgap23
Arhgap31
Arhgdia
Arhgdib
Arhgef7
Arid1a
Arid1b
Arid2
Arl6ip5
Armcx3
Armcx6
Arpc1b
Arpc3
Arpc4
Arpc5
Arrb1
Arrb2
Arsa
Dnlz
Dnm2
Dnmt3a
Dok1
Dok2
Dopey2
Dpf2
Dpy19l1
Drap1
Drg1
Dscr3
Dusp16
Dusp23
Dusp3
Dync1i2
Dync1li2
Dynlt1a
Dyrk1a
Edc3
Edf1
Eef2k
Eepd1
Efemp2
Ehbp1l1
Ehd3
Ehd4
Eif1ad
Eif2b2
Elavl1
Elf2
Elovl1
Elp5
Emc10
Emilin1
Ensa
Epb4.1l2
Esam
Evi2a
Exoc1
F11r
F2r
F2rl3
Fam105b
Fam114a2
Fam126a
Fam131a
Fam168b
Fam172a
Fam174a
Laptm4a
Laptm5
Lasp1
Lat
Layn
Ldlrap1
Lefty1
Leo1
Leprot
Lgals3bp
Lgals9
Lhpp
Lims1
Lmf2
Lmna
Lmo2
Lrrc25
Lrrc32
Lrrc57
Lrrc59
Lrrc8a
Lrrc8c
Lrrfip1
Lrrk1
Lsm14a
Ltbp1
Lyl1
Lyn
Lypla2
Lyve1
Lyz1
Lyz2
Mad1l1
Mad2l1bp
Mad2l2
Maged2
Maml2
Maml3
Man1b1
Manbal
Map2k1
Map2k3
Map3k6
Map4k4
Map7d1
Mapk3
Mapkapk2
Mapre1
Mapre2
Ppp3ca
Ppp6r1
Pqlc1
Prex1
Prkcdbp
Prkce
Prkcq
Prl8a1
Prmt2
Prr13
Prr5l
Prrc2b
Prrg2
Psen2
Psma5
Psma7
Psmb1
Psmd10
Psmd11
Psmd4
Psmd9
Psme1
Ptbp1
Ptges3
Ptgs1
Ptk2
Ptplad2
Ptpn1
Ptpn12
Ptpn22
Ptpra
Ptpre
Ptrf
Pttg1
Pxdc1
Pxk
Pycard
Pygb
Qk
Qpctl
Qsox1
Rab11b
Rab12
Rab13
Rab22a
Rab31
Rab35
Rab3d
Rab43
Stx6
Sugp2
Sumo1
Sumo3
Supt20
Supt4a
Supt5
Surf1
Surf2
Syf2
Syk
Sys1
Syt11
Tacc1
Tada3
Taf12
Taf1a
Tagln2
Tal1
Taok3
Tapbp
Tapbpl
Tax1bp3
Tbc1d22a
Tbc1d5
Tbc1d9b
Tbcb
Tbcc
Tceb2
Tcf25
Tdrd7
Ten1
Tex30
Tfe3
Tfip11
Tfpt
Tgm2
Thoc3
Tie1
Timm17b
Tjp2
Tk2
Tln1
Tm4sf1
Tmbim1
Tmcc2
Tmcc3
Tmed10
Tmed3

bioRxiv preprint doi: https://doi.org/10.1101/708701; this version posted July 19, 2019. The copyright holder for this preprint (which was not certified by peer review) is the author/funder, who has granted bioRxiv a license to display the preprint in perpetuity. It is made available under aCC-BY-ND 4.0 International license.

Asap1
Asf1b
Asns
Atg16l1
Atox1
Atp13a2
Atp1b3
Atp2a3
Atp6ap1
Atp8a1
Atxn3
Atxn7l3
Atxn7l3b
B230378P21Rik
Bad
Bax
Bbc3
BC005624
BC017643
BC029214
Bcl10
Bcl2
Bcl7b
Bend4
Bet1l
Bhlhe41
Bicd2
Bin1
Bin2
Bin3
Birc2
Blvrb
Bmp2
Brd4
Brd9
Bst2
Btbd7
Bysl
C230081A13Rik
C430049B03Rik
Cald1
Calm1
Calu
Camk1
Camk2g
Cant1
Cap1
Capn2
Capn5
Fam174b
Fam177a
Fam192a
Fam195b
Fam212a
Fam214b
Fam217b
Fam219b
Fam32a
Fam3c
Fam43a
Fam53b
Fam57b
Fam65b
Fam76a
Fam78a
Fam89b
Fancg
Fas
Fbxw2
Fcer1g
Fchsd1
Fermt3
Fez2
Fhl3
Fhod1
Fli1
Flii
Flna
Flot1
Fnbp1
Fnta
Foxj2
Fundc2
Fyn
Gars
Gas2l1
Gata2
Gatad2a
Gemin7
Gfod1
Gga3
Ggh
Ggn
Gimap6
Ginm1
Gipc1
Git1
Git2
Marcks
Marveld1
Mat2b
Mbd2
Mbd6
Mcf2l
Mcl1
Mdc1
Mea1
Med10
Med20
Med4
Mef2a
Mef2d
Meis1
Mest
Mettl10
Mfap1b
Mfap3
Mfng
Mgat1
Mgll
Mgme1
Micu1
Mill2
Mis12
Mis18a
Mknk1
Mknk2
Mkrn2
Mmd
Mob1a
Mob2
Mob3a
Morf4l2
Mprip
Mrgbp
Msl1
Msn
Mtch1
Mtcp1
Mthfd1l
Mtmr12
Mtmr3
Mtss1l
Mtus1
Mus81
Mvp
Mxd4
Rab4b
Rab7
Rab7l1
Rabif
Rac1
Rad9a
Ralb
Ralbp1
Ranbp3
Rap1a
Rap1b
Rap1gds1
Rap2a
Rap2b
Rarg
Rasa3
Rasgrp2
Rasl10a
Rbbp6
Rbck1
Rbm17
Rbms1
Rbpj
Rbpms
Rbx1
Rc3h1
Rcc2
Reep2
Rgs10
Rgs12
Rhbdf2
Rhoa
Rhob
Rhoc
Rhog
Rhoj
Ric8
Rin3
Rit1
Rnf114
Rnf125
Rnf144a
Rnf144b
Rnf166
Rnf187
Rnf19b
Rnf38
Rnf41
Rnf44
Tmem101
Tmem109
Tmem123
Tmem140
Tmem159
Tmem160
Tmem167b
Tmem198b
Tmem222
Tmem234
Tmem241
Tmem248
Tmem43
Tmem50a
Tmem63a
Tmem66
Tmod3
Tnfaip8l2
Tollip
Topbp1
Tor4a
Tox4
Tpd52l2
Tpm3
Tpm4
Tprgl
Tpst2
Traf7
Trafd1
Tram2
Trappc3
Trappc6a
Trappc6b
Trem3
Trim37
Trim5
Trim56
Triobp
Trpv2
Tsc22d3
Tspan14
Tspan17
Tspan18
Tspan32
Tspan9
Tspo
Tspyl1
Tssc1
Tssc4

bioRxiv preprint doi: https://doi.org/10.1101/708701; this version posted July 19, 2019. The copyright holder for this preprint (which was not certified by peer review) is the author/funder, who has granted bioRxiv a license to display the preprint in perpetuity. It is made available under aCC-BY-ND 4.0 International license.

Capns1
Capza1
Capzb
Car7
Cars
Casp3
Casp6
Cbx3
Cby1
Ccar2
Ccdc115
Ccdc12
Ccdc124
Ccdc32
Ccdc71
Ccdc9
Ccnd3
Ccndbp1
Ccng2
Cct7
Cd151
Cd1d1
Cd200r1
Cd274
Cd2bp2
Cd47
Cd81
Cd84
Cd93
Cd97
Cdc26
Cdc42
Cdc42bpb
Cdc42ep2
Cdc42ep4
Cdc42se2
Cdca8
Cdk11b
Cdk19
Cdk2ap1
Cdk6
Cdk9
Cdkn1a
Cdkn1b
Cdkn2aipnl
Cdkn2d
Cds2
Cebpa
Cebpg
Gle1
Glipr2
Glod4
Gltp
Gm11346
Gm12166
Gm15503
Gm16286
Gm20492
Gm26510
Gm26541
Gm4070
Gm4204
Gm5914
Gnai2
Gnaq
Gnas
Gnb1
Gnb2
Gnl2
Golga7
Gpr108
Gpr146
Gpr97
Gpsm3
Gpx8
Grb2
Grk5
Grk6
Grn
Gskip
Gsn
Gtf2e2
Gtf2h5
Gtpbp1
Gtpbp2
Gypc
H2afx
H2afz
H2-D1
H2-K1
H2-T22
H2-T23
H2-T24
H3f3a
H3f3b
Hace1
Haus8
Hcls1
Myd88
Myef2
Myh9
Myl6
Mylk
Myo9b
Myom1
Mysm1
Naa60
Naaa
Nars
Nav1
Ncaph2
Ncf1
Ncoa3
Ncstn
Nde1
Necap2
Nedd8
Nek9
Nelfb
Nelfcd
Neurl3
Nfe2l1
Nfix
Ngfrap1
Nipal3
Nkap
Nmb
Nod2
Nosip
Nr1h2
Nras
Nrbp1
Nsf
Nsfl1c
Nub1
Nucb1
Nudcd3
Nudt18
Nudt3
Nudt9
Numb
Nup62
Nxt1
Ogfr
Oit3
Optn
Orai1
Rnpepl1
Rock2
Rras
Rrp7a
Rsu1
Rtf1
Rtfdc1
Rybp
S100a10
S100a13
S1pr2
Samd1
Samd4b
Sap18
Sar1a
Sav1
Sbf1
Sbno2
Scamp3
Scarb1
Scarf1
Schip1
Scnm1
Sdcbp
Sdf4
Sdpr
Sec11c
Sec13
Sec14l1
Sec22b
Sec24b
Sec61a1
Sec61b
Selk
Selm
Selp
Sema6d
Senp3
Sept2
Sept9
Sept11
Sepw1
Serbp1
Serf2
Serinc3
Serpinb9
Sertad1
Sesn1
Sft2d1
Ttc28
Ttc33
Ttc5
Ttyh3
Tuba1a
Tuba1b
Tubb2a
Twf2
U2af1
Uba1
Uba7
Ubald1
Ubald2
Ubash3b
Ube2g2
Ube2h
Ube2i
Ube2j2
Ube2o
Ube2q1
Ube2s
Ube2z
Ubn1
Ubxn1
Unc119
Unc50
Upp1
Usp22
Usp25
Utp14a
Vamp2
Vamp5
Vasp
Vav1
Vcl
Vdac3
Vezf1
Vps25
Vps28
Vps33a
Vps37b
Vps39
Vps72
Vwf
Was
Wasf2
Wbp4
Wdr1
Wdsub1

bioRxiv preprint doi: https://doi.org/10.1101/708701; this version posted July 19, 2019. The copyright holder for this preprint (which was not certified by peer review) is the author/funder, who has granted bioRxiv a license to display the preprint in perpetuity. It is made available under aCC-BY-ND 4.0 International license.

Cenpo
Cep170
Cerk
Cfl1
Chd4
Chek2
Chmp2a
Chmp2b
Chmp3
Chst12
Chsy1
Chtop
Cinp
Cirbp
Ckap4
Clic1
Clic4
Clk3
Clstn1
Cmip
Cmtm3
Cnbp
Cnn2
Cnot8
Cnp
Cnppd1
Cnpy3
Cnr2
Commd7
Cops7a
Coro1b
Coro1c
Cpne8
Cr1l
Creb3
Crebbp
Crlf2
Crtap
Crybb3
Csk
Csnk1d
Csnk1e
Csnk1g2
Csrp1
Ctbp1
Ctdnep1
Ctdsp2
Ctif
Ctnna1
Hcrtr1
Hcst
Hdac5
Hdac7
Herpud2
Hexa
Hexdc
Hgsnat
Hhex
Hipk2
Hist3h2a
Hivep2
Hk1
Hmg20a
Hmha1
Hnrnpab
Hnrnpc
Hnrnpdl
Hnrnpf
Hnrnph2
Hnrnpk
Hnrnpl
Hnrnpm
Hnrnpu
Hnrnpul1
Homer3
Hp1bp3
Hpcal1
Hpgd
Hsd3b7
Hsdl1
Htra2
I830012O16Rik
Ica1
Idua
Ifi27
Ifit3
Ifitm10
Ifitm2
Ifitm3
Ifnar1
Ifrd1
Ift20
Ift27
Igtp
Ikbip
Ikbkb
Ikbkg
Il21r
Orai2
Orai3
Ormdl3
Ostc
Ostf1
Oxr1
Pacs1
Pacsin1
Paf1
Pafah1b2
Pagr1a
Palm
Pan3
Panx1
Pard6a
Parvb
Patl1
Pbx2
Pcif1
Pck2
Pcp4l1
Pdcd10
Pdcd5
Pde2a
Pdgfa
Pdia3
Pdk1
Pdlim1
Pdlim7
Pea15a
Pear1
Pecam1
Peg12
Pfkfb3
Pfkfb4
Pfn1
Pgm1
Phc2
Phf1
Phf20
Phf23
Pik3c2b
Pim1
Pip4k2a
Pip5k1a
Pip5k1c
Pithd1
Pitpna
Pitpnc1
Sgce
Sh2b3
Sh3gl1
Sh3glb1
Sh3glb2
Shc1
Shfm1
Sigmar1
Sin3b
Sirt2
Skap2
Ski
Skil
Sla
Sla2
Slc16a3
Slc18a2
Slc24a3
Slc25a24
Slc35a4
Slc35e4
Slc39a6
Slc44a1
Slc44a2
Slc6a6
Slc7a5
Slc9a1
Slc9a9
Slpi
Slu7
Smap2
Smarcd2
Smc1a
Smim12
Smox
Smtn
Smu1
Smurf1
Snd1
Snf8
Snrnp27
Snrpc
Snw1
Snx1
Snx11
Snx17
Snx3
Snx5
Sp2
Whamm
Wipf1
Wrap73
Xab2
Yap1
Yif1b
Ypel3
Ywhab
Ywhae
Ywhag
Ywhah
Zbtb38
Zc3h13
Zc3h4
Zcchc10
Zcchc6
Zdhhc18
Zdhhc20
Zdhhc7
Zfand2b
Zfand5
Zfand6
Zfp281
Zfp36l2
Zfp414
Zfp646
Zfp652
Zfp710
Zfp746
Zfyve27
Zmat2
Zmiz2
Zmynd11
Znfx1
Znhit1
Zrsr2
Zyx
0610010K14Rik
1110004F10Rik
1110007C09Rik
1500011B03Rik
1700017B05Rik
1700037C18Rik
1810009A15Rik
2310011J03Rik
2310036O22Rik
2310047M10Rik
2510009E07Rik
2510039O18Rik

bioRxiv preprint doi: https://doi.org/10.1101/708701; this version posted July 19, 2019. The copyright holder for this preprint (which was not certified by peer review) is the author/funder, who has granted bioRxiv a license to display the preprint in perpetuity. It is made available under aCC-BY-ND 4.0 International license.

Ctnnb1	*Il27ra*	*Pitpnm1*	*Spin1*	*2610001J05Rik*
Ctsw	*Ilk*	*Pitpnm2*	*Sppl3*	*2810428I15Rik*
Ctsz	*Incenp*	*Pkm*	*Spred2*	*2900026A02Rik*
Cuedc1	*Inf2*	*Pla2g16*	*Sptlc2*	*3110082I17Rik*
Cuedc2	*Ing1*	*Pld2*	*Sqstm1*	*4931406P16Rik*
Cuta	*Ino80c*	*Plek*	*Srd5a3*	*5031439G07Rik*
Cyth1	*Inpp4a*	*Plekha2*	*Srf*	*5330426P16Rik*
Cyth3	*Inpp5a*	*Plekho1*	*Srgap2*	*6330409D20Rik*
D030056L22Rik	*Inpp5d*	*Plekho2*	*Srgn*	*6430548M08Rik*
D17H6S56E-5	*Inpp5k*	*Plscr1*	*Sri*	*9430023L20Rik*
D930015E06Rik	*Ipo11*	*Plvap*	*Srp19*	*9530082P21Rik*
Dapp1	*Irak3*	*Plxna4*	*Srp68*	
Dcaf12	*Irak4*	*Pmp22*	*Srpr*	
Dcaf4	*Irf3*	*Pnkp*	*Srsf5*	
Dcaf7	*Isg15*	*Pnrc1*	*Srsf9*	

Liver

Aagab	*D8Ertd738e*	*Isg15*	*Pofut1*	*Stra13*
Aamp	*D930015E06Rik*	*Itfg3*	*Pofut2*	*Strip1*
Aar2	*Dapp1*	*Itga6*	*Poldip3*	*Strn*
Abca7	*Dcaf12*	*Itgal*	*Pole3*	*Strn4*
Abcc1	*Dcaf7*	*Itgb1*	*Polr2a*	*Stx11*
Abcc4	*Dck*	*Itgb2*	*Polr2d*	*Stx12*
Abcc5	*Dcp1b*	*Itgb4*	*Polr3gl*	*Stx18*
Abhd12	*Dctn1*	*Itgb5*	*Pop7*	*Stx2*
Abhd16a	*Dctn3*	*Itm2b*	*Ppap2b*	*Stx4a*
Abhd17a	*Dctn4*	*Itm2c*	*Ppil1*	*Stx5a*
Abi1	*Dctn5*	*Itpkb*	*Ppm1g*	*Stx6*
Acd	*Dctn6*	*Itsn1*	*Ppp1ca*	*Stx7*
Acer2	*Dcun1d2*	*Itsn2*	*Ppp1cc*	*Stx8*
Actb	*Dcun1d5*	*Jak1*	*Ppp1r12c*	*Stxbp2*
Actg1	*Dda1*	*Jak2*	*Ppp1r13b*	*Sugp2*
Actn1	*Ddah2*	*Josd2*	*Ppp1r16b*	*Sumf1*
Actn4	*Ddrgk1*	*Kansl2*	*Ppp1r18*	*Sumo1*
Actr1a	*Ddx47*	*Katna1*	*Ppp1r2*	*Sumo3*
Actr3	*Ddx5*	*Kcmf1*	*Ppp1r9b*	*Supt20*
Adam10	*Dedd*	*Kctd20*	*Ppp2ca*	*Supt4a*
Adam17	*Degs1*	*Kdm2a*	*Ppp2cb*	*Supt5*
Adarb1	*Dennd2c*	*Kdr*	*Ppp2r4*	*Supt6*
Add1	*Dennd2d*	*Keap1*	*Ppp3ca*	*Surf1*
Add3	*Dennd4c*	*Khsrp*	*Ppp3r1*	*Swi5*
Adipor1	*Dennd5a*	*Kidins220*	*Ppp4r2*	*Syf2*
Adprh	*Dgkd*	*Kif13a*	*Ppp6r1*	*Syk*
Aebp2	*Dgkz*	*Kif3c*	*Ppt1*	*Syngr2*
Aen	*Dhps*	*Kif5b*	*Ppt2*	*Synrg*
Afap1l1	*Dhrs3*	*Klc1*	*Prcp*	*Sys1*
Aga	*Dhx38*	*Klhdc4*	*Prdm2*	*Syt11*
Agap3	*Diap1*	*Klhl6*	*Prdx5*	*Tab2*

bioRxiv preprint doi: https://doi.org/10.1101/708701; this version posted July 19, 2019. The copyright holder for this preprint (which was not certified by peer review) is the author/funder, who has granted bioRxiv a license to display the preprint in perpetuity. It is made available under aCC-BY-ND 4.0 International license.

Agpat1
Agpat5
Agtrap
Ahsa1
AI597468
AI837181
Aip
Akirin1
Akirin2
Akr1b10
Akt3
Aktip
Aldh18a1
Aldoa
Alkbh5
Alkbh6
Alox12
Alox5ap
Amdhd2
Anapc11
Anapc16
Anapc2
Ankfy1
Ankib1
Ankmy2
Ankrd13a
Ankrd17
Ankrd40
Ano6
Anp32a
Anxa5
Ap1b1
Ap1m1
Ap1s1
Ap1s2
Ap2a2
Ap2s1
Ap4s1
Aplf
Apoa1bp
Apold1
Aqp1
Arap1
Arf1
Arf3
Arf5
Arf6
Arfgap1
Arfgap3
Dlgap4
Dmwd
Dnajc1
Dnajc10
Dnajc17
Dnajc4
Dnajc7
Dnal4
Dnase1l1
Dnlz
Dnm2
Dnmt3a
Dock11
Dok1
Dok2
Dpcd
Dpf2
Dpp8
Drap1
Drg1
Dscr3
Dtnbp1
Dusp19
Dusp23
Dusp3
Dut
Dync1i2
Dync1li1
Dync1li2
Dynlt1a
Dyrk1a
Ecm1
Edc3
Efcab14
Efemp2
Efr3a
Ehbp1l1
Ehd1
Ehd3
Ehd4
Ehmt2
Eif1ad
Eif2ak1
Eif2b2
Eif3k
Eif4g3
Eif5b
Elavl1
Elf2
Klhl9
Kmt2e
Knop1
Kpna4
Kpnb1
Lamp1
Lamtor1
Lamtor2
Laptm4a
Laptm5
Lasp1
Lat
Layn
Ldlrap1
Lefty1
Leo1
Leprot
Lgals3bp
Lgalsl
Limd1
Lims1
Lin7c
Lmo2
Lrp10
Lrrc25
Lrrc32
Lrrc58
Lrrc61
Lrrc8a
Lrrc8c
Lrrc8d
Lrrfip1
Lrrk1
Lsm1
Lsm14a
Ltbp1
Ly6g6d
Lyl1
Lyn
Lypla2
Lyve1
Lyz1
Lyz2
M6pr
Mad1l1
Mad2l1bp
Maea
Maf1
Mafg
Prex1
Prkaa1
Prkacb
Prkar1a
Prkcd
Prkcdbp
Prkce
Prkcq
Prmt2
Prorsd1
Prpf38b
Prr13
Prr24
Prr5l
Prrc2b
Psap
Psen1
Psma5
Psma7
Psmb1
Psmb4
Psmb5
Psmd10
Psmd4
Psme1
Ptbp1
Ptbp3
Ptges3
Ptgs1
Ptk2
Ptk2b
Ptov1
Ptplad2
Ptpn1
Ptpn11
Ptpn12
Ptpn18
Ptpn22
Ptpra
Ptpre
Ptprj
Ptrf
Ptrhd1
Pttg1
Pum2
Pura
Purb
Pxk
Pycard
Tacc1
Tada3
Taf1
Taf12
Taf13
Taf9
Tagln2
Tal1
Taldo1
Tamm41
Taok1
Tapbp
Tapbpl
Tax1bp3
Tbc1d14
Tbc1d22a
Tbc1d5
Tbc1d9b
Tbca
Tbcb
Tbcc
Tbxas1
Tceanc2
Tceb2
Tcf25
Ten1
Tex261
Tfe3
Tfip11
Tfpt
Tgfb1
Tgm2
Thap7
Thoc3
Tie1
Timm22
Tinf2
Tjp2
Tk2
Tlk1
Tln1
Tlr12
Tm2d3
Tm4sf1
Tmbim1
Tmcc2
Tmcc3
Tmed10
Tmed3

bioRxiv preprint doi: https://doi.org/10.1101/708701; this version posted July 19, 2019. The copyright holder for this preprint (which was not certified by peer review) is the author/funder, who has granted bioRxiv a license to display the preprint in perpetuity. It is made available under aCC-BY-ND 4.0 International license.

Arhgap1
Arhgap10
Arhgap23
Arhgap31
Arhgdia
Arhgdib
Arhgef7
Arid1a
Arid1b
Arid2
Arl2
Arl3
Arl6ip5
Arl8a
Arl8b
Armcx1
Armcx3
Armcx6
Arpc1b
Arpc2
Arpc3
Arpc4
Arpc5
Arrb1
Arrb2
Arrdc1
Asap1
Asb1
Asb6
Asf1b
Asna1
Atg10
Atg4b
Atic
Atox1
Atp13a2
Atp1b3
Atp2a3
Atp2c1
Atp5h
Atp6ap1
Atp6v0b
Atp6v0c
Atp6v1b2
Atp6v1e1
Atp6v1g1
Atp8a1
Atpaf1
Atpif1
Elovl1
Elp5
Emc3
Emilin1
Enoph1
Ensa
Ep400
Epb4.1l2
Epn1
Epor
Erlec1
Erp29
Esam
Etv6
Evi2a
Evi5l
Exoc1
Exoc2
Exoc5
Ezh1
F11r
F2r
Fadd
Fam102b
Fam104a
Fam114a2
Fam120a
Fam126a
Fam131a
Fam168b
Fam172a
Fam174a
Fam174b
Fam175b
Fam177a
Fam192a
Fam195b
Fam212a
Fam214b
Fam219b
Fam222b
Fam32a
Fam3c
Fam43a
Fam53b
Fam53c
Fam58b
Fam63b
Fam65b
Maged2
Maml2
Man2b1
Manbal
Map1lc3a
Map2k7
Map3k6
Map4k4
Map7
Map7d1
Mapk1
Mapk14
Mapk3
Mapkapk2
Mapkapk3
Mapre1
Mapre2
Marcks
Mark2
Mat2b
Maz
Mbd2
Mbnl2
Mcf2l
Mcl1
Mcu
Mdc1
Mdm1
Mea1
Med10
Med11
Med13l
Med16
Med20
Med4
Med9
Mef2a
Mef2d
Meis1
Mesdc2
Mest
Mettl10
Mfap1b
Mfap3
Mff
Mfng
Mga
Mgat1
Mgme1
Pygb
Qk
Rab1
Rab10
Rab11b
Rab12
Rab13
Rab1b
Rab27a
Rab28
Rab2a
Rab31
Rab32
Rab35
Rab3d
Rab4b
Rab6a
Rab7
Rab7l1
Rac1
Rad21
Rad9a
Ralb
Ralbp1
Ralgps2
Ranbp3
Rap1a
Rap1b
Rap1gds1
Rap2a
Rap2b
Rarg
Rars
Rasa3
Rasgrp2
Rbck1
Rbfa
Rbm17
Rbms1
Rbpj
Rbpms
Rbx1
Rcan1
Rcbtb2
Rcc2
Rce1
Reep5
Rfesd
Rfk
Tmed8
Tmem101
Tmem109
Tmem123
Tmem127
Tmem140
Tmem14c
Tmem159
Tmem160
Tmem164
Tmem167b
Tmem175
Tmem191c
Tmem198b
Tmem234
Tmem241
Tmem242
Tmem246
Tmem261
Tmem29
Tmem40
Tmem43
Tmem50a
Tmem59
Tmem60
Tmem63a
Tmem66
Tmem86a
Tmem9b
Tmod3
Tmppe
Tmub1
Tmub2
Tmx1
Tnfaip8l2
Tnfsf14
Tnik
Tnks2
Tnnt1
Tollip
Tomm22
Tomm7
Topbp1
Tor1aip1
Tor4a
Tox4
Tpd52
Tpd52l2
Tpm1

bioRxiv preprint doi: https://doi.org/10.1101/708701; this version posted July 19, 2019. The copyright holder for this preprint (which was not certified by peer review) is the author/funder, who has granted bioRxiv a license to display the preprint in perpetuity. It is made available under aCC-BY-ND 4.0 International license.

Atxn7l1
Atxn7l3
Atxn7l3b
Aurkaip1
B230378P21Rik
B4galt1
Bad
Bag1
Bax
Bbc3
BC005537
BC005624
BC017643
BC033916
Bcas3
Bcat2
Bckdk
Bcl10
Bcl2
Bcl7b
Becn1
Bend4
Bet1l
Bicd2
Bin1
Bin2
Bin3
Blcap
Bloc1s1
Blvrb
Bmp2
Bmp2k
Bola2
Brd4
Brd9
Brk1
Brox
Bst2
C230081A13Rik
C330006A16Rik
C430049B03Rik
Cab39
Calm1
Calm3
Calu
Camk1
Camk2g
Cant1
Canx
Fam69a
Fam76a
Fam78a
Fam89b
Fam96a
Fancg
Fas
Fastk
Fbxl17
Fbxl3
Fbxo46
Fbxw11
Fbxw5
Fcer1g
Fchsd1
Fermt3
Fez2
Fgd3
Fgfr1op2
Fhl3
Fhod1
Fis1
Flcn
Fli1
Flii
Flna
Fnbp1
Fnta
Foxj2
Foxk2
Frmd8
Fuca1
Fundc2
Fut8
Fyn
G3bp2
G6pdx
Gab2
Gabarap
Gadd45g
Gak
Galk2
Galnt1
Gas2l1
Gata2
Gatad1
Gatad2a
Gbas
Gemin7
Micu1
Mien1
Mill2
Mink1
Minos1
Mis18a
Mkrn1
Mlf2
Mllt11
Mob1a
Mob2
Mob3a
Mon1b
Morf4l2
Mpp1
Mprip
Mras
Mrp63
Mrpl20
Mrpl44
Mrpl48
Mrpl51
Mrpl54
Mrps25
Msantd4
Msl1
Msn
Msrb2
Mtch1
Mtcp1
Mtdh
Mtf1
Mtmr12
Mtmr3
Mtmr6
Mtss1l
Mtus1
Mus81
Mvb12b
Mvp
Mxd1
Mxd4
Myd88
Myef2
Myeov2
Myh9
Myl6
Myo9b
Myom1
Rgs10
Rgs12
Rhbdf2
Rhoa
Rhob
Rhoc
Rhog
Rhoj
Ric8
Rin3
Rit1
Rlim
Rnasel
Rnf114
Rnf141
Rnf144a
Rnf144b
Rnf166
Rnf167
Rnf185
Rnf187
Rnf34
Rnf38
Rnf41
Rnf44
RP24-176F12.14
Rpain
Rpp21
Rqcd1
Rras
Rrp7a
Rsu1
Rtf1
Rtfdc1
Rybp
S100a10
S100a13
S1pr2
Safb2
Samd1
Samd4b
Sar1a
Sars
Sat1
Sav1
Sbf1
Sbno2
Scamp2
Scamp5
Tpm3
Tpm4
Tpp1
Tprgl
Tpst2
Traf7
Trafd1
Trappc2l
Trappc3
Trappc5
Trappc6a
Trappc6b
Trem3
Treml2
Treml4
Trim37
Trim5
Trim56
Trim8
Triobp
Trip12
Trove2
Trpv2
Tsc22d1
Tsc22d3
Tsc22d4
Tsg101
Tspan14
Tspan17
Tspan18
Tspan32
Tspan9
Tspyl1
Tssc1
Tssc4
Ttc28
Ttc3
Ttc5
Ttc7b
Ttc9c
Ttll1
Ttyh3
Tuba1a
Tuba1b
Tubb1
Tusc2
Twf1
Twf2
Txn1

bioRxiv preprint doi: https://doi.org/10.1101/708701; this version posted July 19, 2019. The copyright holder for this preprint (which was not certified by peer review) is the author/funder, who has granted bioRxiv a license to display the preprint in perpetuity. It is made available under aCC-BY-ND 4.0 International license.

Cap1
Capn2
Capn5
Capns1
Capza1
Capzb
Car7
Cbl
Cbx3
Cby1
Ccar2
Ccdc115
Ccdc12
Ccdc124
Ccdc32
Ccdc41os1
Ccdc50
Ccdc71
Ccdc9
Ccnd1
Ccnd3
Ccndbp1
Ccser2
Cct7
Cd200r1
Cd274
Cd2bp2
Cd44
Cd47
Cd55
Cd81
Cd84
Cd93
Cd97
Cdc26
Cdc42
Cdc42bpb
Cdc42ep2
Cdc42ep4
Cdc42se2
Cdca8
Cdipt
Cdk11b
Cdk16
Cdk19
Cdk2ap1
Cdk2ap2
Cdk9
Cdkn1a
Gfod1
Gga1
Gga2
Gga3
Ggh
Gid8
Gimap6
Ginm1
Gipc1
Git1
Git2
Gle1
Glg1
Glipr2
Glod4
Gltp
Gm11346
Gm11669
Gm12166
Gm12942
Gm13476
Gm13840
Gm14446
Gm15051
Gm16211
Gm16286
Gm20492
Gm26510
Gm26782
Gm4070
Gm4204
Gm561
Gmpr
Gna13
Gnai2
Gnaq
Gnb1
Gnb2
Gnb5
Gnl3l
Gnpda2
Golga2
Golga7
Golph3l
Gpaa1
Gpalpp1
Gpr108
Gpr137
Gpr97
Mysm1
Naaa
Nacc2
Naga
Nars
Nav1
Ncaph2
Ncf1
Nck2
Ncoa3
Ncor1
Ncstn
Nde1
Ndel1
Ndufa1
Ndufa7
Ndufa8
Ndufb3
Ndufb8
Ndufs4
Necap2
Nedd8
Nek7
Nek9
Nelfb
Neurl1a
Neurl3
Nfe2l1
Ngfrap1
Ngrn
Ninj1
Nkap
Nkiras2
Nlk
Nmb
Nme1
Nosip
Nr1h2
Nras
Nrbp1
Nsf
Nsfl1c
Nt5m
Nub1
Nubp2
Nucb1
Nucks1
Nudcd3
Nudt16
Scarf1
Schip1
Scnm1
Sdcbp
Sdccag8
Sdf2
Sdf4
Sdhaf2
Sdpr
Sec11a
Sec11c
Sec13
Sec14l1
Sec22b
Sec62
Selk
Selm
Selp
Sema4b
Sema4d
Sema6d
Senp3
Sept2
Sept9
Sept11
Sept15
Sepw1
Serbp1
Serf2
Serinc3
Serpinb9
Sertad1
Sertad2
Sesn1
Setd3
Sfn
Sft2d1
Sgce
Sgip1
Sh2b3
Sh3gl1
Sh3glb1
Sh3glb2
Sharpin
Shfm1
Sin3b
Sirt2
Skap2
Ski
Txnl4a
U2af1
Uba5
Uba7
Ubald1
Ubald2
Ubash3b
Ubb
Ube2a
Ube2d2a
Ube2e1
Ube2g2
Ube2i
Ube2j2
Ube2o
Ube2q1
Ube2s
Ube2v1
Ube2z
Ubl7
Ubn1
Ubxn1
Ubxn2b
Ufm1
Unc13d
Unc50
Upf3a
Upp1
Urm1
Usp12
Usp25
Usp48
Utp14a
Vamp5
Vamp8
Vapa
Vasp
Vav1
Vcp
Vdac3
Vezf1
Vill
Vipas39
Vps25
Vps28
Vps29
Vps33a
Vps37b
Vps39

bioRxiv preprint doi: https://doi.org/10.1101/708701; this version posted July 19, 2019. The copyright holder for this preprint (which was not certified by peer review) is the author/funder, who has granted bioRxiv a license to display the preprint in perpetuity. It is made available under aCC-BY-ND 4.0 International license.

Cdkn1b
Cdkn2aipnl
Cdkn2d
Cebpg
Cenpb
Cenpo
Cep170
Cerk
Cfl1
Cggbp1
Chd2
Chd4
Chek2
Chfr
Chmp1a
Chmp2a
Chmp2b
Chmp3
Chmp4b
Chmp6
Chmp7
Chrac1
Chst12
Chsy1
Chtop
Cib1
Cinp
Cirbp
Ckap4
Ckb
Clec1b
Clec4d
Clec4g
Clic1
Clic4
Clk3
Clstn1
Cluap1
Cmas
Cmc2
Cmip
Cmtm3
Cnbp
Cnep1r1
Cnn2
Cnot6
Cnot8
Cnp
Cnppd1
Gpsm3
Grb2
Grcc10
Grk6
Grn
Gskip
Gsn
Gtf2a1
Gtf2e2
Gtf2h5
Gtpbp1
Gypc
H2afj
H2afv
H2afx
H2afz
H2-D1
H2-K1
H2-Ke2
H2-T22
H2-T23
H2-T24
H3f3a
H3f3b
Hace1
Haus8
Hcfc1r1
Hcls1
Hcst
Hdac3
Hdac5
Hdac7
Hexa
Hexdc
Hexim1
Hgsnat
Hipk1
Hipk2
Hira
Hist3h2a
Hivep2
Hk1
Hmg20a
Hmha1
Hnrnpab
Hnrnpc
Hnrnpdl
Hnrnpf
Hnrnph2
Nudt18
Nudt3
Nudt9
Numb
Nup50
Nup62
Nxt1
Oas3
Oaz2
Ociad1
Ogfr
Ogg1
Oit3
Orai1
Orai2
Orai3
Oraov1
Ostc
Ostf1
Ostm1
Otub1
Otud7b
P2ry1
P2ry13
P4ha1
Pacs1
Padi2
Paf1
Pafah1b2
Pagr1a
Palld
Palm
Pam
Pan3
Panx1
Parp11
Parvb
Patl1
Pbx2
Pbxip1
Pcbp1
Pcif1
Pck2
Pdap1
Pdcd10
Pdcd5
Pdcd6
Pddc1
Pde2a
Skil
Sla
Sla2
Slc12a6
Slc16a3
Slc18a2
Slc25a24
Slc25a35
Slc25a4
Slc30a1
Slc35a4
Slc35e4
Slc39a1
Slc39a13
Slc39a6
Slc3a2
Slc44a1
Slc44a2
Slc45a4
Slc4a1ap
Slc7a5
Slc9a1
Slc9a9
Slco3a1
Slmo2
Slpi
Slu7
Smagp
Smap2
Smarcd2
Smc1a
Smdt1
Smg6
Smg7
Smim12
Smim3
Smox
Smtn
Smu1
Smurf1
Smyd3
Snap29
Snapin
Snf8
Snn
Snrnp25
Snrnp27
Snrpc
Snw1
Vps4b
Vps51
Vps52
Vps72
Vsig2
Vti1b
Vwa9
Vwf
Was
Wasf2
Wbp4
Wdr1
Wdr26
Wdr31
Wdsub1
Wipf1
Wipi1
Wwp2
Xab2
Xcr1
Xpnpep1
Ybx1
Yif1b
Ykt6
Ypel2
Ypel3
Ywhab
Ywhae
Ywhag
Ywhah
Zbtb38
Zc3h4
Zcchc10
Zdhhc18
Zdhhc20
Zdhhc7
Zfand5
Zfp106
Zfp362
Zfp36l2
Zfp414
Zfp422
Zfp646
Zfp652
Zfp664
Zfp710
Zfp715
Zfp746
Zfp773

bioRxiv preprint doi: https://doi.org/10.1101/708701; this version posted July 19, 2019. The copyright holder for this preprint (which was not certified by peer review) is the author/funder, who has granted bioRxiv a license to display the preprint in perpetuity. It is made available under aCC-BY-ND 4.0 International license.

Cnpy3	*Hnrnpk*	*Pdlim1*	*Snx1*	*Zfp830*
Cnr2	*Hnrnpl*	*Pdlim7*	*Snx11*	*Zfyve27*
Coa3	*Hnrnpm*	*Pea15a*	*Snx17*	*Zmat2*
Commd1	*Hnrnpu*	*Pear1*	*Snx3*	*Zmiz2*
Commd6	*Hnrnpul1*	*Pecam1*	*Snx5*	*Zmym4*
Commd7	*Homer3*	*Peg12*	*Sp2*	*Zmynd11*
Comtd1	*Hp1bp3*	*Pet100*	*Specc1*	*Znfx1*
Coro1b	*Hpcal1*	*Pfkfb4*	*Spic*	*Znhit1*
Coro1c	*Hpgd*	*Pfn1*	*Spire1*	*Znhit2*
Cox14	*Hps1*	*Pgd*	*Spns1*	*Zrsr2*
Cox8a	*Hpse*	*Pggt1b*	*Sppl2b*	*Zyx*
Cpe	*Hs1bp3*	*Pgm1*	*Sppl3*	*0610010K14Rik*
Cpne8	*Htatip2*	*Pgs1*	*Spred2*	*0610031J06Rik*
Cr1l	*Htra2*	*Phc2*	*Sptbn1*	*1110001A16Rik*
Creb3l1	*I830012O16Rik*	*Phf1*	*Sptlc2*	*1110004F10Rik*
Crk	*Ica1*	*Phf20*	*Spty2d1*	*1110007C09Rik*
Crlf2	*Iffo1*	*Phf23*	*Srd5a3*	*1110058L19Rik*
Crtap	*Ifit3*	*Pigc*	*Srf*	*1500011B03Rik*
Cryzl1	*Ifitm10*	*Pik3c2b*	*Srgap2*	*1600012H06Rik*
Csk	*Ifitm2*	*Pin1*	*Srgap3*	*1700017B05Rik*
Csnk1a1	*Ifitm3*	*Pip4k2a*	*Srgn*	*1700037H04Rik*
Csnk1d	*Ifrd1*	*Pip5k1a*	*Sri*	*1810009A15Rik*
Csnk1e	*Ift20*	*Pip5k1c*	*Srp19*	*1810043H04Rik*
Csnk1g2	*Ift27*	*Pisd*	*Srp9*	*2210015D19Rik*
Csrp1	*Igbp1*	*Pithd1*	*Srsf9*	*2310011J03Rik*
Ctbp1	*Ikbip*	*Pitpna*	*Ss18*	*2310036O22Rik*
Ctdsp2	*Ikbkb*	*Pitpnc1*	*Ssbp2*	*2310047M10Rik*
Ctdspl	*Il21r*	*Pitpnm1*	*Ssbp4*	*2510009E07Rik*
Ctnna1	*Il27ra*	*Pja2*	*Ssna1*	*2510039O18Rik*
Ctnnal1	*Ilk*	*Pkm*	*Ssu72*	*2610001J05Rik*
Ctnnb1	*Incenp*	*Pla2g16*	*St3gal1*	*2610507B11Rik*
Ctps2	*Ing1*	*Pla2g4a*	*St3gal2*	*2610524H06Rik*
Ctsa	*Ino80c*	*Pld2*	*St3gal4*	*2810428I15Rik*
Ctsd	*Ino80d*	*Pld3*	*Stard3*	*3110062M04Rik*
Ctsw	*Inpp4a*	*Plek*	*Stard3nl*	*3110082I17Rik*
Ctsz	*Inpp5a*	*Plekha2*	*Stat5b*	*4931406P16Rik*
Cttn	*Inpp5b*	*Plekha3*	*Stat6*	*5031425E22Rik*
Cuedc1	*Inpp5d*	*Plekhm1*	*Stim2*	*5031439G07Rik*
Cuedc2	*Inpp5k*	*Plekho1*	*Stk11ip*	*5330426P16Rik*
Cuta	*Ints12*	*Plekho2*	*Stk19*	*5430417L22Rik*
Cyb561a3	*Ip6k1*	*Plvap*	*Stk24*	*6430548M08Rik*
Cyba	*Ipo11*	*Pmm2*	*Stk25*	*9130230N09Rik*
Cyth1	*Iqsec1*	*Pmp22*	*Stk3*	*9130401M01Rik*
Cyth3	*Irak3*	*Pnkd*	*Stk4*	*9430023L20Rik*
D030056L22Rik	*Irak4*	*Pnkp*	*Stom*	*9530082P21Rik*
D17H6S56E-5	*Irf3*	*Pnrc1*	*Ston2*	

Lung

bioRxiv preprint doi: https://doi.org/10.1101/708701; this version posted July 19, 2019. The copyright holder for this preprint (which was not certified by peer review) is the author/funder, who has granted bioRxiv a license to display the preprint in perpetuity. It is made available under aCC-BY-ND 4.0 International license.

Aagab
Aamdc
Aamp
Aars
Abhd16a
Abhd17a
Abi1
Abtb1
Acaa1a
Acat1
Acbd3
Acbd4
Acd
Acer2
Acot8
Actb
Actg1
Actr1a
Actr3
Acy3
Adam10
Adam17
Add1
Add3
Adipor2
Adprh
Aebp2
Aen
Afap1l1
Afp
Aga
Agpat1
Agpat5
Agtrap
Ahsa1
AI837181
Aip
Akirin2
Akr1a1
Aldh2
Aldh9a1
Aldoa
Alg14
Alkbh6
Amdhd2
Anapc11
Anapc16
Ankmy2
Ankrd13a
Daam1
Dcaf12
Dcaf7
Dcp1b
Dctn1
Dctn2
Dctn3
Dctn5
Dctn6
Dctpp1
Dcun1d5
Dda1
Ddah2
Ddi2
Ddrgk1
Ddx47
Deb1
Dennd2c
Derl1
Dffa
Dgcr6
Dgkz
Dhcr24
Dhps
Dhrs1
Dhx38
Dlgap4
Dmwd
Dnajb11
Dnajc17
Dnajc3
Dnajc4
Dnajc7
Dnal4
Dnlz
Dnm2
Dnmt3a
Dnpep
Dok1
Dok2
Dpcd
Dpf2
Dph3
Drg1
Dusp11
Dusp16
Dusp19
Dusp23
Dusp3
Josd1
Josd2
Jup
Kalrn
Kansl2
Katna1
Kcmf1
Kcna3
Kctd20
Kctd21
Kdm2a
Kdr
Khk
Kif13a
Kif3c
Klc1
Klf9
Klhdc3
Klhdc4
Klhl6
Knop1
Kpna1
Lamp1
Lamtor2
Lasp1
Layn
Ldlrap1
Ldoc1l
Lefty1
Leprot
Lgals3bp
Lgals9
Lgalsl
Lias
Lims1
Lman2
Lmna
Lmo2
Lpcat3
Lrp10
Lrrc25
Lrrc32
Lrrc57
Lrrc8a
Lrrc8b
Lrrc8d
Lsm1
Lsm14a
Ly6g6d
Polr2d
Polr2e
Polr2m
Polr3gl
Pop7
Ppib
Ppif
Ppil1
Ppm1g
Ppme1
Ppp1ca
Ppp1cc
Ppp1r12c
Ppp1r13b
Ppp1r15b
Ppp1r16b
Ppp1r18
Ppp1r2
Ppp1r3d
Ppp1r9b
Ppp2ca
Ppp2cb
Ppp2r1a
Ppp2r4
Ppp2r5a
Ppp3r1
Ppp4r2
Ppp6r1
Ppp6r3
Ppt2
Pqlc1
Pqlc2
Prcp
Prdm4
Prdx5
Preb
Prelid1
Prex1
Prkab1
Prkag1
Prkcdbp
Prkce
Prkcq
Prkcsh
Prorsd1
Prr13
Prr24
Prrc2b
Prrg2
Stub1
Stx12
Stx18
Stx2
Stx4a
Stx6
Stx8
Suds3
Sumo3
Supt4a
Supt5
Supt6
Surf1
Swi5
Syf2
Syk
Syngr2
Sys1
Tab2
Tada3
Taf12
Taf13
Taf9
Tagln2
Tal1
Taldo1
Tamm41
Tapbp
Tapbpl
Tarbp2
Tax1bp3
Tbc1d14
Tbc1d17
Tbc1d22a
Tbc1d9b
Tbca
Tbcb
Tbcc
Tceb2
Tcf25
Tcn2
Tdrd7
Ten1
Tesc
Tex2
Tex261
Tex30
Tfpt
Tgfb1

bioRxiv preprint doi: https://doi.org/10.1101/708701; this version posted July 19, 2019. The copyright holder for this preprint (which was not certified by peer review) is the author/funder, who has granted bioRxiv a license to display the preprint in perpetuity. It is made available under aCC-BY-ND 4.0 International license.

Ankrd17
Anp32a
Anxa7
Ap1m1
Ap1s1
Ap1s2
Ap2s1
Ap4b1
Ap4s1
Aph1a
Aplf
Aqp1
Araf
Arap1
Arf1
Arf5
Arfgap1
Arfgap3
Arhgap23
Arhgap6
Arhgdia
Arhgdib
Arhgef12
Arhgef7
Arid1a
Arl2
Arl2bp
Arl8a
Armcx1
Arpc1b
Arpc2
Arpc3
Arpc4
Arpc5
Arrb1
Arrb2
Arsa
As3mt
Asb1
Asb6
Asb8
Asf1b
Asl
Asna1
Asnsd1
Atg16l1
Atg4b
Atox1
Atp13a2
Dut
Dync1i2
Dynlt1a
Ech1
Ecm1
Edc3
Edf1
Eef2k
Eepd1
Egln2
Ehbp1l1
Ehd1
Ehd4
Eif1ad
Eif2ak1
Eif2b2
Eif4e2
Eif4ebp3
Eif4g1
Eif4g3
Elavl1
Elf2
Elp5
Emc10
Emilin1
Eno1
Enoph1
Ensa
Eps15
Ercc3
Ergic3
Erlec1
Erp29
Erp44
Esam
Etfb
Etv6
Evi5l
Ezh1
F10
Fadd
Fam102b
Fam104a
Fam105b
Fam107b
Fam114a2
Fam134a
Fam134c
Fam160b2
Ly6g6f
Lyl1
Lyn
Lypla2
Lyrm4
Lyrm9
Lyve1
Mad1l1
Mad2l1bp
Mad2l2
Madd
Maf1
Maml2
Maml3
Man1a2
Man2b1
Manf
Map1lc3a
Map2k5
Map4k4
Map7d1
Mapk14
Mapk3
Mapk6
Mapkap1
Mapre1
March2
Marcks
Mark2
Marveld1
Mat2b
Mavs
Maz
Mbd2
Mbd6
Mcf2l
Mcl1
Mdh1
Mdm1
Mea1
Med10
Med11
Med4
Med9
Mef2d
Meis1
Mepce
Mesdc2
Mettl10
Psap
Psd3
Psen2
Psma5
Psma7
Psmb1
Psmb4
Psmb5
Psmb6
Psmb7
Psmc3
Psmc4
Psmd1
Psmd10
Psmd11
Psmd13
Psmd2
Psmd4
Psmd8
Psmd9
Psme1
Ptcd2
Ptdss1
Pten
Ptgs1
Ptk2
Ptplad2
Ptpn1
Ptpn12
Ptpn18
Ptpn22
Ptpra
Ptrf
Ptrhd1
Pttg1
Pttg1ip
Pum2
Pwp1
Pxdc1
Pycard
Pygl
Qpctl
Qsox1
R3hdm1
Rab11b
Rab12
Rab14
Rab1b
Rab21
Thap7
Thoc3
Tie1
Timm13
Timm17b
Timm22
Tinf2
Tk2
Tlk1
Tm2d2
Tm2d3
Tm4sf1
Tm7sf3
Tmcc2
Tmcc3
Tmco1
Tmed10
Tmed3
Tmed4
Tmed8
Tmem101
Tmem109
Tmem115
Tmem140
Tmem14c
Tmem158
Tmem160
Tmem191c
Tmem198b
Tmem208
Tmem222
Tmem223
Tmem234
Tmem241
Tmem242
Tmem246
Tmem261
Tmem50a
Tmem60
Tmem63a
Tmem66
Tmem86a
Tmem9
Tmem9b
Tmppe
Tmub2
Tnfaip8l2
Tnip3
Tollip

bioRxiv preprint doi: https://doi.org/10.1101/708701; this version posted July 19, 2019. The copyright holder for this preprint (which was not certified by peer review) is the author/funder, who has granted bioRxiv a license to display the preprint in perpetuity. It is made available under aCC-BY-ND 4.0 International license.

Atp1b3
Atp2a3
Atp5c1
Atp5e
Atp5f1
Atp5g3
Atp5h
Atp5j
Atp5j2
Atp5k
Atp6ap1
Atp6v0b
Atp6v0c
Atp6v0d1
Atp6v1b2
Atp6v1e1
Atp6v1g1
Atpaf1
Atpif1
Atxn3
Atxn7l3
Atxn7l3b
AU023871
Auh
Aurkaip1
B230219D22Rik
B230378P21Rik
B3gat3
Bad
Bak1
Bap1
Bax
Bbc3
BC004004
BC005624
BC017643
BC029214
Bckdk
Bcl2
Bcl7b
Bet1l
Bicd2
Bid
Bin1
Bin3
Blmh
Bloc1s1
Bloc1s5
Bmp2k
Fam162a
Fam168b
Fam174a
Fam192a
Fam195b
Fam212a
Fam214b
Fam217b
Fam219b
Fam222b
Fam32a
Fam3c
Fam43a
Fam53c
Fam57b
Fam58b
Fam63a
Fam63b
Fam69a
Fam76a
Fam78a
Fam89b
Fam96a
Fars2
Fas
Fastk
Fau
Fbxl17
Fbxo46
Fbxo9
Fbxw2
Fbxw5
Fcer1g
Fez2
Fgfr1op2
Fhl3
Fis1
Fkbp8
Fli1
Flii
Flot1
Fmo5
Fnbp1
Foxj2
Foxred1
Frmd8
Fuca1
Fundc2
Fxr1
Mfap3
Mfng
Mfsd2b
Mgat1
Mgll
Mgmt
Mgst3
Micu2
Mief1
Mien1
Mink1
Minos1
Mis12
Mis18a
Mkks
Mknk1
Mknk2
Mkrn1
Mlec
Mlf2
Mllt10
Mllt11
Mmadhc
Mob1a
Mob2
Mospd3
Mpi
Mpl
Mpp1
Mpv17
Mras
Mrp63
Mrpl14
Mrpl20
Mrpl27
Mrpl28
Mrpl44
Mrpl48
Mrpl51
Mrpl53
Mrps11
Mrps17
Mrps24
Mrps25
Mrrf
Msl1
Msrb1
Mtcp1
Mtdh
Rab22a
Rab27a
Rab2a
Rab30
Rab31
Rab32
Rab43
Rab4a
Rab4b
Rab7
Rab7l1
Rabggtb
Rabif
Rad51d
Rad9a
Rai2
Ralb
Ralbp1
Ranbp3
Rap1a
Rap1gds1
Rap2b
Rarg
Rars
Rasgrp2
Rbbp6
Rbck1
Rbfa
Rbm17
Rbm38
Rbms1
Rbpms
Rbx1
Rcan1
Rcbtb2
Rcc2
Rce1
Rcor1
Reep5
Rer1
Rfesd
Rgs10
Rgs12
Rhbdd3
Rhbdf2
Rhoa
Rhoc
Rhog
Rhoj
Tomm22
Tomm7
Topbp1
Tor1a
Tor4a
Tox4
Tpcn1
Tpd52
Tpgs1
Tpi1
Tpm3
Tpm4
Tprgl
Tpst2
Trabd
Traf7
Trafd1
Trappc2l
Trappc3
Trappc5
Trappc6a
Trappc6b
Trappc9
Trem1
Treml1
Treml2
Trim37
Trim8
Triobp
Trpv2
Tsc22d3
Tsc22d4
Tsg101
Tspan14
Tspan17
Tspan18
Tspan9
Tspo
Tsr3
Tssc1
Tssc4
Tstd3
Ttc23
Ttc27
Ttc28
Ttc33
Ttc5
Ttc7b
Ttll1

bioRxiv preprint doi: https://doi.org/10.1101/708701; this version posted July 19, 2019. The copyright holder for this preprint (which was not certified by peer review) is the author/funder, who has granted bioRxiv a license to display the preprint in perpetuity. It is made available under aCC-BY-ND 4.0 International license.

Bola2	*Fyn*	*Mtf1*	*Rhot2*	*Ttyh3*
Brap	*Fzr1*	*Mthfd1l*	*Ric8*	*Tuba1a*
Brd4	*G3bp2*	*Mthfd2l*	*Rin3*	*Tuba1b*
Brd9	*Gab2*	*Mtmr14*	*Riok3*	*Tubb2a*
Brk1	*Gabarap*	*Mtss1l*	*Rit1*	*Tubb2b*
Bsdc1	*Gabarapl1*	*Mtus1*	*Rnf114*	*Tubb4b*
Bst2	*Gale*	*Mul1*	*Rnf125*	*Tusc2*
Btbd7	*Galk2*	*Mvp*	*Rnf141*	*Twf2*
Bysl	*Gapdh*	*Mxd1*	*Rnf144a*	*Txn2*
C530008M17Rik	*Gars*	*Mxd4*	*Rnf144b*	*Txndc15*
Calm1	*Gata1*	*Myd88*	*Rnf167*	*Txnl4a*
Calr	*Gata2*	*Myeov2*	*Rnf185*	*Tyw1*
Camk1	*Gatad2a*	*Myh9*	*Rnf187*	*U2af1*
Camsap1	*Gchfr*	*Myl6*	*Rnf19b*	*Uba1*
Cap1	*Gemin7*	*Napg*	*Rnf41*	*Uba5*
Capn5	*Gfod1*	*Narf*	*Rnf5*	*Uba7*
Capns1	*Gga3*	*Nars*	*Rnpepl1*	*Ubald1*
Capza1	*Ggh*	*Nav1*	*Rom1*	*Ubald2*
Capzb	*Gid8*	*Ncaph2*	*RP24-176F12.14*	*Ubash3b*
Car7	*Gimap6*	*Nck2*	*Rpain*	*Ubb*
Casd1	*Gipc1*	*Ncoa3*	*Rpp21*	*Ube2a*
Casp6	*Git1*	*Ncor1*	*Rps27l*	*Ube2b*
Cbwd1	*Git2*	*Nde1*	*Rps6kb2*	*Ube2d2a*
Cbx3	*Glb1*	*Ndrg1*	*Rps6kc1*	*Ube2g2*
Cby1	*Gle1*	*Ndufa1*	*Rragc*	*Ube2h*
Ccdc115	*Glipr2*	*Ndufa13*	*Rras*	*Ube2j1*
Ccdc12	*Glod4*	*Ndufa2*	*Rrp7a*	*Ube2j2*
Ccdc124	*Gltp*	*Ndufa6*	*Rspry1*	*Ube2m*
Ccdc28a	*Gltpd1*	*Ndufa7*	*Rsu1*	*Ube2q1*
Ccdc32	*Gm12942*	*Ndufa8*	*Rtf1*	*Ube2r2*
Ccdc50	*Gm13840*	*Ndufab1*	*Rtfdc1*	*Ube2v1*
Ccdc58	*Gm15051*	*Ndufb10*	*S100a10*	*Ube2z*
Ccdc71	*Gm16211*	*Ndufb11*	*S100a13*	*Ube4b*
Ccdc9	*Gm16286*	*Ndufb3*	*Samd1*	*Ubfd1*
Ccl3	*Gm16740*	*Ndufb7*	*Samm50*	*Ubiad1*
Ccnd3	*Gm20492*	*Ndufb8*	*Sap30l*	*Ubl7*
Ccndbp1	*Gm26510*	*Ndufb9*	*Sar1a*	*Ubn1*
Ccny	*Gm26863*	*Ndufs2*	*Sars*	*Ubp1*
Ccs	*Gm5506*	*Ndufs4*	*Sat1*	*Ubxn1*
Ccser2	*Gm561*	*Ndufs5*	*Sav1*	*Ufc1*
Cct7	*Gm5914*	*Ndufs6*	*Scamp3*	*Ufm1*
Cd1d1	*Gmpr*	*Ndufs7*	*Scarb1*	*Uhmk1*
Cd200r1	*Gna12*	*Necap2*	*Scarf1*	*Ulk1*
Cd274	*Gna13*	*Nedd8*	*Scnm1*	*Unc119*
Cd2bp2	*Gnai2*	*Nelfb*	*Sdcbp*	*Unc119b*
Cd47	*Gnaq*	*Nelfcd*	*Sdccag3*	*Unc50*
Cd93	*Gnb1*	*Nelfe*	*Sdccag8*	*Upf3a*
Cd97	*Gnb2*	*Neurl3*	*Sdf2*	*Upp1*
Cdadc1	*Gnl2*	*Nfe2*	*Sdf4*	*Uqcr10*

bioRxiv preprint doi: https://doi.org/10.1101/708701; this version posted July 19, 2019. The copyright holder for this preprint (which was not certified by peer review) is the author/funder, who has granted bioRxiv a license to display the preprint in perpetuity. It is made available under aCC-BY-ND 4.0 International license.

Cdc26
Cdc34
Cdc42ep2
Cdc42ep4
Cdc42se2
Cdipt
Cdk11b
Cdk16
Cdk19
Cdk2ap2
Cdk5
Cdk9
Cdkn1a
Cdkn2aipnl
Cdkn2d
Cebpb
Cebpg
Cep170
Cep19
Cerk
Cfl1
Chchd3
Chchd4
Chchd7
Chfr
Chic2
Chid1
Chmp2a
Chmp3
Chmp4b
Chmp6
Chmp7
Chrac1
Chst11
Chsy1
Chtop
Ciao1
Cib1
Cinp
Cirbp
Ckap4
Ckb
Clec1b
Clec4d
Clic1
Clic4
Clint1
Clstn1
Clu
Gnpda2
Gnptg
Golga7
Gorasp2
Got1
Gp5
Gp9
Gpalpp1
Gpcpd1
Gpr137
Gpr146
Gpr97
Gpsm3
Gpx1
Gpx4
Grb2
Grcc10
Grk6
Grn
Gsk3a
Gskip
Gsr
Gstp1
Gtf2e2
Gtf2h1
Gtf2h5
Gtf3c6
Gtpbp2
Gucd1
H2afj
H2afv
H2afx
H2afz
H2-D1
H2-K1
H2-Ke2
H2-T22
H2-T23
H2-T24
H3f3a
H3f3b
Hcfc1r1
Hcls1
Hcst
Hdac5
Hdac7
Hexa
Hexdc
Hexim1
Ngly1
Ngrn
Nipal3
Nkap
Nkiras2
Nlk
Nlrx1
Nmb
Nme1
Nme2
Nosip
Nploc4
Nprl3
Nr1h2
Nras
Nrbf2
Nrbp1
Nsf
Nsfl1c
Nt5m
Nub1
Nubp2
Nucb1
Nucks1
Nudcd2
Nudt16
Nudt18
Nudt3
Nudt7
Nudt9
Numb
Nup50
Nup62
Nxt1
Nyx
Oard1
Oaz2
Ociad1
Odc1
Ogfr
Ogg1
Olr1
Orai1
Orai2
Orai3
Oraov1
Ostc
Ostf1
Ostm1
Sdhaf2
Sdhb
Sdhc
Sdhd
Sdpr
Sec11a
Sec11c
Sec13
Sec14l1
Sec61b
Sec62
Selk
Selm
Selp
Sema6d
Sept9
Sept11
Sept15
Sepw1
Serbp1
Serf2
Serhl
Serinc3
Sertad1
Sertad2
Setd3
Sft2d1
Sgta
Sh2b3
Sh3glb1
Sh3glb2
Sharpin
Shfm1
Siah2
Sigmar1
Sin3b
Sirt7
Skap2
Ski
Skil
Sla2
Slc16a3
Slc25a24
Slc30a1
Slc35a4
Slc35e4
Slc35f5
Slc39a11
Slc39a6
Uqcr11
Uqcrq
Urm1
Uros
Usp12
Usp5
Vamp2
Vamp5
Vasp
Vcl
Vcp
Vdac3
Vkorc1
Vps25
Vps28
Vps29
Vps33a
Vps37b
Vps37c
Vps4a
Vps4b
Vps51
Vps52
Vps53
Vps72
Vrk3
Vti1b
Vwf
Was
Wasf2
Wbp4
Wdr1
Wdr26
Wdr45b
Wdsub1
Wdtc1
Whamm
Wipf1
Wipi1
Wrap73
Wsb2
Xab2
Xpnpep1
Yap1
Yif1b
Yipf3
Ykt6
Ypel2
Ypel3

bioRxiv preprint doi: https://doi.org/10.1101/708701; this version posted July 19, 2019. The copyright holder for this preprint (which was not certified by peer review) is the author/funder, who has granted bioRxiv a license to display the preprint in perpetuity. It is made available under aCC-BY-ND 4.0 International license.

Cmas
Cmc2
Cmip
Cmtm3
Cmtm6
Cnbp
Cndp2
Cnot6
Cnot8
Cnp
Cnppd1
Cnpy3
Cnr2
Coa3
Commd1
Commd6
Commd7
Commd9
Comtd1
Cops2
Cops7a
Copz1
Coro1b
Coro1c
Cox14
Cox4i1
Cox5b
Cox6a1
Cox6c
Cox7b
Cox7c
Cox8a
Cpe
Cpne8
Cpt1a
Cr1l
Crcp
Crk
Crlf2
Crot
Crtap
Csk
Csnk1a1
Csnk1d
Csnk1e
Csnk2b
Ctbp1
Ctdnep1
Ctdsp2
Hhex
Hint2
Hint3
Hira
Hist1h1c
Hist1h2ac
Hist1h4i
Hist3h2a
Hmbs
Hmgcl
Hnrnpab
Hnrnpc
Hnrnpf
Hnrnpk
Hnrnpl
Hnrnpm
Hnrnpu
Hnrnpul1
Hoga1
Homer1
Homer3
HOTAIRM1_5
Hpcal1
Hpgd
Hps4
Hrsp12
Hs1bp3
Hsd17b12
Hsd3b7
Hsdl1
Hsp90b1
Htatip2
Ica1
Icmt
Ifi27
Ifitm10
Ifitm2
Ifitm3
Ifrd2
Ift20
Ift27
Igbp1
Igtp
Ikbkb
Il27ra
Il4
Ilk
Immp1l
Incenp
Otub1
Otud6b
Pacs1
Paf1
Pagr1a
Palm
Pank2
Panx1
Paqr7
Pard6a
Parp11
Parvb
Patl1
Pbx2
Pcbp1
Pcif1
Pck2
Pcmt1
Pcsk7
Pdap1
Pdcd10
Pdcd5
Pdcd6
Pddc1
Pde2a
Pdia3
Pdlim1
Pdlim5
Pdlim7
Pea15a
Pecam1
Pet100
Pex14
Pex19
Pfn1
Pgam1
Pggt1b
Pgm1
Pgm2l1
Pgpep1
Phc2
Phf23
Phlda3
Pigc
Pim1
Pin1
Pip4k2a
Pip5k1c
Pithd1
Slc3a2
Slc45a4
Slc4a1ap
Slmap
Slpi
Slu7
Smagp
Smap1
Smarcd2
Smc1a
Smdt1
Smg7
Smim12
Smim20
Smim7
Smox
Smtn
Smu1
Smurf1
Smurf2
Snd1
Snf8
Snn
Snrnp25
Snrnp27
Snrpc
Snw1
Snx1
Snx11
Snx17
Snx3
Spast
Spg7
Sphk2
Sppl3
Spred2
Sptlc2
Sra1
Srd5a3
Srf
Srgn
Sri
Srp19
Srp68
Srp9
Srpr
Srsf5
Srsf9
Srxn1
Ywhab
Ywhae
Zbtb18
Zc3h13
Zc3h4
Zcchc10
Zcchc2
Zdhhc16
Zdhhc18
Zdhhc6
Zdhhc7
Zfand2b
Zfand3
Zfand5
Zfand6
Zfp281
Zfp36l2
Zfp414
Zfp422
Zfp655
Zfp664
Zfp830
Zfyve20
Zfyve27
Zmat2
Zmiz2
Zmynd11
Znhit1
Znhit2
Znrf2
Zrsr2
Zwint
0610010K14Rik
0610031J06Rik
1110001A16Rik
1110004F10Rik
1110007C09Rik
1110008F13Rik
1110058L19Rik
1500011B03Rik
1700017B05Rik
1700037C18Rik
1700037H04Rik
1810009A15Rik
1810043H04Rik
2010107E04Rik
2210404O07Rik
2310011J03Rik
2310036O22Rik

bioRxiv preprint doi: https://doi.org/10.1101/708701; this version posted July 19, 2019. The copyright holder for this preprint (which was not certified by peer review) is the author/funder, who has granted bioRxiv a license to display the preprint in perpetuity. It is made available under aCC-BY-ND 4.0 International license.

Ctif	*Inf2*	*Pitpna*	*Ss18*	*2310047M10Rik*
Ctnna1	*Ing1*	*Pitpnc1*	*Ssbp4*	*2510009E07Rik*
Ctps2	*Inpp5a*	*Pitpnm1*	*Ssna1*	*2510039O18Rik*
Ctsa	*Inpp5d*	*Pitpnm2*	*Ssr4*	*2610001J05Rik*
Ctsd	*Ipo11*	*Pkd2l2*	*Ssu72*	*2610524H06Rik*
Ctsz	*Irak3*	*Pkm*	*St3gal1*	*2810428I15Rik*
Cttn	*Irak4*	*Pkp4*	*St3gal2*	*2900026A02Rik*
Cuedc1	*Irf3*	*Pla2g16*	*St6galnac3*	*3110040N11Rik*
Cuedc2	*Isca2*	*Pld3*	*Stam2*	*3110062M04Rik*
Cuta	*Iscu*	*Plek*	*Stard3nl*	*4931406P16Rik*
Cxxc5	*Isg15*	*Plekha2*	*Stard4*	*4933426M11Rik*
Cyb5	*Itfg1*	*Plekhm1*	*Stat6*	*5031425E22Rik*
Cyb561a3	*Itga6*	*Plekho1*	*Stim2*	*5031439G07Rik*
Cyb5d2	*Itgal*	*Plekho2*	*Stk19*	*5430417L22Rik*
Cyb5r3	*Itgb3*	*Plscr1*	*Stk4*	*6330409D20Rik*
Cyb5r4	*Itgb4*	*Plvap*	*Stk40*	*6430548M08Rik*
Cyba	*Itgb5*	*Pmm2*	*Stom*	*8430427H17Rik*
Cyth1	*Itm2b*	*Pnkd*	*Stra13*	*9130401M01Rik*
Cyth3	*Itpkb*	*Pnkp*	*Strap*	*9430023L20Rik*
D330023K18Rik	*Itsn2*	*Pnrc1*	*Strip1*	*9530082P21Rik*
D8Ertd738e	*Jagn1*	*Poldip3*	*Strn*	
D930015E06Rik	*Jarid2*	*Pole3*	*Strn4*	

bioRxiv preprint doi: https://doi.org/10.1101/708701; this version posted July 19, 2019. The copyright holder for this preprint (which was not certified by peer review) is the author/funder, who has granted bioRxiv a license to display the preprint in perpetuity. It is made available under aCC-BY-ND 4.0 International license.

Supplemental references

1. Sanz E*, et al.* (2009) Cell-type-specific isolation of ribosome-associated mRNA from complex tissues. *Proceedings of the National Academy of Sciences of the United States of America* 106(33):13939-13944.
2. de Lange WJ, Halabi CM, Beyer AM, & Sigmund CD (2008) Germ line activation of the Tie2 and SMMHC promoters causes noncell-specific deletion of floxed alleles. *Physiological genomics* 35(1):1-4.
3. Koni PA*, et al.* (2001) Conditional vascular cell adhesion molecule 1 deletion in mice: impaired lymphocyte migration to bone marrow. *The Journal of experimental medicine* 193(6):741-754.
4. Muzumdar MD, Tasic B, Miyamichi K, Li L, & Luo L (2007) A global double-fluorescent Cre reporter mouse. *Genesis (New York, N.Y. : 2000)* 45(9):593-605.
5. Tiedt R, Schomber T, Hao-Shen H, & Skoda RC (2007) Pf4-Cre transgenic mice allow the generation of lineage-restricted gene knockouts for studying megakaryocyte and platelet function in vivo. *Blood* 109(4):1503-1506.
6. Lakso M*, et al.* (1996) Efficient in vivo manipulation of mouse genomic sequences at the zygote stage. *Proceedings of the National Academy of Sciences of the United States of America* 93(12):5860-5865.
7. Andreev DE, O'Connor PB, Loughran G, & Dmitriev SE (2017) Insights into the mechanisms of eukaryotic translation gained with ribosome profiling. 45(2):513-526.
8. Nolan DJ*, et al.* (2013) Molecular signatures of tissue-specific microvascular endothelial cell heterogeneity in organ maintenance and regeneration. *Developmental cell* 26(2):204-219.
9. Bodary PF, Westrick RJ, Wickenheiser KJ, Shen Y, & Eitzman DT (2002) Effect of leptin on arterial thrombosis following vascular injury in mice. *Jama* 287(13):1706-1709.
10. Mudge JM & Harrow J (2015) Creating reference gene annotation for the mouse C57BL6/J genome assembly. *Mammalian genome : official journal of the International Mammalian Genome Society* 26(9-10):366-378.
11. Langmead B & Salzberg SL (2012) Fast gapped-read alignment with Bowtie 2. *Nature methods* 9(4):357-359.
12. Salzman J, Jiang H, & Wong WH (2011) Statistical Modeling of RNA-Seq Data. *Statistical science : a review journal of the Institute of Mathematical Statistics* 26(1).
13. Pfeffer S, Woellhaf MW, Herrmann JM, & Forster F (2015) Organization of the mitochondrial translation machinery studied in situ by cryoelectron tomography. *Nature communications* 6:6019.
14. Anonymous (2015) Gene Ontology Consortium: going forward. *Nucleic acids research* 43(Database issue):D1049-1056.
15. Ashburner M*, et al.* (2000) Gene ontology: tool for the unification of biology. The Gene Ontology Consortium. *Nature genetics* 25(1):25-29.
16. Szklarczyk D*, et al.* (2017) The STRING database in 2017: quality-controlled protein-protein association networks, made broadly accessible. 45(D1):D362-d368.
17. Rowley JW*, et al.* (2011) Genome-wide RNA-seq analysis of human and mouse platelet transcriptomes. *Blood* 118(14):e101-111.
18. Jin E*, et al.* (2009) Differential roles for ETS, CREB, and EGR binding sites in mediating VEGF receptor 1 expression in vivo. *Blood* 114(27):5557-5566.
19. Du P, Kibbe WA, & Lin SM (2008) lumi: a pipeline for processing Illumina microarray. *Bioinformatics (Oxford, England)* 24(13):1547-1548.

bioRxiv preprint doi: https://doi.org/10.1101/708701; this version posted July 19, 2019. The copyright holder for this preprint (which was not certified by peer review) is the author/funder, who has granted bioRxiv a license to display the preprint in perpetuity. It is made available under aCC-BY-ND 4.0 International license.

20. Ritchie ME*, et al.* (2015) limma powers differential expression analyses for RNA-sequencing and microarray studies. *Nucleic acids research* 43(7):e47.
21. Wang F*, et al.* (2012) RNAscope: a novel in situ RNA analysis platform for formalin-fixed, paraffin-embedded tissues. *The Journal of molecular diagnostics : JMD* 14(1):22-29.